Dissertation

submitted to the

Combined Faculties for the Natural Sciences and for Mathematics

of the Ruperto-Carola University of Heidelberg, Germany

for the degree of

Doctor of Natural Sciences

presented by

Dipl.-Biol. Ulrike Hüsken

born in Trier, Germany

Oral Examination:

January 28th , 2013

Role of Tcf7l2 Mediated Wnt/Beta-Catenin Signaling in the Establishment of Habenular Asymmetry

Referees: Prof. Dr. Thomas Holstein
Prof. Dr. Michael Boutros

TABLE OF CONTENT

Summary **1**

Zusammenfassung **2**

1 Introduction **3**

1.1 Asymmetries of the nervous system **3**

1.1.1 Epithlamic asymmetries in vertebrates 3

1.1.2 The habenulo-interpeduncular system of zebrafish 4

1.1.3 Asymmetric habenula neurogenesis 7

1.2 Establishment of habenular asymmetry and laterality **9**

1.2.1 Lateralizing signals 9

1.2.2 Symmetry-breaking signals 11

1.3 Role of Wnt/beta-catenin pathway in the habenula development **12**

1.3.1 Early Wnt signals during late gastrulation and somitogenesis 13

1.3.2 Late Wnt signaling during post-somitogenesis 14

1.3.3 The Wnt pathway component Tcf7l2 16

2 Aim of this thesis **19**

3 Results **20**

3.1 Phenotypic characterization of *tcf7l2* mutant **20**

3.1.1 *tcf7l2* mutants show left-right symmetric patterns of epithalamic neuron differentiation 20

3.1.2 Habenular neurogenesis is not overtly altered in *tcf7l2* mutant 24

3.2 Role of *tcf7l2* in the establishment of habenular asymmetry **26**

3.2.1 *Axin1* acts upstream of *tcf7l2* during the formation of habenular asymmetry 27

3.2.2 Transient downregulation of Wnt/beta-catenin signaling mimics the *tcf7l2* mutant habenula phenotype 28

3.3 Function of Tcf7l2 mediated Wnt signaling in the establishment of habenular asymmetry **31**

3.3.1 Wnt signaling is required during habenular cell neurogenesis 32

3.3.2 Tcf7l2 is asymmetric expressed along the left-right axis 34

3.3.3 Tcf7l2 is expressed in habenular cells as they differentiate as dHb neurons 38

3.3.4 Tcf7l2 expression is influenced by altered Wnt signaling 40

3.4 The epistatic relation of Tcf7L2, Nodal and parapineal signals **42**

3.4.1 Asymmetric Tcf7l2 expression is Nodal independent 43
3.4.2 The absence of Tcf7l2 function renders parapineal cell signals redundant 46

4 Discussion 50
4.1 Tcf7l2 mediated Wnt/beta-catenin signaling needs to be tightly controlled during asymmetric habenula establishment 50
4.2 Tcf7l2 mediated Wnt signaling acts Nodal independently during asymmetric habenula neurogenesis 52
4.3 Asymmetric Tcf7l2 influences cell type specification 55
4.4 Parapineal and asymmetric Tcf7l2 mediated Wnt signals establish the habenular left-right asymmetry 60

5 Experimental procedure 64
5.1 Fish Maintenance 64
5.2 Identification of *tcf7l2* mutant fish 65
5.2.1 DNA extraction 65
5.2.2 PCR 65
5.2.3 Restriction Analysis 67
5.3 *In Situ* Hybridization Procedures 67
5.3.1 Bacteria transformation - Isolation of plasmid DNA 67
5.3.2 Preparation of *in situ* probes 69
5.3.3 Whole mount *in situ* hybridization 70
5.4 Whole mount antibody staining 72
5.5 Labeling of habenular efferent projections 73
5.6 Laser cell ablation 74
5.7 Heatshock and IWR treatments 74
5.8 Temperature shift and Morpholino injection 75
5.9 Microscopy, Image manipulation and Statistical analysis 75

6 References 76

7 Appendix 87
7.1 Transient interference with Wnt/beta-catenin signaling 87
7.2 Original pictures of anti-Tcf7l2 stainings 88
7.3 Numbers of Tcf7l2 and/or HuC/D expressing cells 88
7.4 Lists of figures and abbreviations 92

Acknowledgement 96

SUMMARY

Brain asymmetries are a conserved feature of the vertebrate nervous systems that allows an efficient processing of complex neuronal tasks. Given that alterations in asymmetrically formed areas of the human brain can have devastating consequences it is surprising that the genetic basis underlying their development is still poorly understood.

In the zebrafish epithalamus, medial and lateral neurons of the habenulae are differentially distributed on the left and right side of the brain. Recent advances shed light on signaling pathways involved in the establishment of asymmetric habenulae. However, the underlying mechanisms and epistatic relationships between them are unclear.

This study reveals that Tcf7l2 is a key component of habenular asymmetry establishment. In its absence the habenulae develop symmetric neuronal specification as habenular progenitors differentiate mainly into lateral neurons on both sides of the brain. Interestingly, Tcf7l2 is expressed asymmetrically in habenular precursor cells. The data obtained are consistent with a model by which Tcf7l2 mediated Wnt/beta-catenin signaling switches the differentiation program of precursor cells and promotes medial habenula cell fate. On the left side, this activity is suppressed by signals derived from the adjacent parapineal cells, which results in continued generation of lateral habenula neurons. Thus, a combination of parapineal and Tcf7l2 signals can promote the asymmetric habenular organization.

ZUSAMMENFASSUNG

Der asymmetrische Aufbau des Gehirns ist eine konservierte Besonderheit des vertebraten Nervensystems und gewährleistet eine effiziente Verarbeitung komplexer neuronaler Aufgaben. Obwohl ein veränderter Aufbau solcher Areale drastische Konsequenzen im Menschen zur Folge haben kann, ist überraschend wenig über deren Entwicklung und die zugrunde liegende Genetik bekannt.

Im Epithalamus des Zebrafisches sind die medialen und lateralen Neurone der Habenulae auf der linken und rechten Gehirnhälfte unterschiedlich verteilt. Trotz der Identifizierung einiger Signalkaskaden, welche in der Etablierung der asymmetrischen Habenulae involviert sind, ist es nach wie vor unklar, wie diese subnuklearen Unterschiede über die hemispherischen Grenzen hinweg entstehen.

Diese Arbeit zeigt, dass Tcf7l2 eine Schlüsselkomponente in der Etablierung der habenularen Asymmetrie ist. Durch die Abwesenheit des Proteins entwickeln die Habenulae symmetrische neuronale Spezifizierungen. In diesem Fall differenzieren sich die habenularen Vorläuferzellen auf beiden Gehirnhälften vorwiegend zu lateralen Neuronen. Interessanterweise ist Tcf7l2 zunächst asymmetrisch während der habenularen Differenzierung expremiert. Die hier vorliegenden Daten weisen drauf hin, dass das Tcf7l2 vermittelte Wnt/beta-catenin Signal ein mediales Zellschicksal bewirkt indem es das Differenzierungsprogramm der Vorläuferzellen verändert. In der linken Habenula ist diese Differenzierung durch die benachbarten Parapinealzellen unterdrückt, wodurch dort hauptsächlich laterale Neuronen gebildet werden. Somit kann die Kombination von Parapinealsignalen und Tcf7l2-Signalen den asymmetrischen habenularen Aufbau bewirken.

1 INTRODUCTION

1.1 Asymmetries of the nervous system

Neuroanatomical asymmetries are a common feature in the animal kingdom. Already in the basic nervous system of the nematode *caenorhabditis elegans* left-right differences can be found as bilateral paired odorsensory neurons show different setup of receptors (Yu et al., 1997). The asymmetric receptor distribution increases the diversity of the functional repertoire and allows the animals thereby to distinguish between different attractive chemicals (Oritz et al., 2009; Wes and Bargmann, 2001).

Neuronal asymmetries exist in the highly complex vertebrate brain too. Several studies revealed size differences of bilateral structures and asymmetric expressed neurotransmitters (Zilles et al., 1996; Galaburda 1991; Glick et al., 1982; Toga et al., 2003). In humans the most obvious brain asymmetry is given by the differential large left and the right temporal planum, an auditory processing structure in the posterior temporal lobe (Geschwind and Levitsky, 1968). The size difference is concordant with the left-biased language production and comprehension (Dapretto et al., 1999; Binder 2000).

In general, brain asymmetries increase the efficiency of neural processing and prevent interhemispheric conflicts. Reduced or absent hemispheric asymmetry can have drastic consequences in humans as correlations to mental diseases like dyslexia, dementia and schizophrenia were reported (Oertel et al., 2010; Teufel et al., 2010; Larsen et al., 1990; Cro et al., 1989; Loewenstein et al., 1989). In addition to the relevance in human health the question how anatomical left-right brain asymmetries are established in a bilateral symmetric organism has become an important field of developmental neuroscience. Several studies tried to answer the question from studies in frog, mouse, chick and zebrafish embryos.

1.1.1 Epithalamic asymmetries in vertebrates

The best described brain asymmetries in vertebrates are found in the highly conserved epithalamus. The epithalamus is a subdivision of the diencephalon and functions as a relay station between the forebrain and midbrain. Its major nuclei, the bilaterally habenulae and the adjacent pineal complex, are lateralized in many species.

The dorsal diencephalic conduction system (DDC) encompasses the connection of the habenulae and pineal complex, the afferent inputs from the forebrain and innervations of the

ventral midbrain (Fig. 1.1). Since the DDC is connected to limbic parts of the forebrain, the emotional center of the human brain, the neuronal network influences various psychological conditions like depression, anxiety, schizophrenia and neuropathological responses to addictive drugs (Caldecott-Hazard et al., 1988; Yang et al., 2008; Lecourtier et al., 2004; Ellison, 2002; Agetsuma et al., 2011). A further function of the habenulae and the DDC is to regulate the activity of nuclei in the ventral midbrain. Mainly by interaction with the pineal organ the DDC controls the secretion of melatonin and thereby sleep and circadian rhythm (Falcon et al., 1999; Klein and Moore, 1979; Valjakka et al., 1998). Furthermore, the modulation of dopaminergic and GABAergic neurons through the DDC influences motor behaviors and learning (Lisoprawski et al., 1980; Lee and Huang, 1988; Lecoutier and Kelly, 2005). The multitude of different tasks of the DDC probably requires an asymmetric construction to allow a complex and highly efficient processing.

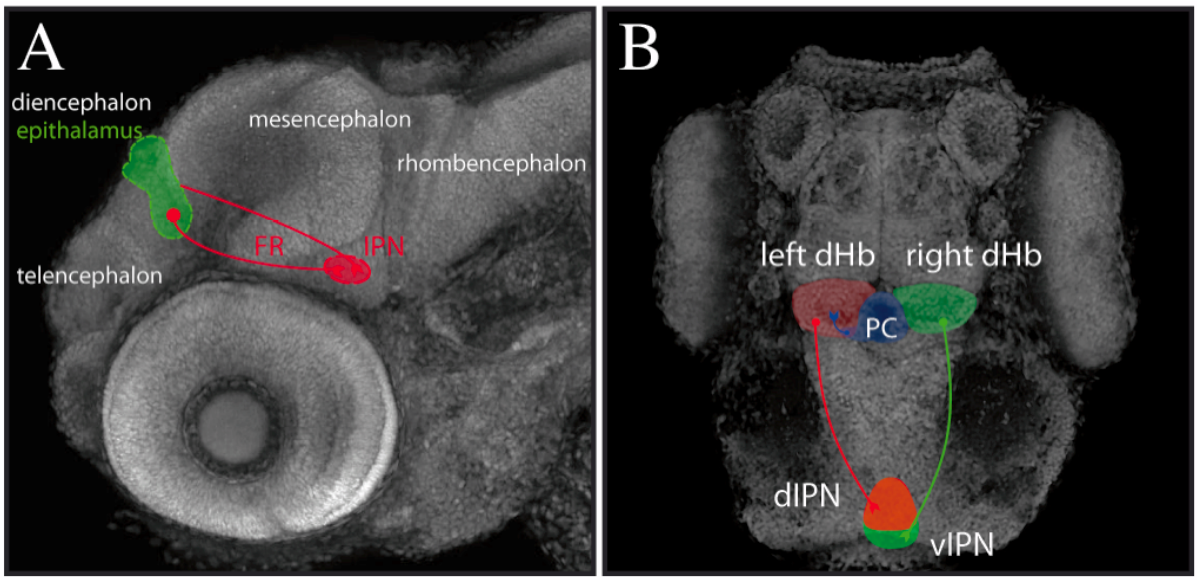

Figure 1.1: Asymmetric regions of the zebrafish brain.
(A) Lateral view on the brain of a 4 dpf old zebrafish larva. The brain areas telencephalon and diencephalon (both forebrain), mesencephalon (midbrain) and rhombencephalon (hindbrain) are labelled. Asymmetries can be found in the diencephalic eptithalamus (green) and in its projection via the fasciculus retroflexus (FR, red) to the interpeduncular nucleus (IPN, red). (B) Dorsal view of the habenular neuronal circuit show that the left dorsal habenula (left dHb, red) project to the dorsal IPN (dIPN, red) whereas the right dorsal habenula project to the ventral part (vIPN, both green). The left habenula is innervated by projections from the medial positioned pineal complex (PC, blue).

The habenular complex consists of two separate bilateral symmetric nuclei: the medial and lateral habenulae in mammals or the ventral and dorsal in amphibians, fish and reptiles. It is probable that the different positions of the homolog nuclei are developed by displacements of the brain region over evolution (Amo et al., 2010). In contrast to the bilateral symmetric lateral/ventral habenula the medial/dorsal nucleus is left-right asymmetric organized.

In fish and amphibian the dorsal habenulae (dHb) obviously exhibit different sizes up to 20% while a more subtle but significant size asymmetry of the homologous medial habenulae, of less than 5% can be found in birds and mammals (Wree et al., 1981; Zilles et al., 1976; Halpern et al., 2003). The mode of lateralization, i.e. which side develops larger, differs depending on the species (Concha and Wilson 2001; Harris et al., 1996; Kemali et al., 1990).
Amphibians, reptiles and fish exhibit asymmetries in the subnuclear organization of the medial habenulae. Cell clusters with different neuronal specifications can be distinguished according to the cell morphology, axonal projection and gene expression. While subnuclei with equal characteristics can be found in both habenulae, their size and distribution differ (Signore et al., 2009; Yanez and Anadon 1994; Concha et al., 2000). Thus, e.g. serotonineric neurons are mainly located in the left habenula of teleost (Ekstrom and Ebbesson 1988; Bianco and Wilson, 2009). Similarly, the neuropil density is more concentrated in the left habenula in teleost, amphibians and some reptiles (Yanez and Anadon 1994; Concha and Wilson, 2001).
The medial habenula of mammals and birds and the dorsal habenula of amphibians and fish respectively receive efferent inputs by the stria medullaris from the forebrain and project almost exclusively via the fasciculus retroflexus to the interpeduncular nucleus (IPN) in the ventral midbrain (Fig 1.1 A, B).
Additionally, the DDC connected photoreceptive pineal complex is also asymmetrically organized in teleost, bowfin, coelacanth, lizards and some reptiles (Concha and Wilson, 2001). It comprises the medial pineal, homologous to the epiphysis in mammals, and the lateralized parapineal organ. The parapineal organ is located on the left side of the brain and sends out ipsilateral projections to the left habenula (Fig. 1.1 B; Ekström and Meissl, 2003; Falcón, 1999; Concha and Wilson, 2001).

1.1.2 The habenulo-interpeduncular system of zebrafish

The zebrafish (*Danio rerio*) has become a popular model system to study the establishment of neural asymmetries since the left-right differences of the habenulo-interpeduncular system are quite distinct and well described. Several genes involved in the establishment of brain asymmetry and laterality were identified using zebrafish mutants. Furthermore, the asymmetric development and behavioral consequences can be studied in living embryos. Thus, it was possible to correlate the epithalamic laterality with the sideness of eye-usage in asymmetric behaviors like the control of response to visual stimuli (Barth et al., 2005).
The dorsal habenula of zebrafish (dHb) develops a clearly defined left-right asymmetric subnuclear regionalization. Two subnuclei, the lateral and the medial, can be distinguished by their expression pattern and neuronal connectivity (Fig. 1.2 A; Concha and Wilson 2001;

Gamse et al., 2003, 2005). For example, three members of the *potassium channel tetramization domain* (KCTD) are expressed in different subnuclei and are thereby asymmetrically distributed along the left-right axis. The *left-over/kctd2.1* gene can mainly be found in cells with lateral dorsal habenula (dHbl) character while *righton* and *dexter* are expressed primarily in cells with medial dorsal habenula (dHbm) specification (Gamse et al., 2005).

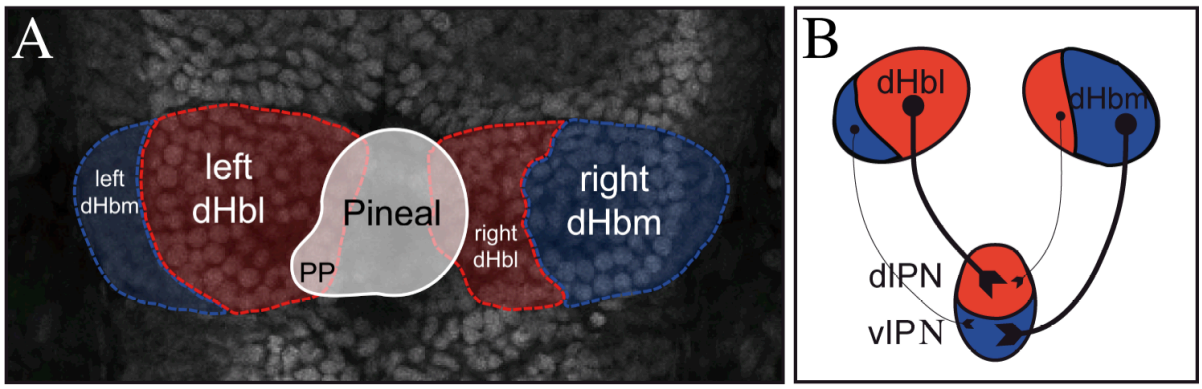

Figure 1.2: Habenula-IPN asymmetry in the zebrafish brain.
Dorsal view focused on the dorsal habenula and pineal complex of a 4 dpf old larvae (A). The pineal complex (white) consists of the medial positioned pineal and the left-sided parapineal cells (PP). The habenulae are asymmetric organized regarding their subnuclear organization and their innervation of the interpeduncular nucleus (IPN, schematic representation in B). A bigger lateral habenular subnucleus (dHbl, red) and a smaller medial subnucleus (dHbm, blue) build up the left dorsal habenula compared to the counterpart organization of the right habenula. The dHbl neurons project to the dorsal IPN (dIPN) while the dHbm cells innervate the ventral (vIPN).

The epithalamic left-right asymmetry is transformed into a dorso-ventral one in the ventral midbrain as the specificity of the habenula cell determinates the innervation side of the IPN. The axons from the dHbl neurons terminate in the dorsal IPN whereas the dHbm axons project to the ventral part (Bianco et al., 2008; Aizawa et al., 2005; Gamse et al., 2005). Since the left habenula consists of a large cluster of dHbl cells and the right habenula of more dHbm cells, axons deriving from the left predominantly end in the dorsal IPN, while most axons from the right end ventral (Fig. 1.2 B).

The asymmetric organized pineal complex is connected to the habenulo-interpeduncular system of zebrafish (Fig. 1.2 A). During the habenula neuron generation, parapineal cells delaminate from the anterior part of the medially positioned pineal, migrate to the left side of the brain and forward to the midline to its final position innervating the left habenula (Fig. 1.3; Concha et al., 2003).

At 4 dpf the asymmetric distribution is already fully developed. A larger cluster of dHbl neurons is located on the left side of the brain while just a few cells have lateral specificity on

the right. The inverse situation is given for dHbm cells (Fig. 1.2 A). At this developmental stage the dHbl cells can be found in a medial position and dHbm cells in a lateral. The subsequent rearrangements of the diencephalon bring about a subnuclear orientation that is in accordance with their designations.

1.1.3 Asymmetric habenula neurogenesis

Several developmental strategies can cause a left-right asymmetric neurogenesis. A main mechanism is the lateralized overproliferation, a process that is involved in directional looping or coiling of organs with tube-like primordia such as heart and gut (Linask et al., 2005; Muller et al., 2003; Qu et al., 2008; Schlueter and Brand, 2007). A second possible scenario is differential cell migration or apoptosis of a tissue as it is described in vascular tree development (Chapple et al., 2012; Augustin et al., 2003). Asymmetric differentiation of single cells or cell cluster usually goes ahead with the referred mechanisms but can also be found in uniform structures to allow differential specifications across the left-right axis. Such an unequal differentiation causes the asymmetry in the already mentioned neuronal network of *C. elegans* (Oritz et al., 2009; Wes and Bargmann, 2001). Furthermore, timely shift of the developmental stage of one side can be used to set up left-right differences. For instance, a faster somitogenesis on the left side was reported in the invertebrate chordate amphiouxus (lancelet) (Minguillon et al., 2002).

During habenula development left-right differences in timing, proliferation and differentiation are given (Fig.1.3; Aizawa et al., 2007). Initially, a bilateral symmetric pool of neuroepithelian stem cells generates the habenular precursor cells. At 24 hpf, after somitogenesis finished, neurogenesis proceeds in the habenular region. BrdU labellings raised the hypothesis that the precursors on the left side start to proliferate earlier compared to those on the right. However, the proliferation finally results in a similar number of left- and right-sided habenular cells.

Subsequent differentiation proceeds asymmetrically too. First differentiating cells were found again on the left side while still further progenitors are born. The differentiation proceeds in two asymmetric waves: Firstly, the early-born progenitors develop lateral characteristics and build up the lateral subnuclei. Slightly delayed, medial habenular cells are generated out of the later born habenular progenitors.

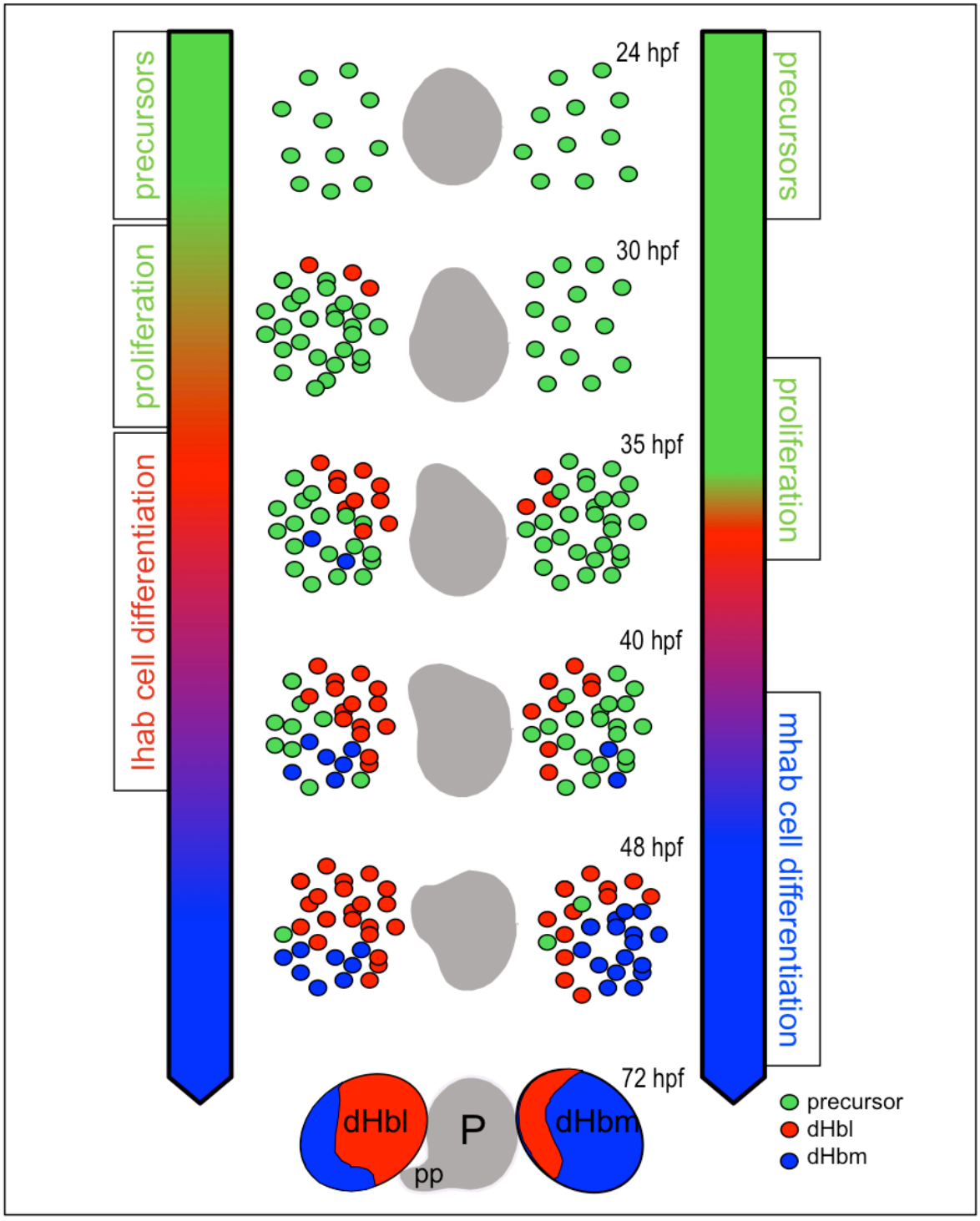

Figure 1.3: Model of asymmetric habenular development.
Initially, habenular stem cells are equally distributed on both sides of the brain (green). The precursor cells start to proliferate earlier on the left side than on the right. Also on the left, first cells start differentiating: while the early born cells develop lateral dorsal habenula character (dHbl, red), the later born differentiate into medial dorsal habenula neurons (dHbm. blue). The parapineal (pp) migrates during the entire process out of the pineal (P) to the left and follows a posterior direction. The model bases on Aizawa et al., 2007.

Thus, neuronal birthdate correlates with the habenular asymmetry. The early born dHbl cells on the left side build up a bigger lateral habenular subnucleus and the later born dHbm cell a smaller medial nucleus compared to its counterpart on the right hemisphere.
Since the maturation of early- and late-born habenular progenitors proceeds temporally overlapping, dHbm and dHbl neurons can be generated at the same time. It was also demonstrated by lineage tracing that single habenular progenitors can give rise to both, dHbm or dHbl neuron (Aizawa et al., 2007). This may suggest that, imposed by a global regulation of neurogenesis timing, the unequal specification of the habenular neurons is promoted by differentially acting signals which bias the neuronal fate at that intermediate time.

1.2 Establishment of habenular asymmetry and laterality

The timing of habenular neurogenesis reveals left-right and lateral-medial asymmetries. Thus, the question arises which signals regulate the process and how its differential progression across the brain hemispheres is established. Several genetic pathways have been identified being involved in the establishment of the diencephalic left-right differences.
Two kinds of signals, that influence the habenula development, should be considered separately: lateralizing signals and symmetry-breaking signals. While symmetry-breaking signals allow the habenulae to develop asymmetrically, lateralizing signals determine the directionality of the habenular asymmetry, i.e. if the habenula with left sided character develops on the left or the right side of the brain.

1.2.1 Lateralizing signals

Most of the work carried out on habenular development has been focused on how their laterality is established. Laterality defines the identity of the habenulae and the sideness of the parapineal. In case of their absence the left-right directionality is randomized but the overall structures are still asymmetrically formed (Gamse et al., 2005).
Nodal, a gene encoding a member of the transforming growth factor-beta superfamily, has an evolutionary conserved role in the development of organ asymmetries (Hamada et al., 2002; Warner et al. 2012; Yanagawa et al., 2011). Left sided Nodal genes expression starting at early somitogenesis is one of the first emergences of left-right asymmetry in fish and other organisms (Concha et al., 2003; Halpern et al., 2003). The unilateral distribution of Nodal signaling is caused by the Kupffer's vesicle (KV) or node in higher vertebrates.

Clockwise rotating cilia located in the inside produce a left-sided flow of morphogens (Tabin, 2006). Downstream to the morphogen flow, the nodal related gene *southpaw* (*spw*) is expressed exclusively in the left lateral plate mesoderm (LPM), the progenitor region of the internal organs. *Spw* mediated signaling does thereby not only determine the laterality of the intestines but is also crucially involved in the establishment of brain laterality. This is caused through the regulation of the left sided expression of Nodal related genes like *cyclops* (*cyc*)*, lefty1* and *pitx2* in the brain progenitor region: the anterior neural plate (ANP) (Long et al., 2003; Ohi and Wright, 2007; Liang, 2000). Other components of the pathway, like *one-eyed pinhead* (*oep*) and *schmalspur* (*sur*), are bilaterally expressed in the epithalamus and are competent to activate bilateral Nodal signaling (Concha et al., 2000; Liang et al., 2000).

It is likely that Nodal signaling is initially repressed in the ANP and subsequently de-repressed on the left side by Nodal-dependent signals deriving from the left LPM as the absence of Nodal activity in the LPM results in bilateral epithalamic Nodal expression (Carl et al., 2007; Inbal et al., 2007). Several signaling pathways like the Retinoic acid, the Notch or the Wnt/beta-catenin pathway seem to be involved in the timely and regional restriction of Nodal signaling activity. For example early alterations of the Notch pathway can cause the absence of asymmetric Nodal genes expression in the LPM what affects the laterality of internal organs (Raya et al., 2003, Niikura et al., 2006).

Nodal related genes are expressed in the anlage of the pineal complex and a left anterior region that could include habenular stem cells (Concha et al., 2000). Thus, the result of unilateral Nodal activity between 18 hpf and 24 hpf in the ANP is the diencephalic left-sideness (Concha and Wilson, 2001; Halpern et al., 2003).

In case of *situs inversus* Nodal signals are right-biased. Parapineal cells migrate to the right and the right habenula exhibits left-characteristic expression patterns while its counterpart on the left side develops right characteristics. Inhibition of Nodal signaling or bilateral Nodal genes expression results in a randomized handeness of the diencephalon (Concha et al., 2000). Half of the embryos exhibit the parapineal cells and the left characteristic habenulae subregionalization on the left side while the other half exhibit the parapineal and the left characteristic habenula on the right (Gamse et al., 2002; Gamse et al., 2003). That the left-characteristic habenula is even in reversal situation on the side of the parapineal may suggest that at least one structure influences the laterality of the other.

1.2.2 Symmetry-breaking signals

Symmetry-breaking signals allow the diencephalon to develop asymmetrically and thus to implement the defined lateralization. In case of altered symmetry-breaking signals both

habenulae develop double right- or double left-sided features (Carl et al., 2007, Aizawa et al., 2007).

Laser ablation experiments of the habenula and the parapineal organ revealed a dependency of each other for their proper development. Despite left-biased Nodal signals, the parapineal cells are not able to migrate to the left side after destruction of the left habenular progenitors. Conversely, ablation of the parapineal cells enables the left habenula to develop the fully penetrant left characteristic subregionalization, although the asymmetric neuronal production is not altered (Gamse et al., 2003; Concha 2003; Roussingé et al., 2009; Bianco et al., 2008). In rare cases in which the parapineal developed bilaterally, both habenulae exhibited left typical pattern (Gamse et al., 2003).

In spite of the fact that both structures need each other for their correct development the nature of interaction is poorly understood. By promoting the left-sided habenula situation on the one hand and ensuring the asymmetric habenula organization on the other, the parapineal could function as a transformation point of laterality and symmetry-breaking signals.

Nodal signals play a pivotal role in directing the habenular laterality. However, beside the lateralization defects caused by misexpressed Nodal related genes, Nodal pathway activity seems to promote the temporal asymmetry of habenular neurogenesis. Recent studies described that early born neurons appear symmetrically in both habenulae when Nodal is absent or bilateral (Roussingé et al., 2009). However, early symmetric patterning results in the loss of laterality but not in the loss of habenular asymmetry. It remains unclear why symmetric neurogenic progression does not result in the formation of symmetric habenulae.

A further signaling pathway involved in the diencephalic development is the Fibroblast growth factor (Fgf) pathway. Bilateral Fgf signals were identified to enable the parapineal to respond to left-guiding Nodal signals (Regan et al., 2009). In addition to the effect on the pineal complex asymmetry, the signaling pathway is involved in the habenula asymmetry establishment. Thus, *acerebellar* (*ace*) zebrafish mutant, which exhibits reduced Fgf8 signaling, develops symmetric habenulae (Regan et al., 2009). However, the habenulae in the mutant show a reduced expression of lateral and medial subnuclei marker indicating that Fgf signals could bias the neurogenesis of habenula per se and not specifically act on the asymmetry decision.

Notch signaling appears not only to be involved in early steps of lateralized development but also in later asymmetry establishing steps. It has been shown that components of the Notch pathway regulate the asymmetric neurogenesis of habenulae as the habenular differentiation relies on intact signaling. In its absence or enhancement the habenulae develop symmetrically (Aizawa et al., 2007).

Genetic hyperactivation of Notch affects the timing of neurogenesis and determines neuronal specificity. The delay in habenula cell differentiation results in the formation of bilateral large

medial and small lateral subnuclei, mimicking a double right-sided habenula phenotype. Conversely, the downregulation of the pathway in *mindbomb/ubiquitin ligase* mutants (*mib*) (Itoh et al., 2003) results in the development of bilateral symmetric habenulae with left-sided character. The symmetry is caused by the differentiation of precursors into equal numbers of lateral dHb neurons while the residual cells develop medial subnuclei characteristics at subsequent stages (Aizawa et al., 2007).

These results demonstrate that Notch signaling is a major component of the habenular asymmmetry establishment and its developmental timing. Given that just the Notch downstream gene *her6* was found to be slightly right-biased upregulated on RNA level (Aizawa et al., 2007), the question occurs how the seemingly uniform signaling mediates differences in the asymmetric processing of habenula neurogenesis and establishes thereby the asymmetric habenular structure.

The Wnt/beta-catenin signaling has been identified as being involved in a high number of decisions during the establishment of non-symmetric habenulae (Hüsken and Carl, 2012; Carl et al., 2007). The following chapter will give a detailed look inside the different roles of Wnt signaling during the regulation of diencephalic asymmetry development and the effects of its alterations.

1.3 Role of Wnt/beta-catenin pathway in the habenula development

The Wnt/beta-catenin signaling pathway, originally described as the wingless pathway in *drosophila*, is known to play a pivotal role in many aspects of embryonic development. The pathway is one of the fundamental signaling cascades that regulates cell proliferation, cell polarity and cell fate determination.

A current model of the pathway assumes that in the absence of the ligand Wnt a destruction complex resides in the cytoplasm, built up by components like Axin, GSK3 and APC. The complex binds, phosphorylates and ubiquitinates beta-catenin followed by the degradation of the protein through proteosomes. In the absence of beta-catenin, a Tcf/Groucho complex occupies and represses the Wnt target genes.

Conversely, the presence of the Wnt ligand induces, by its binding to the Frizzled/LRP receptor, the association of Axin with phosphorylated LRP. Hence, the destruction complex comes apart. Active beta-catenin replaces Groucho from Tcf to drive the target gene expression (reviewed in Clever and Nusse, 2012).

Wnt familiy members act as morphogens and are typically expressed at developmental boundaries (McMahon and Bradly, 1990; Holland and Graham, 1995; McGrew et al., 1995;

Crease et al., 1998). The activity of the Wnt pathway and thus the transcription of Wnt target genes is needed for the axis formation and regionalization of the vertebrate body including the nervous system. Mainly known to provide guidance information during dorso-ventral and anterior-posterior axis formation, its function in the establishment of the left-right axis just started to be uncovered (Zhang et al., 2012; Harvey et al., 2010; Yost, 1998; Geschwind and Miller, 2001; Carl et al., 2007; Rodríguez-Esteban et al., 2001).

The Wnt pathway was identified in several organisms to influence the development of visceral left-right asymmetries. Overactivation of the pathway in *Xenopus* and medaka fish cause a left-right reversal of the internal organs (Danos and Yost, 1995; Nascone and Mercola, 1997; Bajoghli et al., 2007). Furthermore, Wnt signaling is suggested to be a left determinant of Nodal activity in the LPM of chick (Rodriguez-Esteban et al., 2001). In the human brain the expression of the Wnt ligands Wnt2b, 7a and 7b were found to be slightly asymmetric distributed across the left-right axis although the functional reasons are unknown (Geschwind et al., 2001; Geschwind and Miller, 2001; Abu-Khalil et al., 2004).

Manipulations of the pathway and the absence of the repressor Axin1 in zebrafish revealed a multitude of developmental steps during which proper Wnt signaling is needed for the development of diencephalic asymmetry (Hüsken and Carl. 2012; Carl et al., 2007).

1.3.1 Early Wnt signals during late gastrulation and somitogenesis

The earliest reported function of Wnt/beta-catenin signaling so far in the establishment of habenular asymmetry is during gastrulation stage long before the expression of the Nodal related gene *spw* in the left lateral plate mesoderm (LPM) (Fig. 1.4; Carl et al., 2007).

Axin1, a well-characterized inhibitor of the pathway, has been reported to act at late gastrulation stage in the progenitor region of the brain, the anterior neural plate (ANP) (Houart et al., 2002). *masterblind* (*mbl*) mutants, carrying a mutation in the GSK3beta binding domain of Axin1 (Heisenberg et al., 2001), lost the asymmetric Nodal genes expression in the ANP but not in the LPM (Carl et al., 2007). Thus, the laterality of viscera and heart are not altered but the formation of the diencephalon is affected. Consistent with the early function of Axin1, artificial upregulation of Wnt signaling at late gastrula stage, by suppression of GSK3beta function through LiCl treatment, mimics the mutant phenotype and results in a bilateral Nodal genes expression exclusively in the diencephalon too.

This specific effect of early Wnt signaling alterations on Nodal genes expression exclusively in the ANP give rise to the hypothesis that Wnt signaling could repress a repressor of Nodal signaling there. A candidate that could mediate the repression of Nodal genes expression is the Six family transcription factor Six3 (Inbal et al., 2007). Six3 is a Wnt downstream gene (Lagutin et al., 2003), which acts at about the same stage in the ANP (Carl et al., 2002). The

loss of Six3 function results in a similar situation as the upregulation of Wnt during gastrulation: bilateral Nodal genes expression specifically in the ANP but not in the LPM. These findings let suppose that Wnt signals may repress Six3 in the ANP at late gastrulation stages and thereby unblock Nodal genes expression.

Furthermore, latest research has shown that Wnt signaling regulates the development of the Kupffer's vesicle (KV) at early somitogenesis (Caron et al., 2012; Schneider et al., 2010). Via the activation of Foxj1 expression Wnt signaling is needed for the proper generation of cilia. Altered Wnt signals at early somitogenesis influence thereby indirectly the laterality of Nodal genes expression and of the entire body patterning.

At mid-somitogenesis hyperactivation of Wnt signaling results in bilateral or reversed Nodal genes expression in the LPM and the developing epithalamus too (Carl et al., 2007) even though the KV starts to be degraded (Essner et al., 2005). Although Nodal genes are downstream targets of Wnt signaling in several developmental contexts, the mechanism how Wnt signaling is acting independently of the KV during the establishment of Nodal laterality remains unclear.

1.3.2 Late Wnt signaling during post-somitogenesis stages

In addition to its role in regulating Nodal and general laterality, Wnt signaling is crucially involved in the establishment of habenular symmetry per se.

The Wnt signaling mutant *mbl* develops the so-called double right-sided habenula phenotype, reminiscent of embryos with physically ablated parapineal cells or upregulated Notch signaling (Bianco et al., 2008; Concha et al., 2003; Gamse et al., 2003; Kuan et al., 2007; Carl et al., 2007; Heisenberg et al., 2001). The phenotype is characterized by symmetric habenular neuropil and symmetric expression of genes that are normally expressed asymmetrically. Thus, the *mbl* mutant develops an increased number of dHbm characteristic cells and a reduced number of dHbl neurons in the left habenula mirroring the right habenula. Furthermore, the laterotopic segregation of axons projecting to the IPN is lost since the majority of axons from both sides terminates in the ventral IPN (Carl et al., 2007).

Embryos lacking the function of the *adenomatous polyposis coli (apc*) gene, a known inhibitor of the Wnt/beta-catenin pathway like Axin1 (Hurlstone et al., 2003), exhibit a habenula phenotype similar to mbl mutant embryos. The similarity indicates that the upregulation of the Wnt/beta-catenin pathway in these two mutants is responsible for the lack of habenula asymmetry (M. Carl, personal communication).

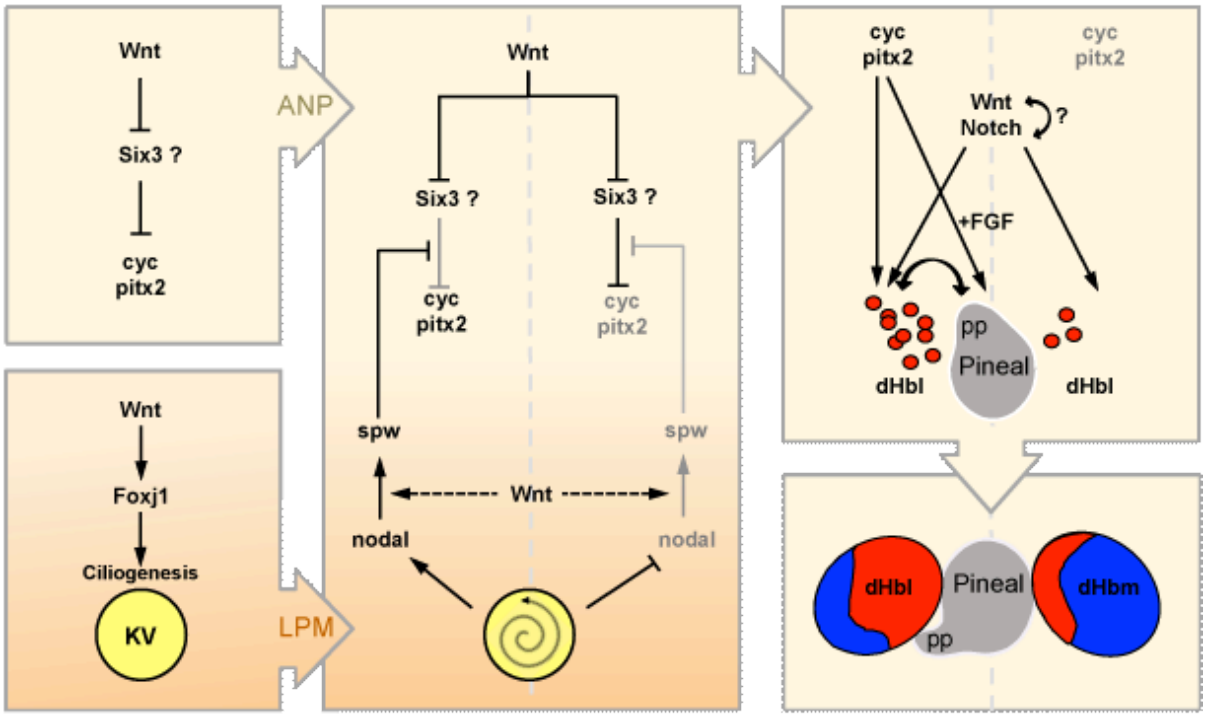

Figure 1.4: Functions of Wnt/beta-catenin signaling during the establishment of brain asymmetry (modified after Hüsken and Carl, 2012)**.**
The scheme is subdivided in early gastrulation stages of Wnt acting (left), intermediate stages during somitogenesis (center) and later morphogenetic stages (right). Black lines and lettering indicate an active state of a gene/pathway, grey coloring an inactive state and dotted lines a presumptive acting. During late gastrulation Wnt represses a repressor of Nodal signaling, likely Six3, in the ANP (anterior neural plate) and regulates thereby the left-biased activity of Nodal related genes *cyclops* and *pitx2* in the developing epithalamus. At a similar time of early development, Wnt signaling activates Foxj1 and promotes thereby the ciliogenesis in the Kuppfer's vesicle (KV). The proper formation of cilia causes a left-sided Nodal flow at somitogenesis in the LPM (lateral plate mesoderm). Upon the regression of the KV, Wnt is involved in the left-sided restriction of Nodal activity. At later stages the left-sideness of the Nodal activity directs together with FGF signals the migration of the parapineal (PP). In addition, Nodal and unknown parapineal signals regulate the laterality of the developing habenulae. Wnt and Notch signals influence the neurogenesis of the habenulae and cause its asymmetric subregionalization. All lateralization and symmetry-breaking signals together thus form a larger population of lateral characteristic cells (dHbl) and a smaller number of medial characteristic neurons (dHbm) on the left side regarding its counterpart on the right.

Transient enhancement of early Wnt signaling results in bilateral Nodal pathway gene expression but does not cause a broken habenular asymmetry (Carl et al., 2007). These results imply that Axin1, APC and thus Wnt signaling play an additional downstream role at later stages like the asymmetric habenular neurogenesis. The hypothesis is further strengthened by the similar habenula phenotype of upregulated Wnt and Notch signaling. It is also possible that the pathways act epistatically during the asymmetric neurogenesis as reported in a number of other developmental processes (Agathocleous et al., 2009; Hayward et al., 2008; Munoz-Descalzo et al., 2011; Nakaya et al., 2005).

The observation that the parapineal cells in Wnt mutants are still able to migrate to the left side of the brain allows to suggest if Wnt signaling may act directly in the habenula cells and enable them to receive inputs from the parapineal or if Wnt may act via the parapineal or adjacent structures to allow parapineal habenula interactions. A direct acting of Wnt/beta catenin signaling in the habenulae but also in the parapineal organ would be possible as the Wnt ligand Wnt8b has been shown to act via the Wnt/beta-catenin pathway and is expressed at the right time in the developing epithalamus (Carl et al., 2007).
However, similar to Notch signaling, no asymmetrically expressed Wnt pathway component has ever been identified in the developing epithalamus. How Wnt signaling functions as a symmetry-breaking signal, how it establishes different subregionalizations and how the epistatic relation to the parapineal cells derives cannot be answered by the current state of research.

1.3.3 The Wnt pathway component Tcf7l2

A small scale ENU-mutagenesis screen was performed in the Wilson lab at the UCL (UK) to identify novel genes that are involved in the determination of the habenular asymmetry. 301 mutagenized genomes were screened by *in situ* hybridization with a cocktail of markers asymmetrically expressed in the body. The gene *left-over/kctd12.1* (*lov*) was used as a marker of dHbl neurons and provided indications for a broken habenular asymmetry. Additionally, pancreas and liver marking RNA expression allowed the determination if the laterality of these internal organs and thus the overall laterality was altered due to a mutation (Fig. 1.5 A, A').
Two non-complementing mutations U754 and U763 were found to exhibit symmetric *lov* expressing habenulae. No other overt morphological defect distinguishes the mutants from wildtype, including an unaltered lateralization of intestines (Fig. 1.5 A, A'). Subsequent mapping localized the mutations to a 9.2Mb interval on LG12 that contains the *t-cell specific transcription factor 7l2* (*tcf7l2*).
Tcf7l2, former known as Tcf4, is a member of the Tcf/Lef family. These proteins act as transcriptional modulators of the Wnt/beta-catenin pathway (Arce et al., 2006; Shitashige et al., 2008; MacDonald et al., 2009). Tcfs can repress the expression of Wnt target genes by interacting with Groucho. Wnt induced beta-catenin stabilization leads to the displacement of Groucho and the formation of a Tcf/beta-catenin complex that can drive the transcription of Wnt target genes (reviewed in Clevers and Nusse, 2012; MacDonald et al., 2010).

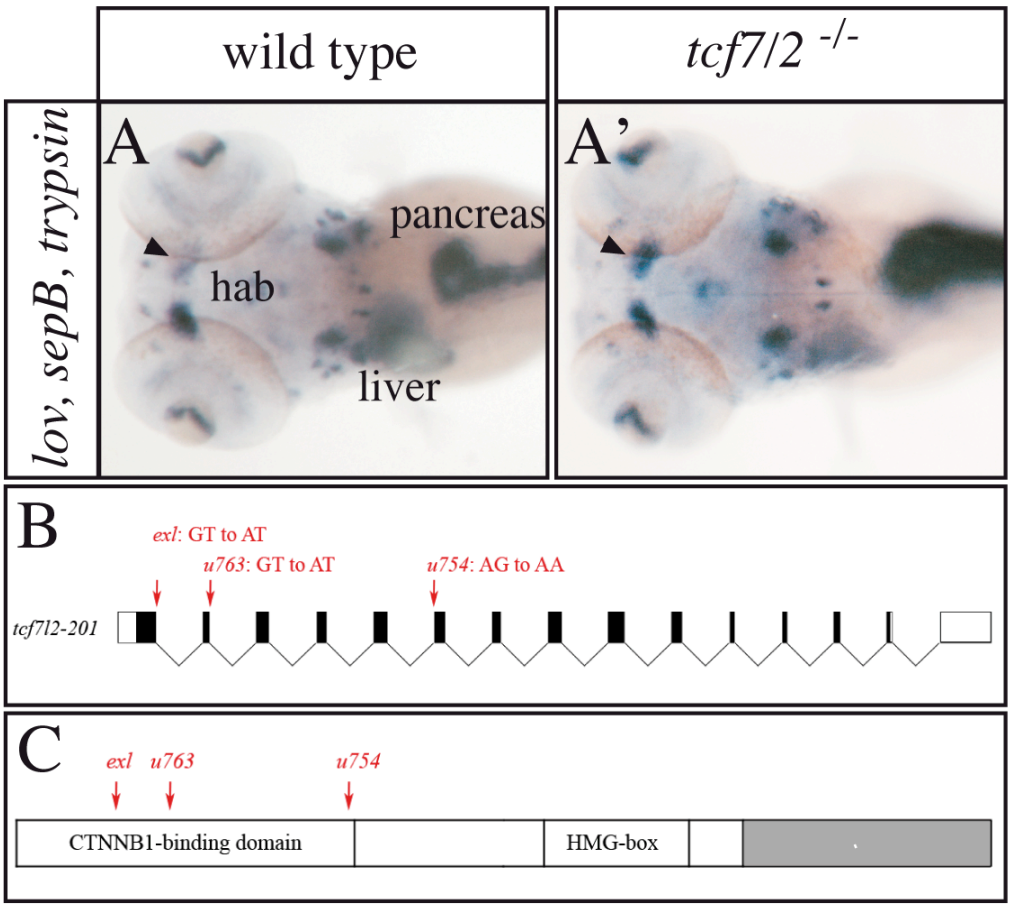

Figure 1.5: Three different *tcf7l2* mutations cause symmetric dHbl marker expression.

(A) Dorsal view on 4 dpf old embryos; anterior to the left. A marker gene cocktail (*lov* - marking dHbl neurons, *sepB* - marking liver, *trypsin* - marking pancreas) was used to identify mutations affecting the habenular asymmetry. The arrows indicate (A) normal and (A') bilateral *lov* expression in the right habenula. (B) The diagram of a *tcf7l2* variant shows the location of tcf7l2^{exi}, U754 and U763 splicing mutations. (C) Schematic showing of the Tcf7l2 protein and the locations at which the different mutations disrupt the protein. The grey box is indicative of the length variation of the protein C-terminal.

In zebrafish and mammals four Tcf genes are known: Tcf7, Tcf7L1, Tcf7L2 and Lef1. While Lef1 was mostly found to act as an activator of target gene transcription, Tcf7, Tcf7l1 and Tcf7l2 can additionally act as repressors (Arce et al., 2006; Hoppler and Kavanagh, 2007). This bipolar function allows Tcf7l2 to play a major role in several Wnt mediated processes like the development of the hindbrain and the gastro-intestinal tract (Korinek et al, 1998; Gregorieff et al, 2004). Furthermore, Tcf7l2 is strongly implicated in diseases like type II diabetes and breast carcinoma (Barker et al., 1999; Grant et al., 2006; Roose and Clevers, 1999).

Similar to the reported functions, zebrafish *tcf7l2* RNA is expressed in midbrain, hindbrain, anterior rhombomeres and the developing gut. The expression can also be found in the anterior neural plate and at later stages in the dorsal diencephalon indicating a function during the epithalamic development (Young et al., 2002).

The zebrafish *tcf7l2* gene is highly regulated at level of RNA splicing as it consists of 17 exons (Fig., 1.5 B; Young et al., 2002). The different variants of protein contain or lack domains that may cause its function as repressor or activator of Wnt target gene transcription. What is common in all protein variants is a N-terminal CTNNB1 binding domain that enables the interaction with beta-catenin and a high mobility group (HMG) promoting the DNA binding (Fig. 1.5 C).

Sequencing the genome of the recently identified U754 and U763 mutants revealed in the U754 mutant a splicer donor lesion at exon II and in U763 a splice acceptor lesion at exon VI of the *tcf7l2* gene (Fig. 1.5 B). Another mutant allele of *tcf7l2*, named *tcf7l2*^{exi}, was already reported harbouring a mutation in the splice acceptor side of exon I (Fig. 1.5 B; Muncan et al., 2007). Preliminary analysis of the *tcf7l2*^{exi} mutant phenotype confirmed a symmetric *lov* expression by the loss of Tcf7l2 function. All mutant alleles carry a point-mutation in the future CTNNB1-binding domain of Tcf7l2 and thereby probably cause the expression of a truncated protein (Fig. 1.5 C).

A main difference between the symmetric *lov* distribution of *tcf7l2* mutants and fish with upregulated Wnt/beta-catenin signaling is the type of broken asymmetry. While *mbl* mutants develop a bilateral symmetric weak *lov* expression, the *tcf7l2* mutants exhibit a symmetric large distribution. Even though a detailed analysis of the habenula situation in *tcf7l2* mutants is needed, the question arises whether the opposite dHbl cell distribution is caused by downregulated Wnt signaling. Furthermore, it remains to answer how Tcf7l2 mediated Wnt signaling is able to establish asymmetrically formed habenulae across the left-right axis.

2 AIM OF THE THESIS

Differences between the left and right side of the body are a universal feature in the animal kingdom and while their laterality has been studied intensively, the genetics underlying their asymmetric development are still poorly understood. In the brain of many vertebrates, the pineal complex and the habenulae develop asymmetric across the left-right axis. Even though the first pathways have been identified that underlie asymmetric habenular development, it remains unclear how they act differentially across the hemispheric borders to define different subregionalizations.

The aim of this thesis is to contribute to the understanding of the mechanism by which neuroanatomical asymmetries are established. Genetic, transgenic and imaging approaches were used to elucidate the function of the T-cell specific factor 7l2 (Tcf7l2) in the establishment of habenular asymmetry in the transparent zebrafish embryo. The following points were to be investigated:

- Characterization of the habenula phenotype caused by a *tcf7l2* loss of function mutation
- Signaling properties of tcf7l2 during establishment of habenula asymmetry
- Timely requirement of Wnt/beta-catenin activity during habenula establishment
- Spatial requirement of tcf7l2 mediated Wnt signaling
- Epistasis of Tcf7l2 and Nodal signaling during habenula establishment
- Epistasis of Wnt/beta-catenin signaling and parapineal mediated asymmetry

I identified the first asymmetrically expressed gene, with a crucial function in the establishment of brain asymmetry. Now it is possible to explain how Tcf7l2 regulates the unequal specification of habenular neurons along the left-right axis in relation to Nodal signaling and signaling from parapineal cells.

3 RESULTS

3.1 Phenotypic characterization of *tcf7l2* mutant

Starting point of my thesis was the notion that the loss of Tcf7l2 function results in the symmetric expression of the normally asymmetrically expressed gene *left-over/kctd12.1* (*lov*) marking dorsal habenula cells with lateral characteristics (dHbl).
For further phenotypic characterization of *tcf7l2*^{exi} mutant embryos, in the following called *tcf7l2*, the fish were analyzed with respect to their dorsal habenula subnuclei organization and their axonal projection to the interpeduncular nucleus (IPN). Since the *tcf7l2* mutant embryos are indistinguishable from wildtype fish all stainings shown in this thesis were done on genotyped embryos.
In order to find potential developmental defects that may cause the broken asymmetry, the distribution and number of habenular precursor and differentiating cells were determined in the mutant background.

3.1.1 *tcf7l2* mutants show left-right symmetric patterns of epithalamic neuron differentiation

An ENU-screen revealed a potentially broken asymmetry of the *tcf7l2* mutant dorsal habenulae. To confirm this indication and to find out if the mutation causes a fully penetrant and specific double-left sided phenotype, further investigations were needed.
In zebrafish the dorsal habenula (dHb) can be subdivided in at least two subdivisions: the lateral and the medial subnucleus. While a large lateral subnucleus and a small medial one build up the left dHb, the inverse situation can be found in the right dHb as it consists of a large medial subnucleus and small lateral one. Several transgenic and *in situ* hybridization markers are known that are left- or right-dominantly expressed and are used for the identification of neurons with lateral characteristic expression pattern (dHbl), building up the lateral subnucleus, or cells with medial characteristics (dHbm) of the medial subnucleus.
To analyze the lateral subnuclei situation the expression pattern of usually asymmetric expressed habenular genes *left-over/kcdt12.1* (*lov*; Gamse et al., 2005) and *cerebellum postnatal development associated protein 2* (*cpd2*; Gamse et al., 2003) were marked by *in situ* hybridization in 4 dpf old fish. According to the sizes of the lateral subnuclei *cpd2* and *lov* RNA are in wildtype more extensively present in the left habenular nucleus than in the right

(Fig 3.1 A, B; n(*lov)* = 31/33, n(*cpd2*) = 4/4). Single staining for *lov* in the *tcf7l2* mutant embryos confirm the already presented increased staining on the right side similar to the distribution on the left (Fig. 3.1 A'; n = 26). Also the left-biased *cpd2* expression is enlarged in the right habenula (Fig. 3.1 B'; n=6/7).

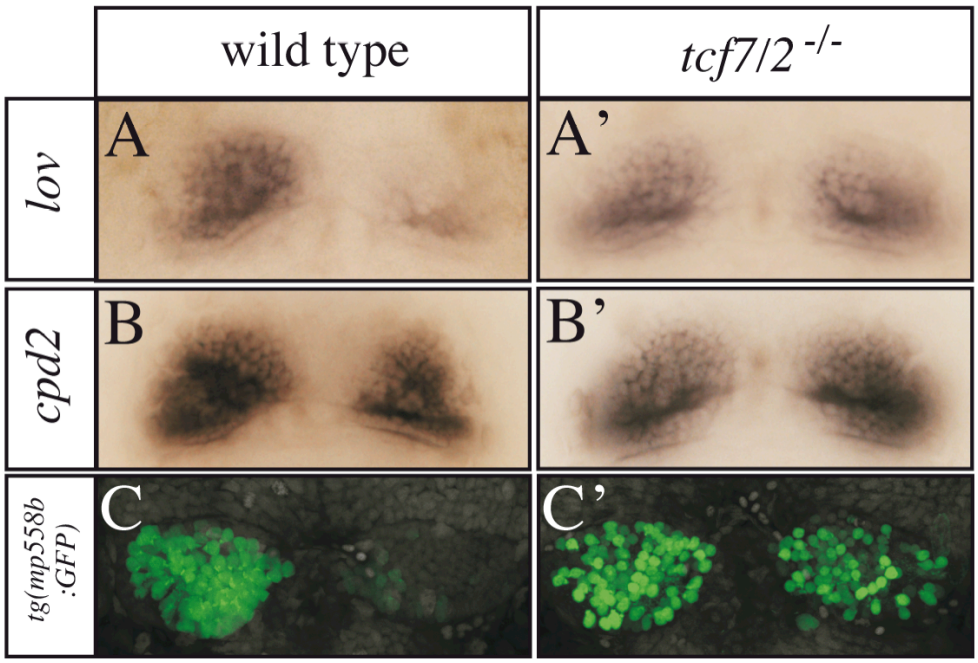

Figure 3.1: *tcf7l2* mutants exhibit double left sided lateral marker expression. Dorsal views focused on the diencephalic area of wildtype and *tcf7l2* mutant at 4 days of development (anterior on the top). DHbl characteristic cells were stained using the in situ hybridization markers *lov and cpd2* and the transgenic marker tg(mp558b:GFP) (subsequently stained by antibody). All markers exhibit a larger expression in the left habenula than in the right in wild type. *tcf7l2* mutant embryos exhibit more marker expressing cells in the right habenula indicating a double left-sided lateral subnucelus. The diencephalic overall structure of mutant fish, counterstained by nuclear marker in grey (C, C') is not distinguishable from wildtypes.

Similar to the left-typical *in situ* markers the novel transgenic line tg(mp558b:GFP) expresses GFP in differentiated dHbl neurons. Hence, transgenic embryos stained for GFP (green) and cell nuclei (grey) show a widespread distribution of mp558b:GFP expressing cells in the left habenula, while just a few GFP expressing dHbl cells can be found on the right side (Fig. 3.1 C; n = 35/36). Consistent with the lateral subnuclei markers, this asymmetric expression is broken in case of Tcf7l2 loss-of-function as the number of GFP expressing cells is strongly increased on the right side (Fig. 3.1 C'; n = 27/28). Thus, usually asymmetric lateral marker expression is in the *tcf7l2* mutant symmetric with left-sided character. Even tough the number of dHbl characteristic cells is increased in the *tcf7l2* mutant right habenula, the nuclear counterstaining does not show an enlargement of the overall anatomy indicating that the total number of cells is not increased (Fig. 3.1 C- C').

For revealing the medial subnucleus situation in the *tcf7l2* mutant, the expression pattern of the right-sided *in situ* hybridization markers *dexter/kctd8* (*dex*; Gamse et al., 2005), *transiently expressed glycoprotein* (*tag1*; Gamse et al., 2003) and the dHbm marker *right-on/kctd12.2* (*ron*; Gamse et al., 2005) as well as the transgenic marker tg(hsp70-brn3a:GFP) (Aizawa et al., 2007) were analyzed.

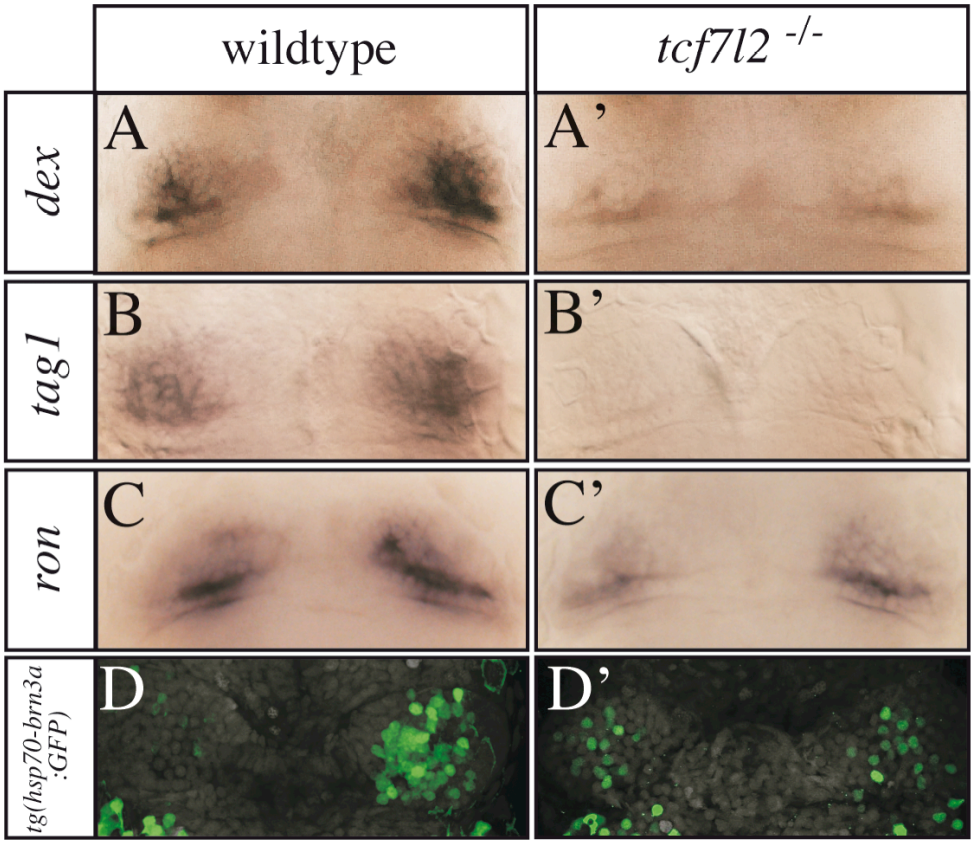

Figure 3.2: *tcf7l2* mutant exhibit symmetric medial and absent right-sided marker expression.
Dorsal views focused on the diencephalic area of wildtype and *tcf7l2* mutant at 3 (B) and 4 days (A, C, D) of development (anterior on the top). Right and medial characteristic cells were stained using the in situ hybridization markers *dex*, *tag1* and *ron* as well as the transgenic marker tg(hsp70-brn3a:GFP) (subsequently stained by antibody; nuclei counterstaining in grey). Markers exhibit a larger expression in the right habenula than in the left in wild type. *tcf7l2* mutant embryos exhibit absence of markers (A', B') or symmetric reduction (C', D') in *tcf7l2* mutants.

Wildtype fish exhibit the staining mainly localized in the right habenula and rarely in the left habenula (Fig. 3.2 A - D; n(*dex*) = 21/22, n(*tag1*) = 8/11, n(*ron*) = 5/6; n(tg(hsp70-brn3a:GFP) = 12/12). Contrasting, in *tcf7l2* mutants the asymmetric markers *dex* and *tag* are almost absent in both habenulae (Fig, 3.2 A', B'; n(*dex*) = 20/21; n(*tag*) = 7/7). *Ron* is reduced symmetricaly expressed on both sides of the brain in the mutant (Fig. 3.2 C'; n = 9/9). A similarly reduced symmetric expression pattern is given by the tg(hsp70-brn3a:GFP) expression in mutants. However, the transgenic marker has a more varying expression

pattern in *tcf7l2* mutant fish since most of the embryos exhibit a reduced symmetric expression while a few show a more wildtype characteristic asymmetric situation (Fig 3.2 D'; n = 8/12, 4/12 respectively). In total, dHbm markers are reduced in the right habenula to left-sided levels and the right-sided markers are almost absent. Thus, *tcf7l2* mutants do not develop any detectable habenular asymmetries.

The targeting of the habenular efferent axons into the IPN in the ventral midbrain reflects their subnuclear origin (Gamse et al, 2005; Bianco et al., 2008; Beretta et al., 2012). In wildtype the axons deriving from the left habenula (mostly dHbl; red) project preferentially into the dorsal IPN, while most axons from the right habenula (mostly dHbm; green) innervate the ventral IPN (Fig. 3.3 A).

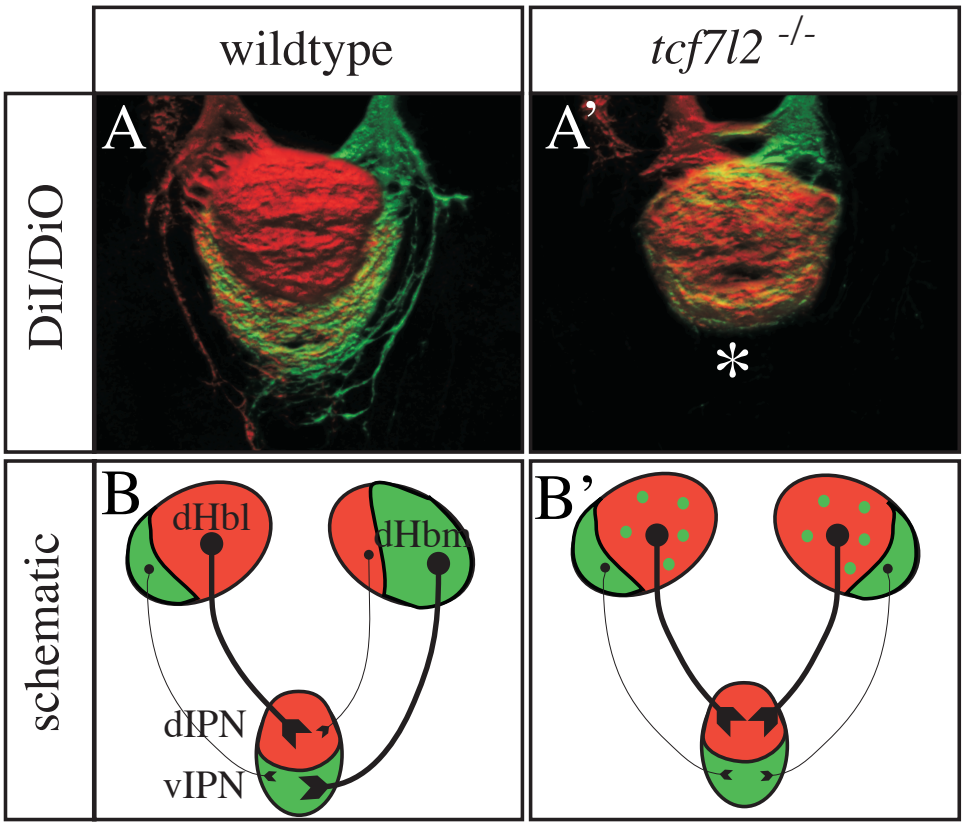

Figure 3.3: *tcf7l2* mutant develop symmetric habenulae with left-sided character symmetrically innervating the dorsal IPN.

Dorsal view focused on the interpeduncular nucleus (IPN) (A, A') and a schematic representation of the habenula – IPN circuit (B, B') of wildtype and *tcf7l2* mutant at 4 days of development (anterior on the top). DiI/DiO labelings for axonal projections from the left (red) and right (green) habenula into the dorsal (dIPN) and ventral (vIPN) IPN show that axons from both sides end in the dIPN in *tcf7l2* mutants. The asterisk marks the absence of innervation into the ventral IPN. The scheme represents the broken asymmetry in *tcf7l2* mutant having bilateral large lateral subnuclei of dorsal habenula (dHbl; red) innervating the dIPN and bilateral reduced medial subnuclei (dHbm; green) innervating the vIPN.

To confirm the dHb marker analysis, axonal bunch labelings were performed in *tcf7l2* mutant. According to the habenula situation, the habenular axonal projections into the IPN show a lack of dorso-ventral asymmetry. The loss of laterotopic segregation leads to a unidirectional innervation of the IPN. Right-sided and Left-sided axons terminate both in the dorsal part (Fig 3.3 A'; n = 6/6).

Thus, the marker and transgene expression as well as the innervation of the IPN confirm a specific and fully penetrant double left sided phenotype in absence of *tcf7l2* function.

3.1.2 Habenular neurogenesis is not overtly altered in *tcf7l2* mutant

Since the *tcf7l2* mutant develops habenulae of similar size and similar number of neurons as the wildtype, it is likely that the differentiation into cells with lateral or medial specification is rather altered than their production. To determine, which early processes may be affected in the Wnt signaling mutant, the expression of the habenula precursor maker *cxcr4b* (*C-X-C chemokine receptor 4b*) (Roussigné et al., 2009) as well as HuC/D expression in post-mitotic differentiated neurons were analyzed.

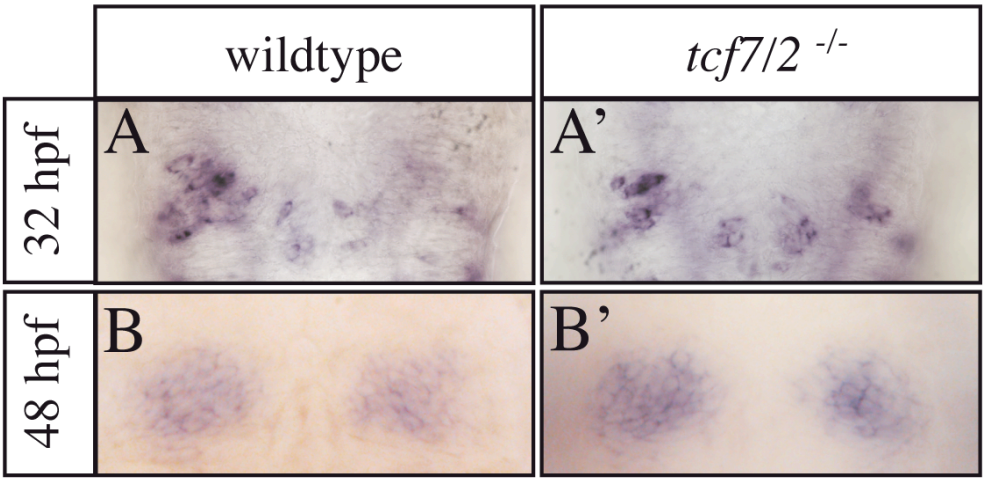

Figure 3.4: The expression of precursor cell marker *cxcr4b* is not altered in *tcf7l2* mutant.
Dorsal views focused on the diencephalic in wildtype, and *tcf7l2* mutant embryos stained for the habenular precursor marker *cxcr4b*; anterior to the top, age as indicated. Neither early asymmetric nor later symmetric precursor expression differs from wildtype in case of *tcf7l2* mutation.

The amount and distribution of habenula precursors at 32 hpf, marked by *cxcr4b*, are not affected in *tcf7l2* mutant (Fig. 3.4 A - A'; n(wt) = 37; n(tcf7l2) = 38). Although the *tcf7l2* mutant lost its asymmetric habenular organization, the early proliferation occurs asymmetrically and primarily on the left side, indistinguishable from wildtype fish.

Furthermore, at 48 hpf, a stage when proliferation is almost completed, wildtype and mutant embryos exhibit a similar expression of the habenular cell marker (Fig 3.4 B - B'; n(wt) = 12; n(*tcf7l2*) = 12).

For the analysis of the post-mitotic state the transgenic marker tg(HuC/HuD:GFP) (Park et al. 2000) was used for late stages while a HuC/HuD specific antibody (Barami et al., 1995) allowed to detect the first emergence of differentiating cells.

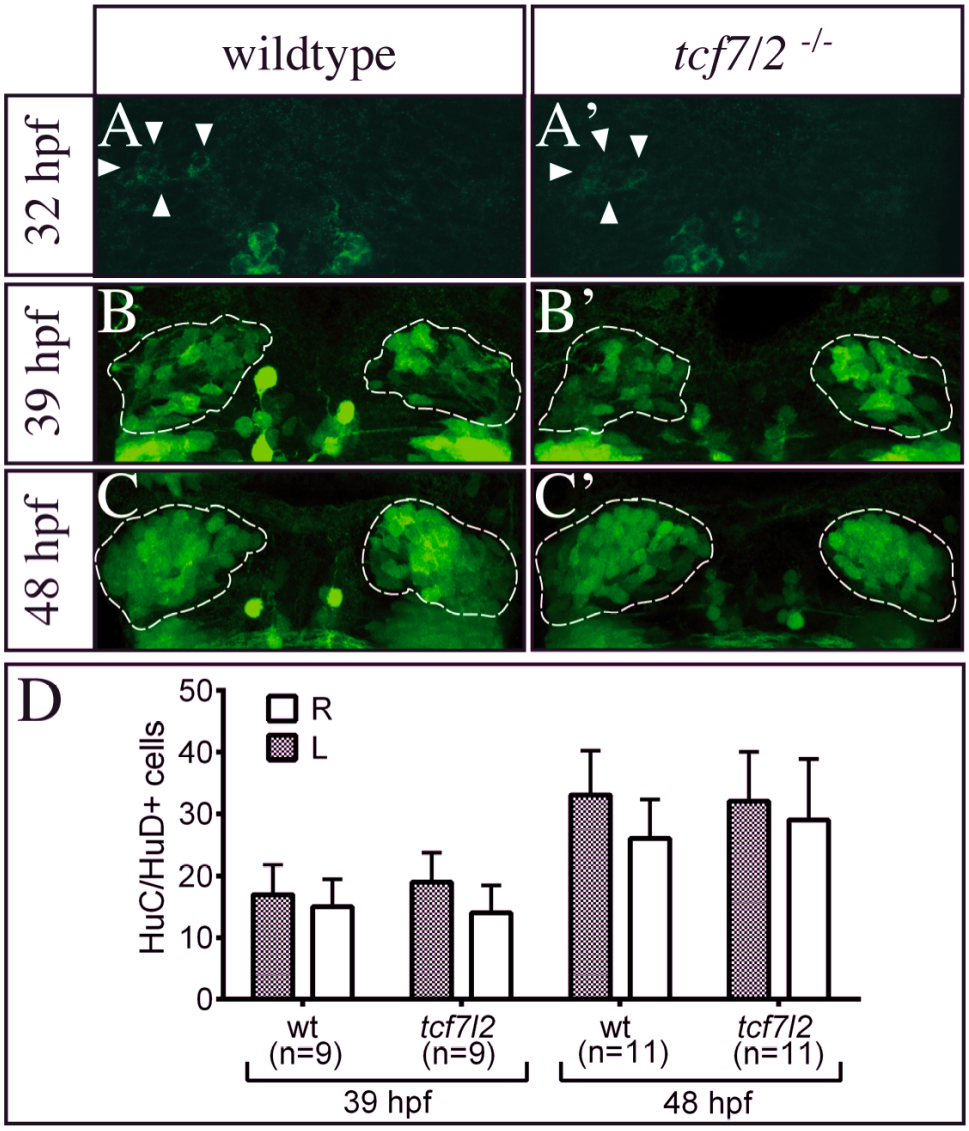

Figure 3.5: The early steps of habenula formation are not affected in *tcf7l2* mutants.

Dorsal views focused on the diencephalic area in wildtype, and *tcf7l2* mutant embryos; anterior to the top, age as indicated. An anti-HuC/D staining, marking the onset of differentiation, does not show a difference between wildtype and *tcf7l2* mutant (A, A'). The arrowheads indicate emerging HuC/HuD+ cells on the left side; HuC expression in habenulae is encircled. Similarly, the amount of GFP expressing cells in wild type and mutant tg(HuC/HuD:GFP) at 39 hpf and at 48 hpf are the same (B - C'). This was also confirmed by calculating the mean and SD of the number of GFP expressing cells (D).

In mutant and wildtype fish the first emergence of HuC/HuD is detectable at 32 hpf on the left side of the brain (Fig. 3.5 A - A'; n(wt) = 22; n(*tcf7l2*) = 10). Similarly, at 39 hpf the amount of HuC expressing neurons does not differ from wildtype to *tcf7l2* mutant. In both cases more cells express GFP on the left side (Fig. 3.5 B - C' n(wt) = 9; n(*tcf7l2*) = 9). A symmetric distribution of post-mitotic cells can be found at 48 hpf in wildtype and mutant fish (n(wt) = 11; n(*tcf7l2*) = 11). The counting of GFP expressing cells confirmed the equal numbers in wildtype and mutant fish at early and later stages (Fig. 3.5 D; detailed numbers in Appendix 7.3). Thus, the start of differentiation and its asymmetric processing is not overtly altered in *tcf7l2* mutant regarding the amount and distribution of newborn neurons marked by HuC/HuD.

3.2 Role of *tcf7l2* in the establishment of habenular asymmetry

Tcf family members are context dependent transcriptional modulators of the Wnt/beta-catenin pathway (Acre et al., 2006; MacDonald et al., 2009). In case of beta-catenin presence they act as activators of the Wnt target gene transcription whereas in absence of beta-catenin, Tcfs function as repressors of transcription. The *tcf7l2* mutant double left-sided habenular phenotype can consequently be the result of the repression or activation of Wnt target genes.

Another component of the pathway whose absence results in the development of symmetric habenulae with right-sided character is the Wnt/beta-catenin signaling inhibitor Axin1 (Carl et al., 2007). The opposing phenotypes support the idea that the loss of *tcf7l2* function results in a downregulation of Wnt signaling and that Tcf7l2 acts as an activator of the Wnt pathway in the process of habenular establishment. However, the function of Axin1 is linked to other pathways, including the planar cell polarity Wnt-pathway (PCP) and the Notch pathway and the protein can also act Wnt independently (Caneparo et al., 2007; DeStroopera and Annaert, 2001).

To investigate if the Axin1 phenotype depends upon the activator activity of Tcf7l2, the epistatic relationship between the proteins was determined by creating double mutant fish.

To prove furthermore if downregulated Wnt/beta-catenin signaling results in a similar phenotype to the *tcf7l2* mutant the signaling activity was transiently suppressed with the drug "IWR1endo" and heatshock treatments of transgenic fish carrying a dominant negative Tcf heatshock inducible construct.

3.2.1 *Axin1* acts upstream of *tcf7l2* during the formation of habenular asymmetry

masterblind (*mbl*) mutants, carrying a mutation in the GSK3beta binding domain of Axin1, have a enhanced Wnt signaling and develop symmetric habenulae with right-sided features (Carl et al., 2007; Heisenberg et al., 2001). Axin1 acts upstream of Tcf7l2 in the Wnt/beta-catenin pathway. However, its involvement in other pathways has been described too (Caneparo et al., 2007; DeStroopera and Annaert, 2001). To test if Axin1 acts specifically through Tcf7l2, the epistatic relationship between the mutations was analyzed in double mutant fish using the dHbl typical marker gene *lov* and the right typical marker gene *dex.*

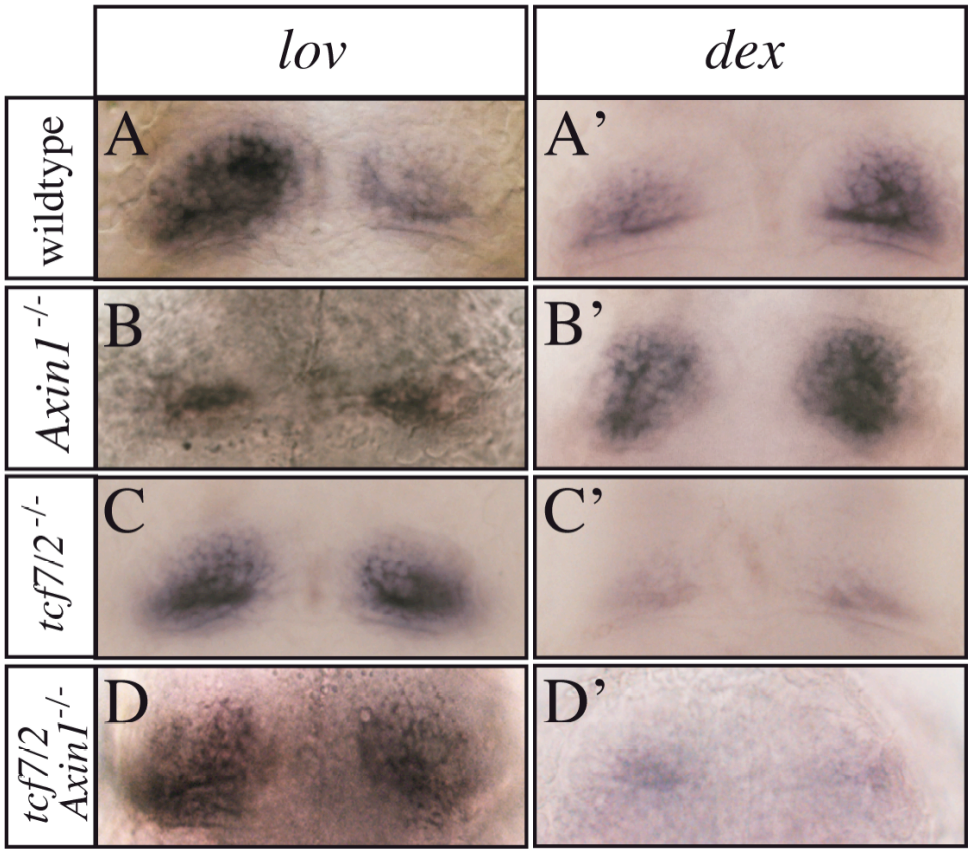

Figure 3.6: *Axin1* acts upstream *tcf7l2* during formation of habenular asymmetry. Dorsal views of 4 dpf wildtype, *Axin1/mbl*, *tcf7l2* single and double mutants focused on the dorsal diencephalon. Whole mount *in situ* hybridization of the asymmetrically expressed marker gene *left over* (*lov*) (A-D), marking lateral neurons, and the right-typical marker *dexter/kcdt8* (*dex* (A'-D') show in double and *tcf7l2* mutant symmetrically expanded *lov* expression and reduced *dex* expression in the right habenula.

As previously shown the dHbl neuron marker *lov* is expressed widespread in the left habenula and weakly in the right while the marker dex is weakly expressed on the left side but highly on the right in wildtype fish (Fig. 3.6 A, A'; Fig. 3.1 A; 3.2 A). In *Axin1* mutant background *lov* is symmetrically weak and *dex* symmetrically widespread distributed (Fig. 3.6 B, B'; n(*lov*) = 32, n(*dex*) = 20/21). The opposite situation can be found in *tcf7l2* mutants as

they express *lov* symmetric large and *dex* symmetric low or absent (Fig. 3.6 C, C'; Fig. 3.1 A'; Fig. 3.2 A').

In the double mutant the *lov* gene is expressed symmetrically at high levels while the *dex* expression is almost absent on both sides (Fig. 3.3 D, D'; n(*lov*) = 15/16 , n(*dex*) = 10/10). The habenular phenotype of *tcf7l2/Axin1* double mutants is thereby reminiscent of *tcf7l2* single mutants. These results provide evidence that *Axin1* acts upstream and specifically through *Tcf7l2* via the canonical Wnt pathway in the process of habenula asymmetry establishment.

3.2.2 Transient downregulation of Wnt/beta-catenin signaling mimics the *tcf7l2* mutant habenula phenotype

The observation that Axin1 acts upstream Tcf7l2 is consistent with the idea of an activating Tcf7l2 function in the Wnt/beta-catenin pathway during the habenular asymmetry establishment. The hypothesis implicates that the double left sided habenula phenotype is caused by a defective activation of the pathway. In order to prove that the downregulation of Wnt/beta-catenin results in left characteristic neuronal specifications in both habenulae, embryos were treated with the drug IWRendo, a known Axin stabilizer and thereby a suppressor of the pathway (Chen et al., 2009; Moro et al., 2012). This drug has been shown to block efficiently the pathway during fin regeneration as well in Wnt read-out line tg(7xTCF-XIa.Siam:GFP), carrying GFP under control of seven multimerized TCF responsive element (Moro et al., 2012). The inactive isoform IWRexo served as a negative control.

As reported Wnt activity is involved in a multitude of decisions during the establishment of non-symmetric habenulae during gastrulation and somitogenesis (Hüsken and Carl, 2012). Beside the investigation of the habenula phenotype caused by downregulated Wnt signaling, the late drug treatments further allow to determine if Wnt signaling can establish the habenular asymmetry exclusively during neurogenesis. Therefore, treatments were started at 32 hpf for an incubation of 16 hrs. By this transient manipulation of Wnt signaling unwanted effects of the early Wnt/beta-catenin activity can be avoided.

In situ hybridization with the dHbl cell population marker *lov* showed that the treatment of embryos with a substance, which suppresses Wnt signaling, results in a double left sided distribution similar to *tcf7l2* mutants. An increased *lov* expression can be found in the right habenula (Fig. 3.7 A'; n = 31/35). As expected, the control drug IWRexo did not influence the wildtype situation (Fig. 3.7 A; n= 21).

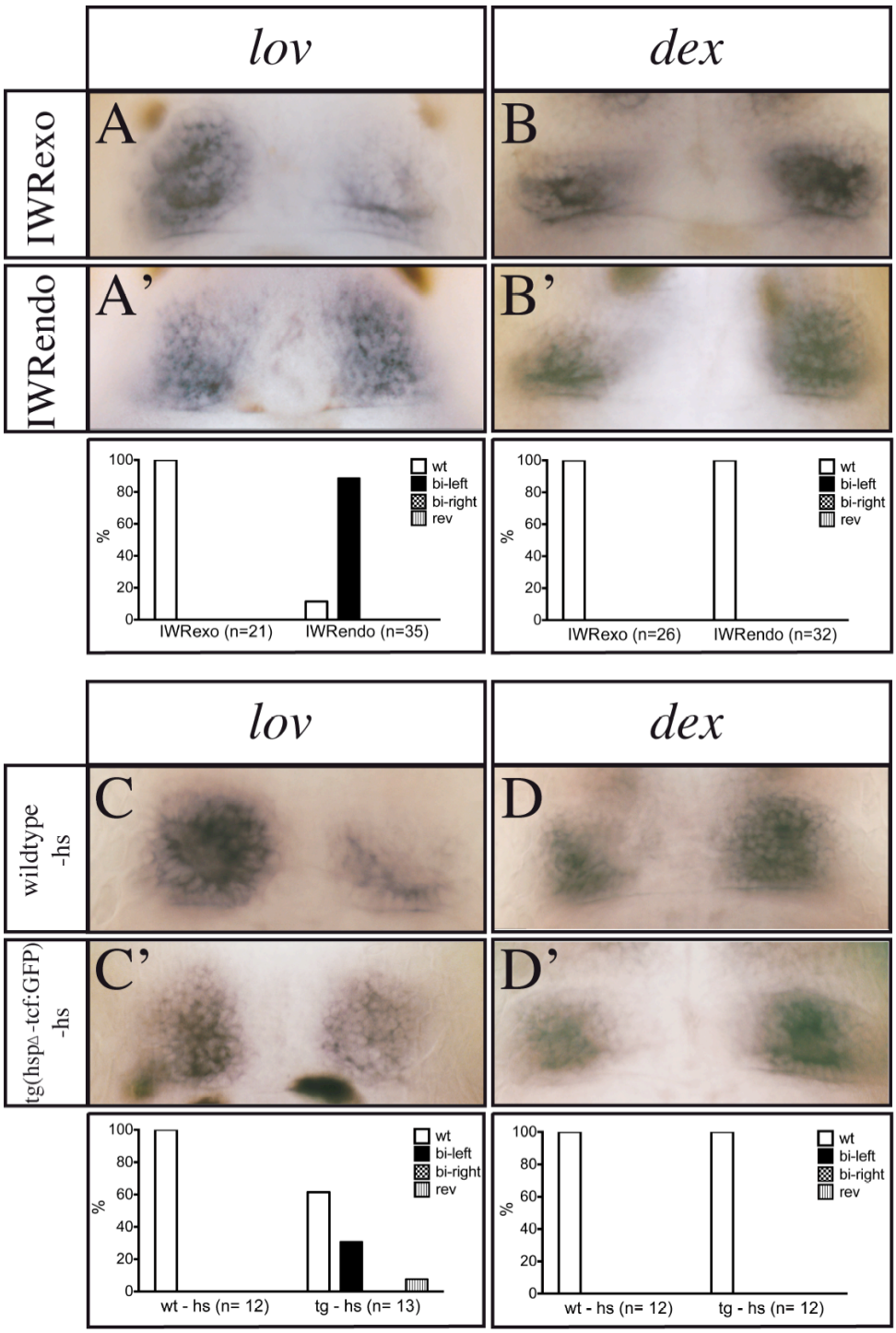

Figure 3.7: Transient inhibition of Wnt/beta-catenin signaling causes an increase of dHbl cells on the right side.

Dorsal view of 4 dpf embryos focused on the dorsal diencephalon. DHbl cells were marked by whole mount in situ hybridization for *left over* (*lov*) (A, A', C, C') and the right-typical marker *dexter* (*dex*) was used (B, B', D, D'). Wildtype embryos were treated with control drug IWRexo (A,B) and Wnt inhibiting drug IWRendo (A', B') (32hpf - 48 hpf) resulting in an increased right dHbl cell population by IWRendo. Heatshock treatment (33hpf) of tg(hsp70-Δ-tcf:GFP) fish (C', D') enlarge the dHbl marker expression on the right side too. (C, D). Neither drug treatments nor heatshock induction influenced the right-typical expression. The graphs illustrate the percentage of embryos showing wildtype (wt), reversed (rev), bilateral-left (bi-left), bilateral-right (bi-right) or no gene expression.

To confirm the result heatshock treatments of transgenic fish carrying a dominant negative Tcf heatshock inducible construct (tg(hsp70-Δtcf:GFP)) were performed (Weidinger et al., 2005). The activation of the transgene at 33 hpf results in a habenula phenotype comparable to the IWRendo treatments (Fig. 3.7 B'; n= 4/13). Although the transgenic double dominant neagtive Tcf expression influences the habenula asymmetry with low frequency as 31% of embryos develop the symmetric expression, it is a significant alteration as only 0 - 3% of non-transgenic wildtype embryos develop a symmetric doule left habenula (Fig. 3.7 C, n = 12; Fig. 3.1 A).

However, in situ hybridizations with the right-sided marker *dex*, which is expressed in dHbm subpopulation amongst other regions of the habenula (Gamse et al., 2005), showed that the downregulation of Wnt signaling by IWRendo and tg(hsp70-Δtcf:GFP) does not affect its asymmetric expression unlike the *tcf7l2* mutant (Fig. 3.7 B, B', D, D'; n(IWRendo) = 32/32; n(hs-tg) = 12/12).

To further understand the habenula phenotype of transient inhibited Wnt signaling drug treated embryos were analyzed with additional habenula markers. Similar to the dHbl cell population marker *lov* the expression of the transgene mp558b:GFP mimics the *tcf7l2* phenotype by symmetric widespread expression too (Fig. 3.8 A', n = 23/27). As exhibited with the marker *dex*, the dHbm cell marking tg(hsp70-brn3a:GFP) confirms the wildtype characteristic asymmetric expression (Fig. 3.8 B', n = 26/28).

Since the morphology of efferent axonal projections into the ventral midbrain can be used as a read-out for the habenula situation, axonal bunch labelings were performed in drug treated embryos. To only label those embryos showing the double left sided dHbl phenotype embryos exhibiting symmetric expression of the transgene tg(mp558b:GFP) were selected. Albeit the expression of the dHbm cell marker and the right-sided marker indicate an unmodified dHbm cell population of the right habenula, the majority of right sided axons innervate the dorsal IPN and mimic thereby the *tcf7l2* mutant phenotype (Fig. 3.8 C', n = 13/16). However a few axons still terminate in a more ventral position.

Thus, the phenocopying of the large dHbl cell specificity on the right side and the partial loss of laterotopic segregation of the IPN demonstrate that reduced activity of Wnt signaling leads to habenular neurons acquiring mainly dHbl fate.

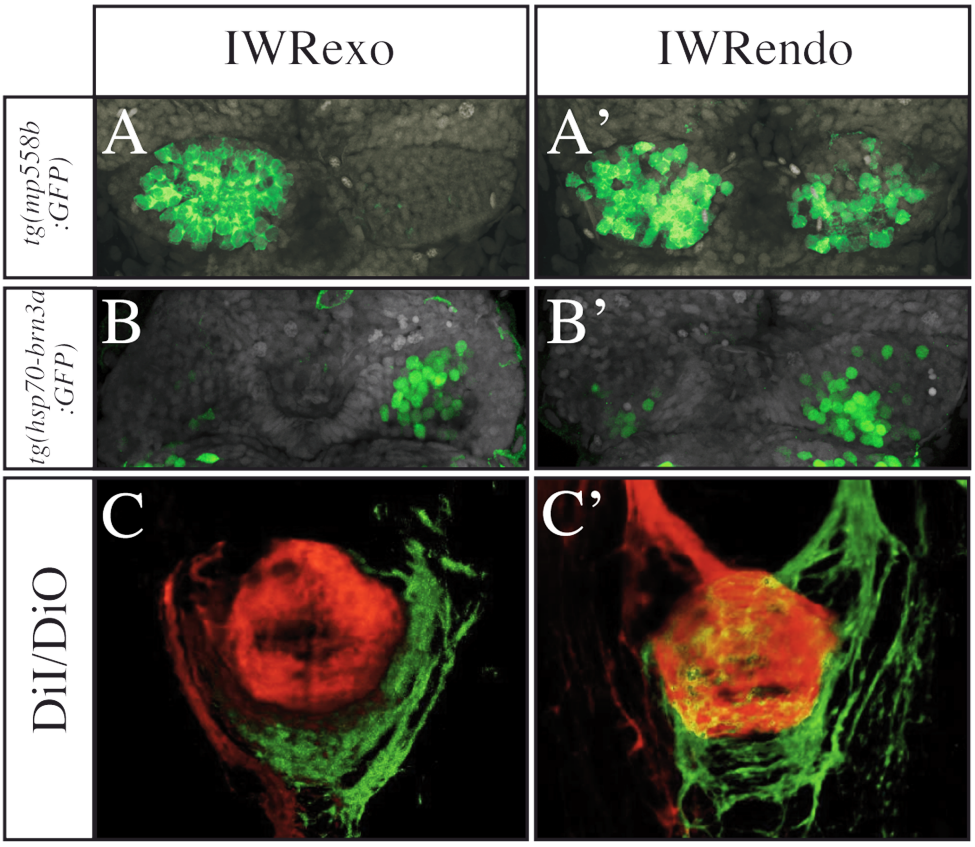

Figure 3.8: Artificial downregulation of Wnt/beta-catenin signaling with IWRendo mimic *tcf7l2* mutant phenotype.
Dorsal views focused on the diencephalic area (A-B'), the interpeduncular nucleus (IPN) (C, C') of 4dpf old transgenic or non-transgenic fish as indicated. The transgenic GFP expression are colored in green, counterstain for nuclei in grey. IWRendo treatment (32-48 hpf) results in more tg(mp558b:GFP) positive lateral habenula cells on the right side while the control treatment with IWRexo shows a unaltered asymmetric distribution (A-A'). The expression of tg(hsp70.brn3a:GFP) medial habenula cells is still asymmetric after incubation in IWRexo or endo (B, B'). (C, C') DiI/DiO labellings for axonal projections from the left (red) and right (green) habenula shows an overlap of left and right axons in the dorsal part of the IPN (yellow) in IWRendo treated embryos.

3.3 Function of Tcf7l2 mediated Wnt signaling in the establishment of habenular asymmetry

The investigations of the role of Wnt signaling points out that the activity of the pathway needs to be precisely regulated to allow the proper formation of habenular asymmetry - overactivation results in symmetric right-sided habenulae, while inhibition leads to the formation of symmetric left-sided habenulae. However, the mechanism by which Wnt signaling acts to establish differentially large neuronal subpopulations is still unclear as no

overt defect in the developmental processes was detectable in the *tcf7l2* mutant. The timely sequence of habenular cell proliferation and subsequent differentiation is well described and can be useful for uncovering the underlying process that cause the set up of habenular asymmetry (Aizawa et al., 2005).

Therefore a timing analysis of Wnt signaling activity was preformed. To find out where and when Wnt signaling is active, fish carrying the Wnt signaling read-out construct tg(7xTCF-Xla.Siam:nslmCherry), in the following called tg(7xTCF:mCherry), were analyzed by confocal timelapse microscopy. Furthermore, the established IWRendo drug treatments were used for timely modulations of the signaling pathway. Thereby the exact time slot when Wnt signaling is needed to establish the habenular asymmetry was found.

After the identification of the relevant time, a detailed expression analysis of *tcf7l2* RNA and protein was performed for these stages. The result further helps understanding if Wnt signaling is needed in habenula cells, acts indirectly onto these cells or may even be activated asymmetrically to establish different habenular subtypes along the left-right axis.

3.3.1 Wnt signaling is required during habenular cell neurogenesis

To investigate the activity of Wnt/beta-catenin signaling during the habenula development the mCherry expression of living embryos carrying the Wnt-read-out construct tg(7xTCF:mCherry) was followed from 30 hpf to 40 hpf by using confocal timelapse imaging (Moro et al., 2012). Two additional transgenes tg(foxD3:GFP) (Concha et al., 2003) and tg(flh:GFP) (Gilmour et al., 2002) were crossed into the Wnt read-out line for visualizing the pineal complex. As the habenulae nuclei are adjacent to the pineal cells their putative positions can be indicated by circles (Fig. 3.9). Wnt activity is detectable in the presumed habenulae region but also in the surrounding tissue. Starting at 34 hpf, mCherry expressing cells are localized in the precursor region and the number of Wnt active cells increases rapidly over time (Fig. 3.9 A - A''').

Notable is a lack of mCherry signal close to the pineal on the right side of the brain indicating asymmetric Wnt activity across the left-right axis (Fig. 3.9 A''; marked by asterisk). Left-right axis randomization, due to raising the embryos at lower temperature (Roussigné et al., 2009), randomizes overall the body laterality. In case of inverted brain laterality as marked by the parapineal cells, the Wnt activity gap is still on the opposite side of the parapineal (Fig. 3.9 B; n = 10). Hence, the asymmetric distribution of Wnt signal depends on the habenula laterality and not on the brain hemisphere.

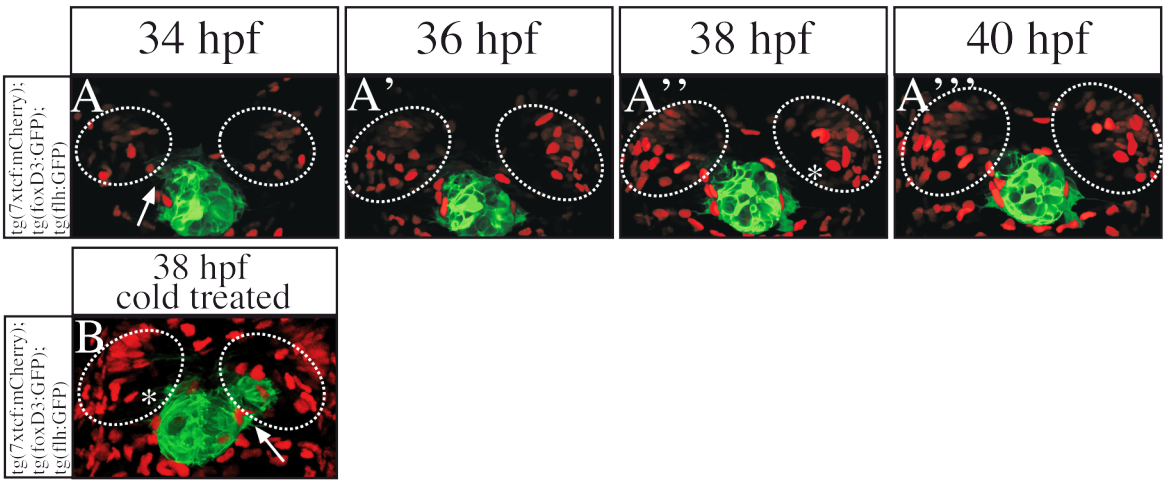

Figure 3.9: Wnt signaling is asymmetric active in the dorsal diencephalon as from 34 hpf.

Dorsal view focused on the dorsal diencephalon of living triple transgenic embryos. The transgenes tg(foxD3:GFP); tg(flh:GFP) mark the pineal complex. The presumed habenula region is encircled. First Wnt activity in the habenulae is detectable at 34 hpf by tg(7xTCF-Xla.Siam:nslmCherry) signal. (B) Embryos were raised at 22 degrees to randomize brain laterality. The parapineal cells are marked by arrow. Asterisks in A" and B mark the lack of mCherry expressing cells on the parapineal opposite side.

The start of Wnt signal activity at 34 hpf in the habenulae is overlapping with the already focused stage of habenula neurogenesis (Aizawa et al., 2007). To assess whether at this time Wnt signaling influences the establishment of the habenula asymmetry, the pathway was transiently inhibited in intervals of for one to four hours between 28 hpf and 55 hpf by drug treatments with IWRendo.

IWRendo incubations before 32 hpf and after 39 hpf causes only in a low number of fish the development of the bilateral widespread expression of the dHbl cell marker *lov* (<20%, Fig. 3.10 B - E; detailed numbers in table 7.1). 20 - 80 % of embryos increase the amount of dHbl cells in the right habenula by incubation between 33 hpf and 39 hpf. The peak of IWRendo efficiency is reached when embryos are treated only for one hour between 35 hpf and 36 hpf since 80% of treated fish exhibit an almost symmetric *lov* expression (n = 20, Fig. 3.10 E). This time is consistent with the stage when the first Wnt activity in habenula cells is detectable by using the tg(7xTCF:mCherry) read-out line.

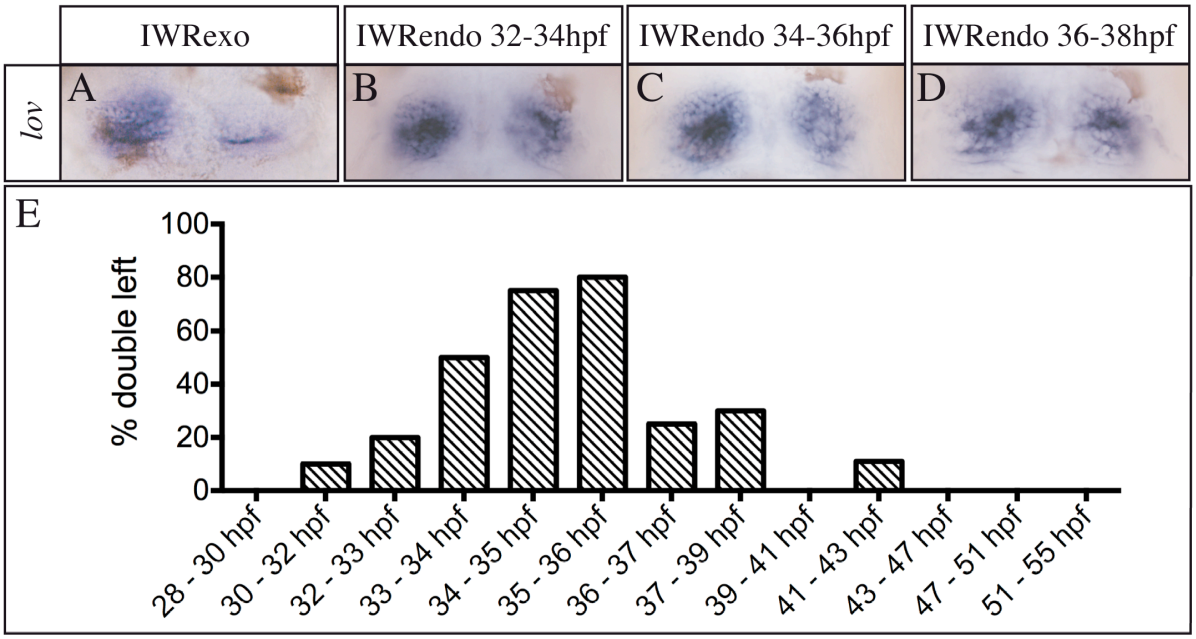

Figure 3.10: Artificial downregulation of Wnt signaling around 35 hpf results in an increased right dHbl subnucleus.
Dorsal views focused on the diencephalic area in drug treated wildtype fish (A-D). Embryos were incubated in an IWRexo solution, as control, and an IWRendo solution, to inhibit Wnt activity, for one to four hours (as indicated). Subsequently the embryos were analyzed regarding their dHbl phenotype at 4 dpf by *in situ* staining with the dHbl marker *left over* (*lov*). Drugs were tested from 28 hpf till 55 hpf (E). Only around 32 hpf till 39 hpf a significant effect was detectable. Incubation for one hour, from 35 hpf till 36 hpf, results in an increased number of right dHbl cells in 80% of embryos.

3.3.2 Tcf7l2 is asymmetric expressed along the left-right axis

In order to understand if the reported Wnt activity in habenula cells and function onto these cells around 35 hpf could be mediated by Tcf7l2, a *tcf7l2* RNA expression analysis was performed between 28 hpf and 42 hpf.

Consistent with previous reports, *tcf7l2* RNA appears to be distributed throughout most of the diencephalic area and covers large parts of the midbrain (Fig. 3.11, Young et al., 2002). The expression domain stretches out highly dynamic from more lateral, posterior and ventral parts of the brain into a medial, anterior and dorsal direction within this period of only 14 hours.

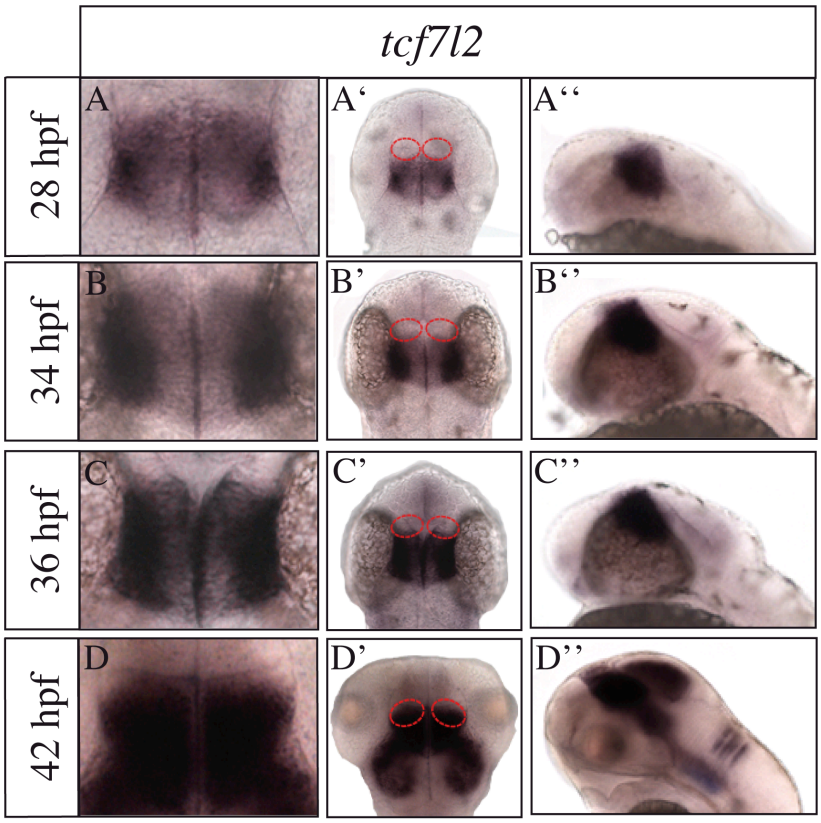

Figure 3.11: *tcf7l2* expression in the diencephalon during habenula development. Dorsal view (A - D') and lateral view (A'' - C'') focused on the diencephalon of 28 hpf, 34 hpf, 36 hpf and 42 hpf olf wildtype embryos. The dotted circles highlight the presumed location of the habenulae. In situ hybridization staining against *tcf7l2* shows a highly dynamic expression of the RNA in the diencephalic region.

It seems to be likely that the cells of the presumed habenula region, marked by red circles, start to express *tcf7l2* within this period (Fig. 3.11). However, the low resolution of *in situ* hybridization staining and the impossibility of three-dimensional analysis made it difficult to conclude about the exact starting point and distribution of *tcf7l2* expression specifically in the habenulae.

A human TCF3,4 antibody allowed to solve the problem as it exhibits a specificity against the zebrafish Tcf7l2 protein (Baker et al., 2001). As a control an antibody staining was performed in the *tcf7l2* mutant allel u754. In contrast to wildtype fish the antibody staining does not detect the protein in *tcf7l2* mutant (Fig. 3.12 A, B; n = 12/12 each). Furthermore, a co-labeling for *tcf7l2* RNA by fluorescence-*in situ* hybridization and for Tcf7l2 protein by the antibody staining was carried out (Fig. 3.12 C, C'). The in situ/immuno co-labeling exhibits a complete overlap of the protein and the RNA detection (Fig. 3.12 C'').

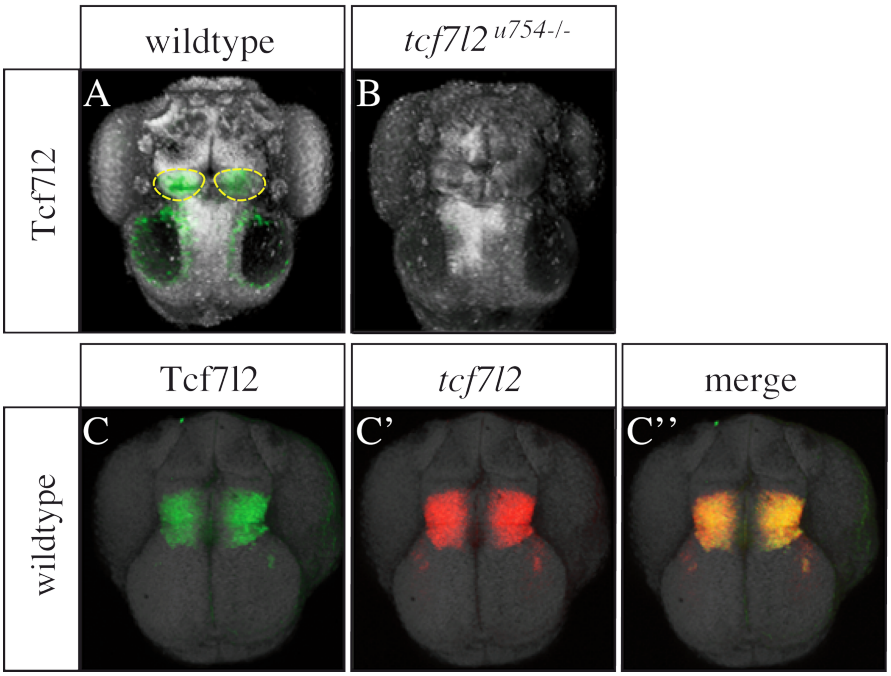

Figure 3.12: Anti-Human TCF3,4 detects zebrafish Tcf7l2 protein.
Dorsal view focused on the brain of 4 dpf (A, B) and 36 hpf (C) old embryos; anterior to the top. Unlike the detection in wildtype, the antibody does not give a signal in *tcf7l2 u754* mutants (A, B). Nuclei stainings (grey) allow to identify the habenular region by morphology (dotted circles, A). Immuno/fluorescent *in situ* hybridization staining shows that the antibody detected Tcf7l2 protein (C, green) and RNA (C', red) are completely overlapping (C'', yellow).

The tool to detect the Tcf7l2 protein by confocal microscopy, instead of using the *tcf7l2* RNA labeling, facilitated a detailed expression analysis: By nuclei counterstaining a morphological orientation for the border of the habenulae were given (for example Fig 3.12 A, dotted yellow circles). Additionally the high resolution enables to detect single cell signals.

Thus, anti-Tcf7l2 stainings were performed in tg(foxD3:GFP); tg(flh:GFP) double transgenic embryos (Fig. 3.13, n = 10 each stage). Between 32 hpf and 3 dpf the parapineal cells migrate first out of the medial positioned pineal complex to the left side and follows then a posterior-ventral direction (Concha et al., 2003). The transgenic expression in the pineal and parapineal supported thereby a staging of embryos according to the parapineal position.

To clearly visualize the Tcf7l2 expressing cells particularly in the habenulae the non-habenular Tcf7l2 positive cells were subsequently pseudo-colored in blue. The original pictures can be found in figure 7.2. For statistical analysis the Tcf7l2 expressing cells were counted for each stage (detailed numbers in Appendix 7.3). The percentage of Tcf7l2 positive cells on each side (Fig. 3.13 F) and the number of newly Tcf7l2 expressing cells on each side were calculated (Fig. 3.13 G).

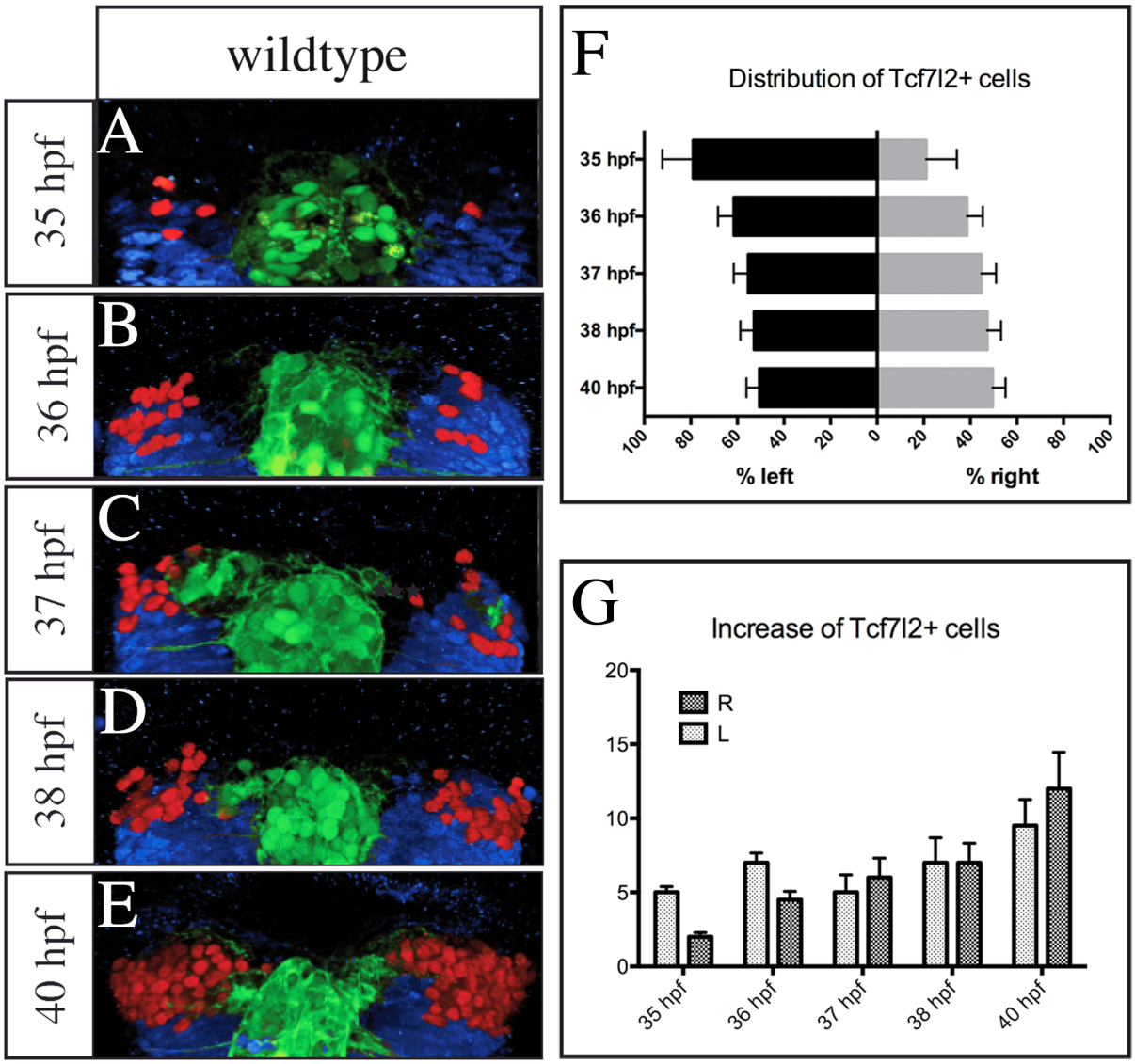

Figure 3.13: Tcf7l2 protein is asymmetrically expressed across the left-right axis. (A-E) Dorsal view focused on the habenulae; anterior to the top. Anti-Tcf7l2 and anti-GFP stainings were performed in wildtype embryos between 35 hpf and 40 hpf. The transgenic background tg(foxD3:GFP); tg(flh:GFP) was used for marking the pineal complex, which allows the staging of embryos. Habenular Tcf7l2 expressing cells are colored in red while more ventral TCF7l2 expressing cells are labeled in blue for clarity. A statistical analysis of the distribution of Tcf7l2 positive habenula cells across the left-right axis shows that the majority of Tcf7l2 expressing cells are on the left side of the brain in early stages (F; mean + SD). At later stages of development the Tcf7l2 positive cells are equally distributed along the left-right axis. The equal distribution occurs by a rapid increase on Tcf7l2 expressing cells on the right side as from 37 hpf while the amount of the right Tcf7l2 cells does not rise as much anymore (G, mean + SD).

Indeed, Tcf7l2 expression can be detected within the presumed habenulae as the signal appears in a dorsal cell layer laterally neighboring the pineal complex (Fig. 3.13 A - E). The protein is highly dynamic distributed over a period of only 5 hours, between 35 hpf and 40 hpf. In this timeframe Tcf7l2 is asymmetrically distributed along the left-right axis and

reminds in its expression pattern to the asymmetric dynamics of the habenular neuronal production (Aizawa et al., 2007).

Consistent with the time when Wnt signaling is active in the habenulae and when Wnt signaling is needed for the formation of diencephalic asymmetry, the first emergence of Tcf7l2 in the presumed habenular cells is detectable at 35 hpf (Fig. 3.13 A). At this early stage the protein is produced in cells of the left and the right habenulae. However, about 75% of Tcf7l2 expressing cells are located on the left side of the brain (Fig. 3.13 A, F).

Subsequently, the number of Tcf7l2 producing cells increases on both sides (Fig 3.13 A - E, G). The asymmetric distribution slowly equates within 5 hours and is nearly absent at 40 hpf when 51% of Tcf7l2 positive cells are on the left side but 49% on the right (Fig. 3.13 E, F). The calculation of newly Tcf7l2 expressing cells (Fig. 3.13 G) shows that this is caused by a stronger increase of Tcf7l2 producing cells in the right habenula as from 36 hpf. The right-sided increase of Tcf7l2 production leads to a decrease of the overall percentage distribution of Tcf7l2 positive cells on the left side. Thus, already at 37 hpf just 54% of the signal can be found in the left habenula (Fig. 3.13 C, F).

3.3.3 Tcf7l2 is expressed in habenular cells as they differentiate as dHb neurons

The proliferation and differentiation of habenula cells and the emergence of Tcf7l2 expressing cells start on the left side of the brain. The previous results showed that differentiation is likely affected by altered Wnt signaling. Thus, the hypothesis arises if Tcf7l2 mediated Wnt signaling could influence the asymmetric neurogenesis of habenula precursor cells. In order to understand the nature of Tcf7l2 expressing cells their developmental stage was analyzed.

To investigate if the dorsal Tcf7l2 positive cells are in fact habenular precursors a co-staining with the precursor marker *cxcr4b* was performed at 35 and 38 hpf (Fig. 3.14 A, B). The first Tcf7l2 expressing cells at 35 hpf on the left side are indeed habenula precursor cells as the antibody staining fully overlaps with the *in situ* marker (Fig 3.14 A; yellow signal marked by arrows; n = 6). Furthermore, *cxcr4b* expression is also detectable in cells without Tcf7l2 staining (red signal). At 38 hpf the co-labeling confirms that the most dorsal layer of Tcf7l2 expressing cells are in fact habenula cells: the Tcf7l2 positive cells clearly co-express *cxcr4b* (Fig 3.14 B, marked by dotted circles; n = 8). The ventral and posterior Tcf7l2 postive cells do not overlap with the habenula marker (green). Consitent with the already detected asymmetric Tcf7l2 distribution at 38 hpf, a high number of *cxcr4b* expressing cells co-express Tcf7l2 on the left sides of the brain while a smaller number of *cxcr4b* cells express Tcf7l2 on the right at this stage too.

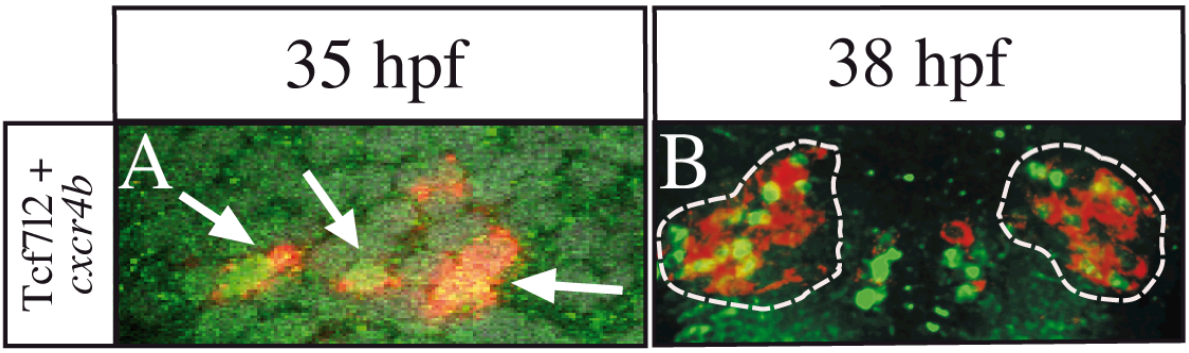

Figure 3.14: Tcf7l2 is expressed in habenula precursor cells.
Dorsal view focused on the diencephalon of co-stained wildtype fish for anti-Tcf7l2 (green) and the precursor marker *cxcr4b;* anterior to the top. 35 hpf old fish are additionally labeled with nuclei staining (grey). Overlapping signals are indicated by arrows (A) and by yellow coloration. The first dorsal Tcf7l2 expressing cells at 35 hpf co-express *cxcr4b* (A; focused on the left side of the brain; marked by arrows). Co-labelings of the dorsal layer (marked by dotted circles) are visible at 38 hpf too. At 38 hpf and 35 hpf precursor cells are detectable which do not express Tcf7l2 (red colored; A, B). However, all dorsal Tcf7l2 positive cells are labeled with the precursor marker.

Subsequently, a co-staining for anti-Tcf7l2 (red) and anti-GFP (green) in a transgenic line with the post-mitotic marker construct tg(HuC/HuD:GFP) was performed (Park et al., 2000). The staining should provide information if the Tcf7l2 expressing cells are differentiating neuronal progenitors.

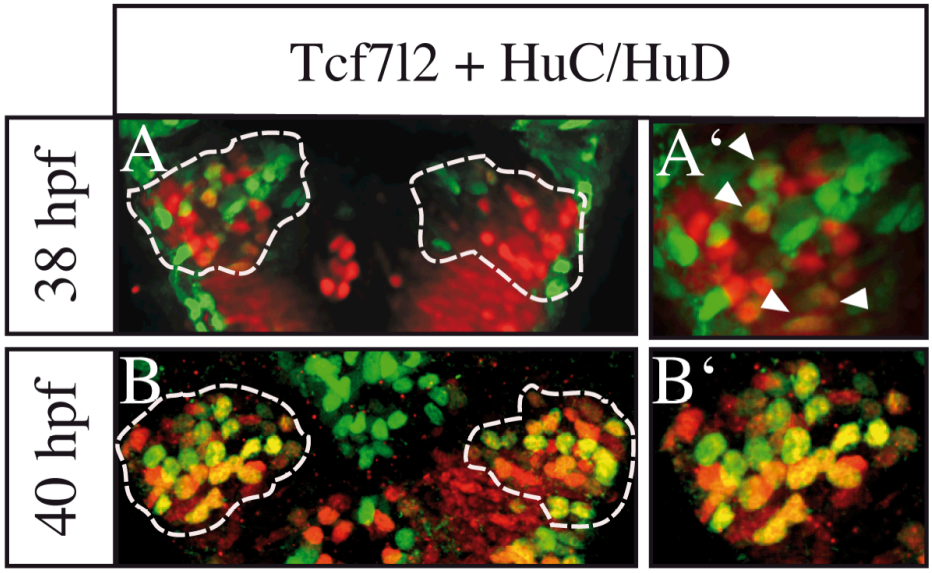

Figure 3.15: Tcf7l2 is expressed in differentiating habenula neurons.
38 hpf and 40 hpf old embryos co-stained for anti-Tcf7l2 (red) and the transgenic differentiation marker tg(HuC/HuD:GFP) (anti-GFP, green; A - B'). Dorsal view focused on the diencephalon (A, B) or on the left habenula (A', B'). Tcf7l2 and HuC/HuD expressing cells in the persumed habenula region are surrounded by dotted circles. Overlapping signals are indicated by arrowheads (A') and by yellow coloration. Tcf7l2 remains to be expressed in differentiating cells predominantly on the left side of the brain at 38 hpf (C) and symmetrically at 40 hpf (D). Single stainings of HuC/HuD or Tcf7l2 in the habenula are detectable at both stages.

At 38 hpf the first overlap of HuC/HuD and Tcf7l2 expression is detectable (Fig 3.15 A, A'; yellow signal, marked by the arrowheads). However, post-mitotic cells, which do not express Tcf7l2, are especially detectable on the left side. As previously reported the number of differentiating habenular cells and Tcf7l2 expressing cells is at this time higher on the left side than on the right side. The left-right asymmetry is also present regarding differentiating Tcf7l2 positive cells: 50% of the HuC/HuD-positive cells on both sides co-express Tcf7l2.
The asymmetric distribution still exists at 40 hpf (Fig. 3.15 B, B'; n=10 or detailed numbers in Appendix 7.3) but Tcf7l2 is almost present in all post-mitotic habenular neurons. Thereby the question occurred if Tcf7l2 is produced in all dHb cells within the course of time or if the protein is preferentially in cells with lateral or medial character.
To further investigate the nature of Tcf7l2 producing cells the expression of the protein was analyzed at 4 dpf with the dHbl cell marker mp558b:GFP and the dHbm cell marker brn3a:GFP. Additionally fish were counterstained for their nuclei to identify the habenula borders (Fig 3.16). At 4 dpf all dorsal habenula cells express Tcf7l2. Hence, tg(mp558b:GFP) and tg(brn3a:GFP) signals of the dHbl and dHbm neurons fully overlap with the Tcf7l2 distribution indicating that the presence of the protein in mature neurons is not an indicator of their subnuclear character.

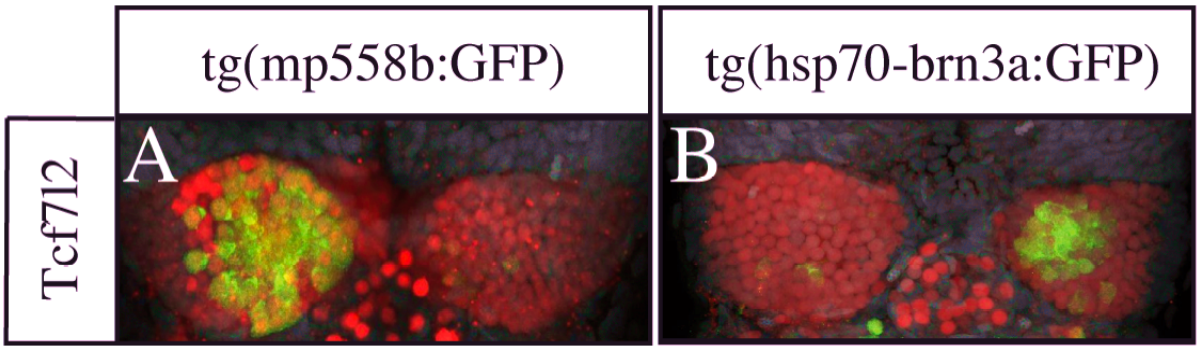

Figure 3.16: Tcf7l2 is expressed in the entire dorsal habenula at 4dpf.
Dorsal view focused on the habenulae of 4 dpf old fish. Transgenic fish for the lateral cell marker tg(mp558b:GFP) (A) and the medial marker tg(hdp70-brn3a:GFP) (B) were stained for GFP (green), Tcf7l2 (red) and nuclei (grey). The Tcf7l2 covers the entire dorsal habenula and shows thereby no preferential overlap with the lateral or medial subnuclei marker.

3.3.4 Tcf7l2 expression is influenced by altered Wnt signaling

Tcf7l2 appears to be asymmetrically expressed in differentiating habenular cells at that time point when Wnt signaling is needed to establish the habenular asymmetry. If the timely and spatial dynamics of Tcf7l2 expression has an influence on the differentiation of habenula

neurons, fish with broken habenula asymmetry could exhibit an altered Tcf7l2 distribution too. To test the hypothesis Tcf7l2 expression was analyzed in embryos with disturbed Wnt/beta-catenin signaling.

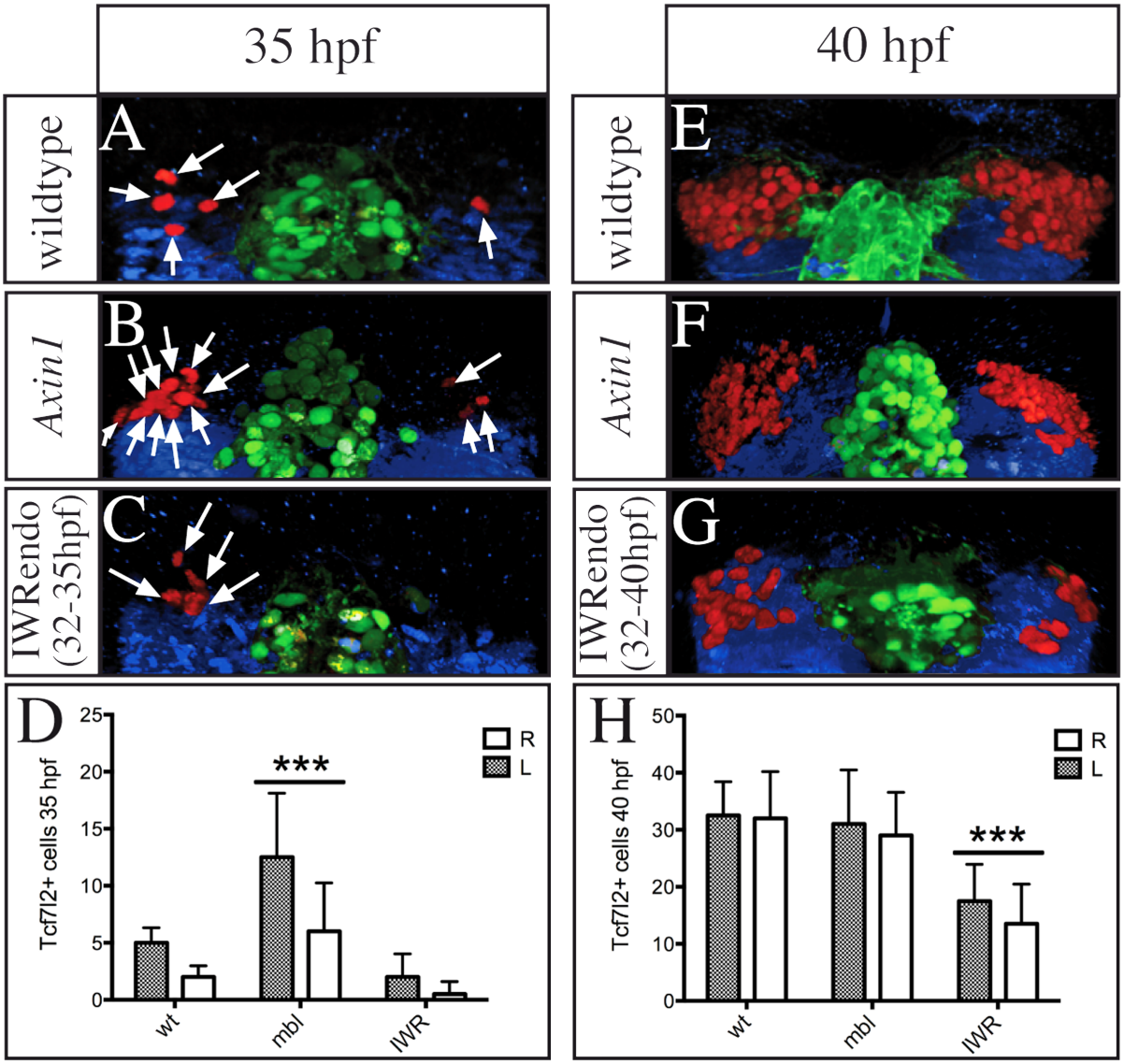

Figure 3.17: Tcf7l2 expression in habenular cells is regulated by Wnt signaling. Dorsal view focused on habenula; anterior to the top. Anti-Tcf7l2 (red) anti-GFP antibody staining in tg(foxD3:GFP); tg(flh:GFP) wildtype (wt; A, E), *Axin1* mutant (B, F) and IWRendo treated (C, G) embryos at 35 hpf (A - C) and 40 hpf (E - G). Non-habenula Tcf7l2 expressing cells are pseudo-colored in blue. Early Tcf7l2 expressing habenula cells are additionally marked by arrows. (D, H) Statistical analysis of the amount of Tcf7l2 positive habenula cells show mean values and standard deviation of TCF expressing left or right habenula cells in 10 embryos each. T-test was performed to identify significant differences between overall cell populations (indicated by stars). *Axin1* mutant embryos exhibit highly significant more Tcf7l2 expressing cells at 35 hpf (B, D; P = 2,23511E-05). On the contrary, IWRendo treated embryos show highly significant less Tcf7l2 positive cells at 40 hpf (G, H; P = 6,6062E-11).

Axin1 mutants, IWRendo treated fish and wildtype carrying the transgenes tg(flh:GFP); tg(foxD3:GFP) were stained at 35 hpf and 40 hpf for the Tcf7l2 (Fig. 3.17). For statistical reason the Tcf7l2 positive habenula cells of 10 embryos were counted separately on each side of the brain at each stage. Mean values and standard derivations were calculated and a student t-test was performed to recover significant differences (Fig. 3.17 D, H; for detailed numbers see Appendix 7.3).

Axin1 mutant fish exhibit symmetrically increased dHbm cell populations and a reduced number of dHbl cells caused by upregulated Wnt signaling (Carl et al., 2007).

The upregulation of Wnt/beta-catenin signaling does not alter the distribution of Tcf7l2 expressing cells. However the number is increased. In wildtype, an average of 6,5 cells expresses Tcf7l2 at 35 hpf, the time when mainly dHbl cells develop (Fig. 3.17 B). *Axin1* mutant fish exhibit a three fold higher number of 19,5 Tcf7l2 expressing cells (Fig. 3.17 D). The differences are confirmed by T-test as a considerable significant probability of $P = 2{,}23511^{-05}$ confirm that the cell numbers of wildtype and mutant do not originate from the same population. At 40 hpf no difference between wildtype and *Axin1* mutant is detectable (Fig. 3.17 F, H).

An opposite effect is detectable in IWRendo treated fish (Fig. 3.17 C, D, G, H). Caused by the *Axin1* stabilizing drug, Wnt signaling is downregulated in these fish. That results in the development of symmetrically increased dHbl cell populations.

Although the average of early Tcf7l2 is reduced to 1,5 cells at 35 hpf, the numbers do not pass the t-test (Fig. 3.17 C, D). However a significant decrease is verifiable at 40 hpf when mainly dHbm cells develop. On average 30,5 cells expresses Tcf7l2 in the habenulae in comparison to 58,5 cells in wildtype ($P = 6{,}6062^{-11}$; Fig. 3.17 G, H). These results may suggest that the Tcf7L2 expression is regulated by Wnt/beta-catenin signaling as the downregulation of the pathway causes a decrease and the upregulation an increase of Tcf7l2 expressing cells.

3.4 The epistatic relation of Tcf7L2, Nodal and parapineal signals

The results support the hypothesis that Tcf7L2 mediated Wnt/beta-catenin signaling influences the neurogenesis of habenula progenitors. It is questionable how the habenula asymmetry is established by Wnt signals across left right axis and which other lateralized signals could be involved.

The laterality of brain asymmetry, in particular the sidedness of habenulae as well as the migration of parapineal cells to the left is dependent on Nodal signaling (Concha et al., 2003;

Gamse et al., 2003). Early Nodal signals as well as the distribution of first Tcf7l2 proteins are left-biased, which raised the possibility that the initiation of the Tcf7l2 expression depends on the Nodal pathway. Insights into the question were obtained by the determination of Nodal laterality in *tcf7l2* mutants and by the investigation of the effect of altered Nodal signals on the early Tcf7l2 expression.

The Parapineal cell cluster migrates in parallel to the onset of asymmetric Tcf7l2 to the left side of the brain and influences the habenula cell differentiation. Laser ablations of the cell cluster results in a double right-sided habenula phenotype reminiscent to *Axin1* mutants (Gamse et al., 2003; Concha et al., 2003; Bianco et al., 2008). Given that the parapineal cell migration in *Axin1* mutants is largely normal (Carl et al., 2007), Tcf7l2 mediated Wnt signaling may be involved in the communication between the parapineal cells and the habenula cells on the left side of the brain. In order to understand the dependency of the structures, the parapineal position was analyzed in case of downregulated Wnt signaling in the *tcf7l2* mutant and conversely the mutant habenula phenotype was analyzed in the absence of parapineal cells. Furthermore, the expression analysis of Tcf7l2 was performed in parapineal-ablated fish.

3.4.1 Asymmetric Tcf7l2 expression is Nodal independent

Nodal signals influence the laterality of the habenulae but not the asymmetry. The activity of Nodal-related genes can be altered by unproper Wnt/beta-catenin signaling (Carl et al., 2007). To test if in the case of Tcf7l2 loss-of-function Nodal gene expression in the lateral plate mesoderm (LPM) and the anterior neural plate (ANP) is still left-sided, *in situ* hybridizations for the Nodal pathway genes *southpaw* (*spw*; Long et al., 2003) and *paired-like homeodomain transcription factor 2* (*pitx2*; Essner et al., 2000) were performed at 24 ss (Fig. 3.18).

Even though Nodal gene expression correlates with Wnt signals in the brain, the *tcf7l2* mutation and thereby the probably downregulated Wnt/beta-catenin signaling does not influence the presence of left-sided of Nodal gene expression neither of *spw* in the lateral plate mesoderm (Fig. 3.18 B, B') nor of *pitx2* in the developing brain (Fig. 3.18 B, B'). The defects of altered Wnt signaling by the loss of Tcf7l2 do not affect the early determination of left-biased Nodal activity.

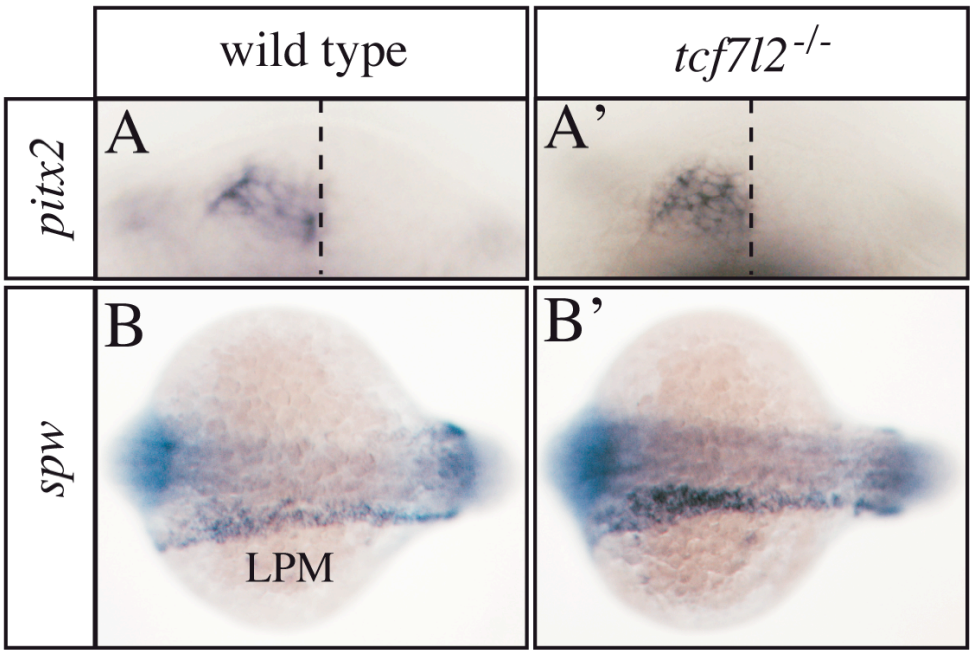

Figure 3.18: Nodal gene laterality is not altered in *tcf7l2* mutants.
Dorsal view on ANP (anterior neural plate; A, A') and LPM (lateral plate mesoderm; B, B') of wildtype and *tcf7l2* mutant fish at 24s. Embryos were stained by *in situ* hybridization for the nodal pathway genes *pitx2* (A) and *spw* (B). Midline is indicated by dotted lines. (A) anterior to the top - (B) anterior to the left. Both genes are in wildtype and mutant exclusively expressed on the left side.

To test whether the left-biased emergence of Tcf7l2 expressing cells is directly regulated by left-sided Nodal signaling or indirectly by defined brain laterality, Nodal signaling and thus the laterality was manipulated in early stages of development. The left habenula and the left-sided parapineal are always concordantly established and mark the sideness of the brain hemispheres (Concha et al., 2003). Thus, parapineal position was marked by the transgenes tg(foxD3:GFP); tg(flh:GFP).

One way to randomize the laterality of Nodal pathway components is to raise embryos for 16 hours after fertilization at 22 degrees (Roussigné et al., 2009). 40% of coldtreated embryos developed an inversed laterality. In addition, the first Tcf7l2 expressing cells at 35 hpf follow the altered sideness as they are always on the same side as the parapineal cells (Fig. 3.19 B, E; n = 10).

Symmetric or absent Nodal activity does not influence the habenular asymmetry but affects its laterality. By morpholino injection against *no tail* (*ntl*) the unilateral Nodal gene expression was altered into a bilateral or absent signal (Concha et al., 2000; Nasevicius and Ekker, 2000). As a consequence 50% of morphants show an outgrowing parapineal on the right side while the remaining fish developed a left-orientated cell cluster (Fig. 3.19 E). The Tcf7l2 expression remains asymmetric and the majority of first Tcf7l2 positive cells are again on the

same side as the parapineal cells (Fig. 3.19 C, E; n = 10). However, the emergence of first Tcf7l2 expression is slightly delayed at 37 hpf.

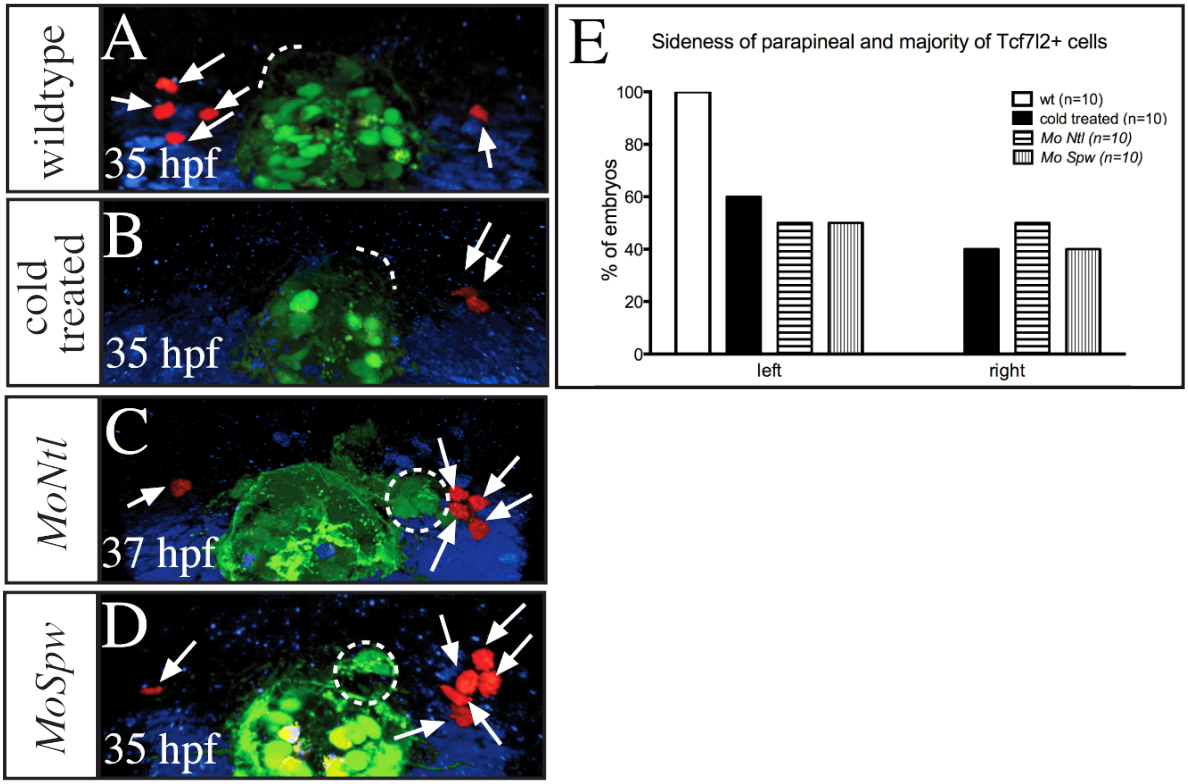

Figure 3.19: Altered Nodal signaling does not influence asymmetrically Tcf7l2 distribution.
Dorsal view focused on the diencephalon of embryos carrying the transgenic pineal complex marker of tg(flh:GFP); tg(foxD3:GFP) (A - D). The fish are stained against GFP (green) and Tcf7l2 (red - habenula cells; blue - non-habenula cells). Altered Nodal signaling, by raising embryos for 16 h at 22 degrees (randomized Nodal; cold treated; B), morpholino (Mo) injection against *no tail* (*Ntl;* bilateral or no Nodal; C) or *southpaw* (*Spw*; no Nodal; D), results in the loss of brain and Tcf7l2 expression laterality. First cluster of Tcf7l2 positive cells (wildtype (wt), coldtreated MoSpw at 35 hpf, MoNtl at 37 hpf) are always on the side of parapineal (PP) cells (A - E; cells marked by arrow, PP position indicated by dotted line/circle).

To confirm the data, the effect of the blocked Nodal signals was tested by an injection of a morpholino targeting the Nodal related gene *southpaw* (*spw*) (Long et al., 2003). Consistent with the previous results, the absence of southpaw protein expression or the absence of Nodal signals does not influence the early asymmetric Tcf7l2 expression but its laterality. In this case 40% of embryos have a right-directed parapineal migration linked with a right-biased expression of first Tcf7l2 expressing cells at 35 hpf (Fig. 3.19 D, E; n =10). In case of left-sided parapineal migration the majority of early Tcf7l2 positive cells are on the left side too (40%).

3.4.2 The absence of Tcf7l2 function renders parapineal cell signals redundant

The habenulae and the pineal complex need each other to develop their asymmetries. In case of parapineal absence the number of dHbl cells does not increase in the left habenula. More dHbm cells arise instead, resulting in the symmetric double right-sided phenotype reminiscent to *Axin1* mutant fish. Conversely, the parapineal is not able to migrate out of the pineal to the left side of the brain when left habenula are absent (Gamse et al., 2003; Concha et al., 2003).

The fact that the *tcf7l2* mutants develop the double left-sided habenula phenotype leads to the question if the parapineal exhibit a disturbed migration caused by bilateral left habenula signals. This question was answered by analyzing the parapineal position in mutant embryos carrying the transgenic pineal complex maker tg(foxD3:GFP). As in wildtype anti-GFP staining in genotyped 2 dpf old embryos show a clear left-sided signal of parapineal cells pseudo-colored in red for clarity (Fig. 3.20 A, A'; n=10).

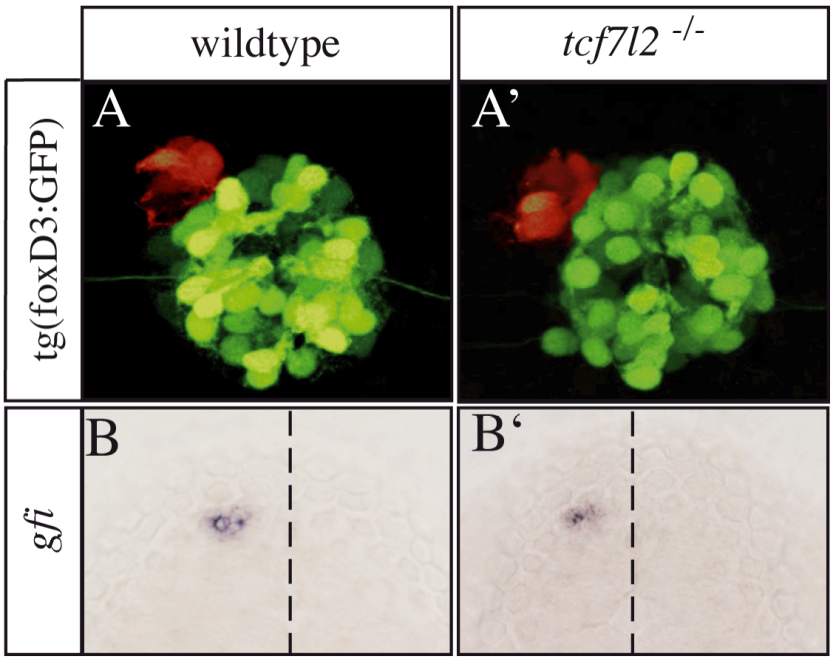

Figure 3.20: Left-directed parapineal migration is not altered in *tcf7l2* mutant.
Dorsal view focused on the pineal complex of transgenic 2 dpf wildtype and *tcf7l2* mutant embryos (A, A') and *in situ* hybridization stained embryos against *gfi*. Anti-GFP staining of the transgenic expression tg(foxD3:GFP) marks the pineal complex consisting of the pineal (green) and the parapineal (pseudo-colored in red). In wildtype and mutant background the parapineal is located on the left side of the brain. *In situ* stainings detect the parapineal in both cases on the left side too (midline marked by dotted line).

For further confirmation an *in situ* staining against the parapineal specific marker *gfi* (Dufourcq et al., 2004) was performed. The expression of *gfi* is in wildtype and mutant restricted to the left side too (Fig. 3.20 B, B'; n =19). Hence, the left-characteristic habenula

on the right side of the brain in *tcf7l2* mutant fish do not influence the outmigration of the parapineal on the one hand, on the other hand parapineal cells are not needed on the right side for the development of the left-typical habenula.

Still, the nature of parapineal signal is unknown. In concordance with the left-sided parapineal position a left characteristic habenular subregionalization develops in *tcf7l2* mutant and wildtype fish. On the contrary the absence of parapineal cells in wildtype fish causes right characteristic expression patterns on the left side.

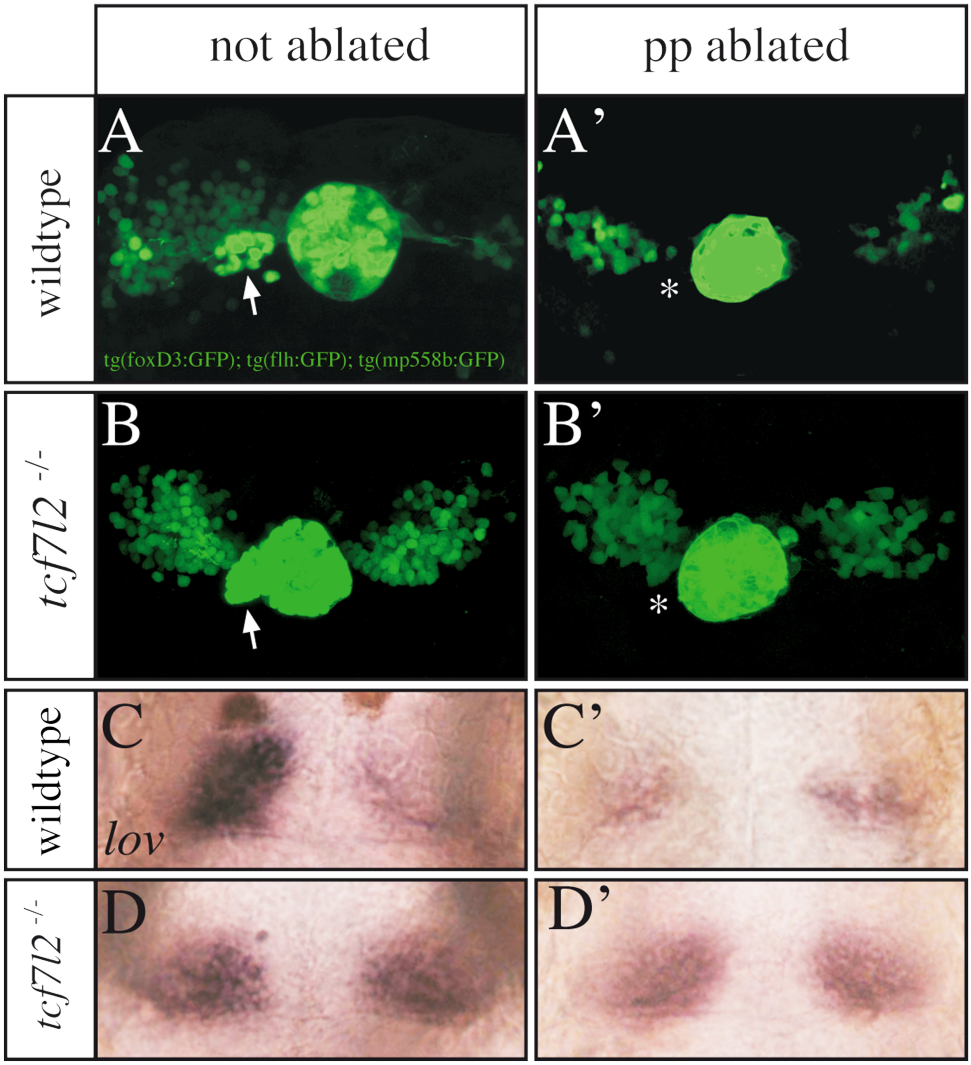

Figure 3.21: Absence of parapineal cells does not influence *tcf7l2* mutant phenotype.

Dorsal view focused on the habenula region of 4 dpf parapineal ablated and not ablated wildtype or *tcf7l2* mutant fish. Embryos are triple transgenic tg(foxD3:GFP); tg(flh:GFP); tg(mp558b:GFP) and stained for GFP (A - B) or *left over* (*lov*; C - D'). Parapineal cells (PP) are marked by arrows (A, B). Absence of parapineal cells (marked by asterisk in A', B') alter the asymmetric distrubtion of the dHbl cell specific marker in wildtype (A, C) to symmetric reduced condition (A' but has no effect on the *tcf7l2* typical double left sided situation.

To investigate if the double left sided habenula phenotype of *tcf7l2* mutant fish develops without signals from the parapineal cells, the cell cluster was ablated and the resulting habenula situation analyzed. The ablation was performed by using 2-photon microscopy before the onset of left direct migration at 27 - 30 hpf. Fish were used carrying the transgenic markers tg(foxD3:GFP); tg(flh:GFP) for pineal complex and the dHbl marker tg(mp558b:GFP). The tg(mp558b:GFP) should provide information about the habenula phenotype at 4dpf in the living embryo. Subsequently, an *in situ* hybridization with the dHbl characteristic marker *left over* (*lov*) was performed.

In concordance with prior investigations, the absence of parapineal cells in wildtype fish leads to a reduced expression of the dHbl marker *lov* but also of the transgene mp558b:GFP on the left side (Fig. 3.21 C', A'; n = 4/14, 1/8). However, the absence of parapineal does not have an effect on the left habenula in *tcf7l2* mutants: as in the not ablated control the marker *lov* and tg(mp558b:GFP) are symmetrically enlarged on both sides of the brain (Fig. 3.21 B, B', D, D'; n = 7/7, 12/12). The differentiation of dHbl cells occurs in the Wnt signaling mutant with or without signals from the parapineal.

The epistasis of the *tcf7l2* mutant phenotype to the parapineal-absent one may hypothesize that the parapineal can influence the habenular cell fate upstream to the Wnt signals. To assess whether parapineal derived signals may influence the expression Tcf in precursor cells and thereby drive precursors towards dhHbm cell fate Tcf7l2 expression was analyzed at early and late stages in parapineal-ablated wildtype fish (Fig. 3.22).

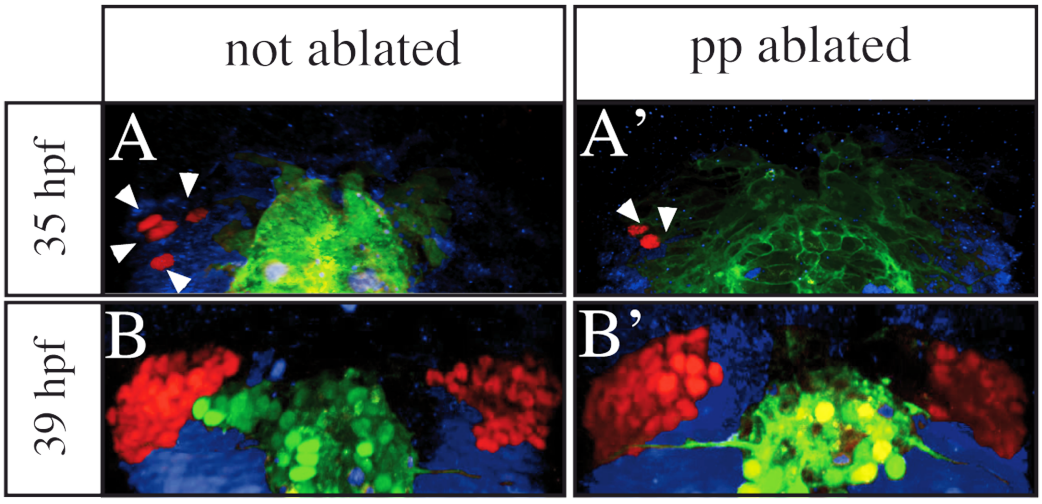

Figure 3.22: Absence of parapineal cells does not influence Tcf7l2 expression. Dorsal view focused on the diencephalon of parapineal-ablated (A', B') and not ablated (A, B) embryos carrying the transgenic pineal complex marker of tg(flh:GFP); tg(foxD3:GFP). Fish are stained against GFP (green) and Tcf7l2 (red - habenula cells; blue - non-habenula cells). Arrowheads mark Tcf7l2 expressing cells at 35 hpf (A, A'). Ablation of parapineal cells neither alters early (35 hpf) nor late (39 hpf) Tcf7l2 expression.

The Tcf7l2 expression is not altered by the absence of parapineal structure or signals. At 35 hpf the first emergence of Tcf7l2 expressing cells is detectable on the left side of the brain in presence and in absence of parapineal cells. The number of first Tcf7l2 expressing cells is neither altered in parapineal-ablated fish (Fig. 3.22 A', B'; n = 8; n = 12; detailed numbers in Appendix 7.3). The amount and equally distribution of Tcf7l2 is also not significant different in case of parapineal absence at 39 hpf in comparison to control fish (Fig. 3.22 A, B; n = 10 both). A translational control of Tcf7l2 by parapineal signals is unlikely.

4 DISCUSSION

How neuroanatomical asymmetries are established across the hemispheric borders has been an unanswered question of neurodevelopmental biology.
Previous research revealed a possible function of Wnt/beta-catenin signaling for the establishment of habenular asymmetry. Following the results of this work, the pivotal role of Tcf7l2 mediated Wnt signaling on the habenula development will be presented. Furthermore, regulatory mechanisms will be discussed, by which Wnt/beta-catenin signaling and parapineal derived signals act to establish the asymmetric habenular cell composition.

4.1 Tcf7l2 mediated Wnt/beta-catenin signaling needs to be tightly controlled during asymmetric habenula establishment

The only reported influence of Wnt/beta.catenin signaling on the establishment of habenular asymmetry showed the effect of a mutant *Axin1* gene on its subregionalization (Carl et al., 2007). The gene mutation causes the development of bilateral symmetric habenulae with right-sided features (Carl et al., 2007).
Axin1 is a component of the destruction complex for beta-catenin and is thereby needed for blocking the transcription of target genes in absence of the Wnt ligand. Consequently, *Axin1* mutant fish have enhanced Wnt signaling activity (Heisenberg et al., 2001). However, beside its prominent role in the Wnt/beta-catenin pathway, Axin1 is also known to act Wnt independently (Caneparo et al., 2007; DeStrooopera and Annaert, 2001). A final proof for the influence of canonical Wnt signaling on the establishment of habenular asymmetry is missing.
Tcf7l2 is acting as a transcription factor exclusively via the Wnt/beta-catenin pathway (Korinek et al., 1998). Indeed, phenotypic characterizations of *tcf7l2* mutant fish corroborate the necessity of proper Wnt/beta-catenin signaling for the establishment of habenular asymmetry. The loss of Tcf7l2 function results in the formation of the opposing phenotype to the double right-sided one of *Axin1* mutant fish: the double left-sided habenular phenotype.
The fully penetrant double left-sided habenular phenotype comprises of symmetric large neuronal subpopulation with dHbl characteristic expression and projection patterns, while the amount of dHbm typical neurons is reduced. In concordance with this definition all dHbl specific markers used, are bilaterally widespread expressed in *tcf7l2* mutant fish and confirm the presence of symmetric large lateral subnuclei on both sides of the brain.

The right-sided markers *dex* and *tag1* are almost absent in the mutant background. It is likely that the absence is caused by a direct regulation through altered Wnt signaling since dHbm markers like *ron* and brn3a:GFP are still present in the mutant. In addition, nuclei staining and habenula cell staining by *cxcr4b* or HuC/HuD do not indicate a reduction of total habenular cell number. Thus, the reduced symmetric expression patterns of the medial markers indicate the presence of symmetric small medial subnuclei.
The loss of laterotopic segregation confirms the double left-sided habenula phenotype too. Consistent with the increased number of lateral characteristic cells on the right side, most axons innervate dHbl-characteristic the dorsal IPN.
Bilateral symmetric habenulae with left-sided characteristics have been described before in two mutant backgrounds. Embryos mutant for *sec61a-like-1*, a subunit of the endoplasmatic reticulum translocation channel, exhibit an increased expression of lateral subnuclei marker on the right side (Doll et al., 2011). However, the axons deriving from both habenulae terminate in the ventral IPN. It is unclear if the mutated gene also influences axonal guidance due to its function in other brain structures or if it influences the target information additionally to the expression pattern.
Double left-sided habenular specifications can also be found in embryos carrying a mutation for *mindbomb* (*mib*) (Aizawa et al., 2007). The defective gene causes reduced Notch signaling activity (Itoh et al., 2003). The Notch signaling mutant shows several additional morphological defects and does not develop beyond 3 dpf (Jiang et al., 1996; Haddon et al., 1998). A detailed description of the habenula phenotype, including the axonal projection pattern, does not exist since the fully developed structure is formed as from 4 dpf.
In contrast, *tcf7l2* mutant fish can reach an age of 6 weeks and carries no other overt cerebral defects (Faro et al., 2007; Muncan et al., 2007). The specific malformation of double left sided habenulae points out a pivotal role of Tcf7l2 in the establishment of epithalamic asymmetry.

Tcfs are context-dependent transcriptional modulators of Wnt/beta-catenin signaling. Many developmental processes are known in which Tcf7l2 acts as a repressor or activator of the pathway (Vacik and Lemke, 2011; Wang et al., 2011; Tran et al., 2010; Arce et al., 2006; MacDonald et al., 2009). All data obtained indicate that the double left-sided phenotype is the result of downregulated Wnt signaling. It is therefore likely that Tcf7l2 acts as an activator in context of habenular asymmetry establishment.
For instance, IWRendo drug treatment or heatshock activation of a dominant negative Tcf construct demonstrate that embryos with downregulated Wnt signaling mimic the main aspects of the *tcf7l2* mutant phenotype. The treated fish exhibit the generation of more dHbl neurons in the right habenulae.

Surprisingly, the alteration of the signaling does not influence the expression pattern of the right-sided and medial markers. However, the majority of axons from the right habenula innervate the dorsal IPN in most drug treated fish, similar to the projection patterns of *tcf7l2* mutant fish. It is conceivable that a population of dHbl neurons exists, which co-expresses right-sided markers, while their projection pattern is mainly lateral characteristic. Thus, the fully suppression of medial specifications seems to be just feasible when Tcf7l2 mediated Wnt signaling is completely repressed.
A further support for Tcf7l2 acting as an activator of Wnt target gene transcription is the phenotype of *Axin1/tcf7l2* double mutants, which is indistinguishable from *tcf7l2* single mutants. The mirroring of the *tcf7l2* mutant phenotype makes it probable that Axin1 acts through Tcf7l2 to establish the habenular asymmetry by canonical Wnt signaling. The result supports the idea that exclusively Tcf7l2, and not another Tcf, mediates Wnt signaling in the establishment of asymmetric epithalamus, since the loss of protein prevents the development of the habenula phenotype caused by enhanced Wnt pathway activity.

The findings emphasize, that Wnt/beta-catenin signaling needs to be precisely regulated to allow the formation of proper asymmetric habenulae. It can be assumed that Wnt signaling activity is required to suppress the dHbl character or promotes dHbm character: Both habenulae develop small medial and big lateral subnuclei when Wnt signaling is upregulated while the abrogation of the pathway results in symmetric habenulae with big lateral and small medial subnuclei.
The effects of up- and downregulated Wnt signaling are similar to those of altered Notch signaling activity. Hyperactivation of Notch signal results in double right-sided habenulae while *mib* mutants, having a downregulated Notch activity, develop double left-sided characteristics (Aizawa et al., 2007). These similarities and the fact that the pathways are epistatically related in a number of developmental processes (Agathocleous et al., 2009; Hayward et al., 2008; Muñoz-Descalzo et al., 2011; Nakaya et al., 2005) lead to the hypothesis that the pathways may interact in the habenular asymmetry establishment.

4.2 Tcf7l2 mediated Wnt signaling acts Nodal independently during asymmetric habenula neurogenesis

Previous research highlighted two developmental stages when proper Wnt signaling is needed for the proper sidedness of habenulae (Carl et al., 2007). At late gastrulation and at

somitogenesis Wnt interfering LiCl drug treatments influence the left-restricted expression of Nodal-related genes and thus the establishment of habenular laterality.
These early functions of Wnt signaling only regulate the establishment of habenular laterality, whereas the asymmetry is subsequently established (Carl et al., 2007). The evoked downregulation of Wnt pathway activity causes the loss of habenular asymmetry only as from 33 hpf, 15 hours later than the described effect of LiCl during somitogenesis. In addition, the emergence of the Tcf7l2 protein and the start of Wnt signaling activity in the developing diencephalon around 35 hpf, further confirm a subsequent role of the pathway. The results lead to the conclusion that Wnt signaling indeed regulates the habenular asymmetry at an later developmental stage than the laterality.

Previous work assumed that Wnt signaling blocks a repressor of Nodal activity in the ANP. At somitogenesis this repressor is inhibited on the left by the activity of the Nodal-related gene *southpaw* (*spw*) deriving from the left LPM (Fig. 1.4; Carl et al., 2007). This effect allows unliateral Nodal signaling activity in the brain.
Altered Wnt signaling in *Axin1* mutants does not influence the left-sided expression of Nodal pathway genes in the LPM but causes defects in the ANP (Carl et al., 2007). However, *tcf7l2* mutant fish do not exhibit an alteration of the lateralized expression of Nodal pathway components neither in the ANP nor in the LPM.
Albeit *tcf7l2* expression can be found in the ANP during somitogenesis (Young et al., 2002), it is conceivable that Wnt/beta-catenin signaling acts through another member of the Tcf family to regulated the restriction of Nodal signaling activity. Possible candidates are Tcf7 and Tcf7l1, which are expressed in the region too (Thisse et al., 2004; Veien et al., 2005).
Still, it is questionable why the enhancement of Wnt signaling in *Axin1* mutants should cause the loss of the blockade in the right ANP. One possible explanation for this phenomenon may be a transcription-supporting role of Wnt signals that competes with transcription-inhibiting signals.
Similar to the mentioned assumption, the presumed repressor blocks the transcription of Nodal-related genes on both sides of the brain and is inhibited on the left by *spw*. However, the repressor activity is in this case not downstream to the Wnt pathway. Instead, Wnt activity directly stimulates the expression of Nodal-related genes. The weak promotion of transcription by Wnt signaling cannot cause the start of gene expression on the right side since it is prevented by the stronger inhibition of the repressor. On the left, the repressor is inhibited and Wnt supports the transcription.
Assuming that the transcription can also proceed without Wnt activity explains why downregulation of the pathway does not change the scenario. However, an upregulation of Wnt signaling superimpose the repressor signal on the right side. The final outcome is a

bilateral expression of Nodal components as it is described in *Axin1* mutants and LiCl treated fish.

In addition to its role in regulating general laterality, Nodal signaling appears to influence the asymmetric habenular neurogenesis too (Roussingé et al., 2009). Bilateral Nodal signals result in symmetric neurogenesis. This observation led to the presumption that left-sided Nodal signals promote the neurogenesis on the left side. If the support of neurogenesis is caused by alterations during early stages or if Nodal regulates the process directly during morphogenesis is not known.

Nodal and Wnt signaling interact in many developmental processes (Schier, 2001; Carl et al., 2007; Rodriguez-Esteban et al., 2001) and an epistatic relationship during habenular asymmetry establishment cannot be excluded. It is rather unlikely that the symmetry-breaking Wnt signal depends on Nodal mediated asymmetric neurogenesis. On the one hand the habenular precursors of *Axin1* mutants differentiate asymmetrically although the embryos exhibit bilateral Nodal activity in the brain (Carl et al., 2007; M. Carl personal communication). On the other, the *tcf7l2* mutants develop symmetric habenulae but neither exhibits bilateral Nodal activity nor a symmetric differentiation.

However, a downstream role of Wnt signaling during the neurogenesis process would allow the connection of the findings. The fact that Nodal expression in *tcf7l2* mutants is unaltered restricted to the left side and that the first emergence of Tcf7l2 protein in the habenular precursors is left-biased in wildtype fish, raises the possibility that Tcf7l2 expression depends on the pathway.

Insights into the questions were obtained from embryos exhibiting varied Nodal signaling activity caused by raising the fish for 16 hours at 22 degrees (randomized Nodal), morpholino injection against the Nodal-related gene *no tail* (*ntl*; bilateral or no Nodal) or *spw* (no Nodal). The outcome of the experiment demonstrates that Tcf7l2 expression is just indirectly affected by altered Nodal. The randomization, absence or bilateral presence does not alter the asymmetry but causes the loss of laterality.

Although the manipulation of Nodal signaling does not break the asymmetric Tcf7l2 expression, *ntl* morphants start to express the protein with a delay of 2 hours in contrast to the proper timing in *spw* morphants. The *ntl* morphants and mutant fish develop, in addition to the loss of left-right laterality, various defects (Nasevicius and Ekker, 2000; Marlow et al., 2004). Thus, it is unlikely that the delayed Tcf7l2 expression is a specific effect on the habenular asymmetry establishment. The results confirm that Nodal signaling does not regulate the left-biased expression of Tcf7l2.

Fish with defective habenular asymmetry, due to altered Notch signaling, exhibit reduced or enhanced neurogenesis activity (Aizawa et al., 2007). It is therefore rather probable that the effect of Nodal on the asymmetric neurogenesis is rather connected to Notch signaling than

to Wnt signaling. It remains to be determined how the signaling pathways interact to allow the proper habenular organization.

4.3 Asymmetric Tcf7l2 influences cell type specification

Habenular asymmetry is evidenced by differences in the number of neurons that belong to each subnucleus. How Wnt/beta-catenin signaling promotes the asymmetric organization is not known. The symmetric habenulae in *tcf7l2* mutants could be the result of altered proliferation or altered subnuclear cell specification.

The timing of habenular neurogenesis is well described and helps to identify the Wnt regulated developmental process that causes the asymmetry. Previous work demonstrated that dHbl and dHbm neurons develop in two asymmetric waves of proliferation and differentiation (Aizawa et al., 2007). On the left side of the brain, the proliferation of habenular precursors begins at 24 hpf and peaks around 32 hpf, while the precursors on the right start proliferating with a delay of approximately 6 hours. Following cell maturation, differentiation starts again on the left and begins slightly delayed on the right too. Photoconversion experiments provided evidence, that first differentiating cells develop into dHbl neurons while dHbm neurons specify with a time lag of a couple of hours.

The efficiency of Wnt interferences, the start of Wnt signaling activity and the Tcf7l2 expression in the epithalamus demonstrate, that the period between 34 and 36 hpf is the stage when Wnt/beta-catenin signaling influences the habenula asymmetry. This timeframe mainly overlaps with post-mitotic neuron specification. Differences in the rate of proliferation and in the final amount of precursor cells were not detectable in the *tcf7l2* mutant compared to wildtype. It is therefore likely that Wnt signaling is acting at another developmental step than proliferation to regulate the establishment of proper asymmetric habenulae.

Similarities of the Wnt and Notch pathway can be found in the habenular organization of fish with altered signaling and in the time of acting on the asymmetry establishment (Aizawa et al., 2007; Carl et al., 2007). Up- or downregulation of the pathways results in similar symmetric phenotypes. Notch signaling acts on the habenular development as from 32 hpf and Wnt signaling only three hours later.

Notch signaling activity regulates the timing of asymmetric habenula development since modifications of the pathway leads to delayed or excessive neurogenesis (Aizawa et al., 2007). As Wnt signaling is known to cause comparable delays in retinal cell differentiation

(Meyers et al., 2012; Agathocleous et al., 2009), the pathway could influence the timing of habenula neurogenesis too.
Unknown signals during the habenular differentiation define the specification to first lateral subnuclei neurons and subsequently medial neurons (Aizawa et al., 2007). Wnt signaling could influence the amount and distribution of differentiating cells that receive the signal. Thereby the pathway could regulate the habenular cell composition.
However, no alterations of the timing, amount or distribution of post-mitotic HuC/HuD positive habenular cells were detected in *tcf7l2* mutant fish. Thus, the symmetrically large lateral subnuclei do not develop by excessive early differentiation. Likewise, the small medial subnucleus on the right side is not the product of a delayed late differentiation. Despite of all similarities, Wnt signaling seems to promote the habenula asymmetry in a different way than Notch.

Asymmetric neurogenesis can lead to symmetric habenulae, like in Wnt mutants, and a symmetric neurogenesis to asymmetric habenulae, like in Nodal morphants. These observations may suggest, that the establishment of habenular asymmetry is mainly regulated by asymmetric cell type specifications and not by symmetric differentiation per se. Wnt/beta-catenin has been reported to determine neuronal character in several cases (Bluske et al., 2012; Huang et al., 2007; Hirabayashi 2004). It is conceivable that Wnt signaling regulates the habenular asymmetry by a direct promotion of the cell type specification and not indirectly by the retardation or acceleration of the cell development till a further signal drives the specification.
The identified period, when Wnt signaling has an effect on the habenular differentiation, begins slightly after the start of differentiation. A transient suppression of Wnt signaling activity by IWRendo only between 35 and 36 hpf can already break the habenula asymmetry. Even though the habenular differentiation occurs quite dynamically, it is unlikely that the majority of habenular cell specification processes within one hour. It is possible that the drug is not completely removable by washing and that it thereby influences Wnt signaling over a longer period. Thus, also treatments after 36 hpf show an effect. However, drug treatments after 39 hpf do not have a significant effect on the asymmetry anymore.
The restricted timing of Wnt signaling activity explains why still populations of dHbl neurons in *Axin1* mutants and dHbm cells in *tcf7l2* mutants respectively are made. Already before the start of Wnt acting some lateral subnuclei cells are specified whereas after the necessity of Wnt signaling and the latest IWRendo effect still medial specification proceeds.
Hence, Wnt activity is needed between 34 and 36 hpf to regulate the specification into lateral or medial subnuclei neurons. Consequently, the number of precursor cells and the rate of differentiation do not have to be altered for this process. Following the hypothesis, the upregulation of Wnt activity in *Axin1* mutants causes an increased specification into dHbm

neurons, whereas the downregulation of Wnt signaling in *tcf7l2* mutants results in a reduced specification into neurons with dHbl character. However, it is unanswered what the default stage of habenular neurons is and if Wnt suppresses lateral cell fate or promotes medial cell fate.

Although the cell type specification is likely to be regulated by Wnt signaling, it remains to be elucidated how Wnt/beta-catenin signaling mediates the differential specifications across the left-right axis.

Tcf7l2 is the first asymmetrically expressed protein identified to be involved in asymmetric habenula establishment. Tcf7l2 starts to be left-biased expressed as from 35 hpf, directly in habenular precursor cells. The left-dominant distribution slowly equates over the next 5 hours till Tcf7l2 expressing cells are equally distributed on both sides of the brain.

The dynamic and left-biased distribution of Tcf7l2 is reminiscent to the observations that the specification of the different subnuclear characters always starts on the left side. Thus, Wnt signaling could promote dHbm specification, following the expression pattern of Tcf7l2. It is remarkable that no other component, regulating the habenular asymmetry and neurogenesis, has been found asymmetrically expressed yet.

Several indications point into the direction of a Tcf7l2 promoted medial specification and not a role of Tcf7l2 in the promotion of cell type independent differentiation. For instance, the location of Tcf7l2 expressing cells let assume a function, that is not related to lateral subnuclei cells. Tcf7l2 expression is not present close to the pineal on the right side. This region was identified to harbor right dHbl characteristic cells at later stages (Aizawa et al., 2007). In concordance with the avoidance of this region, tg(7xTCF:mCherry) expression, reflecting Wnt signaling activity, has never been found there too.

The time of first protein expression at 35 hpf gives further confirmation for the hypothesis. The stage fits perfectly to the elucidated start of Wnt activtity in the habenulae. As already mentioned, it is likely that before this period early born progenitors differentiate into lateral subnuclei neurons (Aizawa et al., 2007). Thus, 35 hpf could be the start point of medial specification. The observation that some fish exhibit an IWRendo effect earlier than 35 hpf is explainable by an incomplete drug removal that causes this rare alteration of habenular asymmetry.

Tcf7l2 is expressed in post-mitotic HuC/HuD expressing habenula precursor cells and the amount of co-labeling increases drastically within the course of time. The presence of HuC/HuD positive cells at 38 hpf that do not co-expresses Tcf7l2, further strengthens the conclusion that these early post-mitotic cells differentiate into dHbl neurons.

Additional support for a medial cell fate promoting role of Tcf7l2 is given by the observation that the first post-mitotic Tcf7l2 positive cells are localized on the left side at the time when according to Aizawa et al., 2007 the amount of dHbl cell differentiation starts to decrease.

Since the total amount of differentiating cells increase over this period, it seems reasonable that the Tcf7l2 expressing cells differentiate into medial neurons. Following the decrease of dHbl cells and the increase of dHbm neurons, the amount Tcf7l2 and HuC/HuD co-expressing cells gains drastically within the next two hours on both sides.
However, a medial specification independent function of Tcf7l2 mediated Wnt signaling could be argued regarding the facts that the number of newly Tcf7l2 expressing cells increase after 39 hpf while the downregulation of Wnt signaling by IWRendo does not influence the asymmetric habenula development anymore. Furthermore, at 4 dpf all habenula cells express Tcf7l2 independent of their subregionalization.
It should be noted that Tcfs are also needed to regulate maintenance processes (Oh et al., 2012; Mao and Byers 2011; Kanwar et al., 2012). Hence, it seems reasonable that the late Tcf7l2 expression may be related to its role as a maintenance protein.
Despite the strong indications that support the specifying signaling by Tcf7l2, the function cannot be proven directly, as no early marker for medial cell fate exists. A future goal would be the generation of a transgenic line expressing a fluorescent marker under the control of the Tcf7l2 promoter. A combination with lateral or medial transgenic markers and the utilization of photoconvertible cellular tracers would allow the cell fate determination of early Tcf7l2 positive cells and would provide a final proof for the protein function.

Still, it remains unclear if Tcf7l2 expression follows the asymmetric neurogenesis or if the distribution of Tcf7l2 mediates asymmetric Wnt signals that imposes the asymmetric cell specifications. A timely and spatial specificity of the Wnt/beta-catenin signaling activity is often ensured by the cell-context-dependent expression of its components (Mao and Byers 2011; Veeman et al., 2003). The expression pattern of other Wnt signaling components could answer if Tcf7l2 exclusively triggers the activity patterns of Wnt signaling in case of habenular asymmetry establishment. It would also be useful to analyze the expression of Tcf7l2 in fish with altered cell maturation and specification caused by improper Notch signaling.

A support for a maturation independent expression of Tcf7l2 is its expression pattern in *Axin1* mutant. The timing of neurogenesis is grossly unaffected in those fish (M. Carl, personal communication). However, alterations of Tcf7l2 expression patterns are detectable. The modified Tcf7l2 expression in fish with altered Wnt signaling strongly correlates the spatial and timely distribution of Tcf7l2 to the regulation of medial cell fate. In accordance with the bilateral large medial subnuclei formation, *Axin1* mutants exhibit an increase of Tcf7l2 positive cells. The enhancement of Wnt signaling activity mainly influences the amount of Tcf7l2 positive cells at early stages when predominantly dHbl cells are generated. Thus it is

likely that upregulated Tcf7l2 expression causes the overproduction of dHbm characteristic cells on the left side. Conversely, transient inhibition of Wnt signaling by IWRendo results in a reduced number of Tcf7l2 expressing cells. The amount of Tcf7l2 positive cells is decreased at later stages when mainly dHbm cells specialize.

The hypothesis implicates the existence of a positive feedback loop for Tcf7l2 expression driven by Wnt signaling activity. Regulatory feedback circuits of the Wnt/beta-catenin pathway are well known (Tanaka, et al., 2011; Acre et al., 2006; Hoppler and Kavangh 2007; Struewing et al., 2010). Additionally, it has been reported that Wnt signaling activity has the capacity to enhance specifically the tcf7l2 expression (Saegusa et al., 2005). Since recent findings indicate that the transcription of Wnt target genes can also trigger the secretion of Wnt ligands (Fu et al., 2011), one may speculate that not only the intercellular expression but also the amount of Tcf7l2 expressing cells multiplies by the positive feed forward circuit.

Surprisingly, the IWRendo has an effect on the Tcf7l2 expression around 40 hpf while the asymmetry influencing time of treatment is a couple of hours earlier. What might at first sight seem contradictory can be explained by the presumed feedback loop. The early downregulation of Wnt also triggers the feedback circuit down. Hence, the deceleration of the cycle may influence later stages too. The feedback mechanism of Tcf7l2 mediated Wnt pathway activity elucidates why even slight modifications of proper signaling can result in drastically subnuclear changes.

Both Tcf7l2 emergence as well as progenitor cell differentiation still takes place asymmetrically in case of up- and downregulation of Wnt/beta-catenin signaling although alterations result in the formation of symmetric subnuclei. A very precise interplay of the cell maturation state and specification signals seems to be needed for the final habenular setup. Before the Wnt activity in the habenular cells starts, small clusters of dHbl and dHbm cells specify, while at the time of Wnt acting medial neurons develop probably by following the distribution of Tcf7l2.

Thus, the assumed mechanism explains how the switch from early lateral to late medial specification proceeds across the left-right axis and gives an idea why improper Wnt signaling results in alterations of the subnuclear organization.

4.4 Parapineal and asymmetric Tcf7l2 mediated Wnt signals establish the habenular left-right asymmetry

It is doubtful whether the different habenular subregionalizations along the left-right axis are exclusively caused by Tcf7l2 mediated Wnt signaling, since the proper asymmetric setup requires the presence of a second asymmetric structure: the left-sided parapineal.
The laterality of parapineal cells and of the left habenula always develops concordantly (Concha et al., 2003). Furthermore, parapineal cell migration to the left depends on the presence of a left-characteristic habenula. In its absence the cell cluster is not able to delaminate from the pineal complex (Concha et al., 2003). These facts raised the question if Wnt signaling might guide the migration directly by a left-biased signal or indirectly by causing the development of the large lateral subnucleus on the left. However, neither bilateral symmetric large subnuclei nor downregulated Wnt signaling do effect the left-sided migration in *tcf7l2* mutants.

Habenular cells mainly proliferate before the left-sided migration of the parapineal, while the progenitors mainly differentiate after the orientation of left (Aizawa et al., 2007). The left-sided parapineal cell migration takes place at the same time as the early specification of the left lateral subnucleus. Researchers hypothesized that unidentified parapineal signals could promote the specification of habenular precurors (Aizawa et al., 2007; Gamse et al., 2003; Bianco et al., 2008; Roussigné et al., 2011).
In fact, parapineal derived signals are needed for a proper habenular cell composition. The ablation of the delaminating parapineal cells causes the development of right-characteristic features in the left habenula. In this case the left habenula is built up by a large medial subnucleus and a small lateral one, reminiscent to the habenula situation in *Axin1* mutants (Carl et al., 2007; Bianco et al., 2008; Concha et al., 2003; Gamse et al., 2005; Gamse et al., 2003).
It is a challenging question what the default stage of habenular precursor cells is and if the parapineal positively influence them to acquire dHbl character or negatively by suppressing dHbm fate. It is possible that the neurogenesis occurs on both hemispheres in the same way: A small number of early born precursors follow a lateral cell fate, while the remaining later born cells develop a medial specification, possibly caused by Tcf7l2 presence. The left and the right side could just differ in the timing of neurogenesis and the presence of parapineal signals. Thus, it is conceivable that the presence of the parapineal on the left suppresses this medial specification for a couple of hours or in a restricted area.
Parapineal cells are not needed indeed for the lateral specification of a certain amount of cells since a small cluster still develops in their absence (Gamse et al., 2003). It is further

likely that the small lateral subnucleus is formed by early differentiating cells, as ablation after the described first specifications still results in the parapineal-ablated phenotype.
In addition, the habenular development on the right side occurs probably parapineal-independent. The progenitors are able to develop lateral specifications even without having the parapineal on the same hemisphere. Thus, *tcf7l2* mutants develop a fully penetrant left-characteristic habenular on the right side in the absence of parapineal cells.

Parapineal signals and Wnt signaling have an opposed effect on the habenular phenotype. Wnt signaling promotes medial cell fate while parapineal signals are likely to suppress medial cell fate. The proper subregionalization of the left habenula may be established by an interaction of the signals. Laser ablation experiments revealed that the absence of parapineal cells does not influence the double left-sided phenotype of *tcf7l2* mutant fish.
Two different scenarios can explain the observation: Parapineal signals could directly block Wnt signaling or the signals block the capacity of the cells to respond to Tcf7L2 mediated Wnt signals.
If the parapineal-mediated signaling is acting upstream of Wnt/beta-catenin signaling, the presence could suppress the pathway activity and the mediated dHbm specification. Thus, the absence of parapineal cells could not effect the subregionalization in case of altered Wnt pathway activity.
This assumption is however contradicted by the Tcf7l2 expression pattern in parapineal-ablated wildtype fish. The obtained results indicate that the protein is a key-component for the establishment of medial specification and that it is transcriptionally regulated by Wnt signaling activity. The formation of a large medial subnucleus would require an increased number of Tcf7l2 expressing cells like it was shown in *Axin1* mutant fish (Carl et al., 2007). However, the distribution and amount of Tcf7l2 protein is not altered.
Another way, how a large medial subnucleus can be established on the left side, was described in Notch mutant fish (Aizawa et al., 2007). Timely shifts in neurogenesis can cause an enhanced differentiation into dHbm cells too. How this effect is related to the Tcf7l2 distribution is not known yet. Nevertheless, delays in neurogenesis timing were neither reported in parapineal-ablated fish (Roussigné et al., 2009).
Alternatively, if the parapineal signals prevent the capacity of the habenular precursors to respond to the medial specification promoting Wnt signals, the absence of parapineal and Wnt signaling could result in the observed left-characteristic phenotype too. Thus, a large lateral subnucleus develops in wildtype fish, since the cells cannot process the Tcf7l2 mediated specification. However, Tcf7l2 promoted fate determination can specify medial neurons when the parapineal caused inhibition of cell response is broken.
This hypothesis is strengthened by the less successful attempts to break the habenular asymmetry by artificial enhancements of Wnt signaling. Drug treatments that inhibit Wnt

signaling activity and heatshock-induced downregulation of the pathway in transgenic fish easily modify the habenula subregionalization on the right side. However, artificial upregulation of the signaling with drugs like BIO or ALP (Moro et al., 2012) or heatshock induction of Wnt8 in tg(hspWnt8:GFP) transgenic embryos (Weidinger et al., 2005) has nearly no effect on the specification of the left habenula (M. Carl; personal communication). Only the strong overactivation of Wnt/beta-catenin signaling, caused by the absence of its inhibitor Axin1, results in a change of left-sided subnuclear arrangement. This finding provides further support for a model in which parapineal cells prevent medial differentiation independent or downstream of Tcf7l2 mediated Wnt signaling.

Transplantation experiments could answer if parapineal signals are able to prevent Tcf7l2 mediated medial specification. The right-sided cell fate should change from medial to lateral and the left-sided from lateral to medial by the conversed placement of parapineal cells.

The mentioned combination of a Tcf7l2:mCherry transgenic line with the lateral or medial transgenic markers and the utilization of photoconvertible cellular tracers would also be helpful to answer the question. Thus, the potential switch of specification could be analyzed in parapineal presence and in ablated fish.

The developed hypothesis contributes to the understanding how the habenular asymmetry is established. On the right side Tcf7l2 mediated Wnt signaling promotes medial specification. On the left side this signal is partially suppressed by the adjacent parapineal cells (Fig. 4.1). The combination of asymmetric Tcf7l2 emergence and left-sided parapineal signals allows the specification into differentially large subnuclei across the left-right axis.

It remains a challenging task to figure out how exactly Tc7l2 mediated Wnt signaling, Nodal and Notch interact on molecular level during the habenular neurogenesis. In addition, it will be useful to investigate the Wnt regulatory circuit that regulates the Tcf7l2 expression, as neither the process-initiating Wnt ligand nor the downstream targets are known.

Finally, the complex signal interaction, the precise triggering of developmental timing and the importance of adjacent structures leads to the question what the function of habenular asymmetry is. The rising number of tools to study the activity of neuronal circuits and their behavioral consequences may allow to link the asymmetric habenulae to its physiological function e.g. by the usage of the asymmetry defective *tcf7l2* mutant fish.

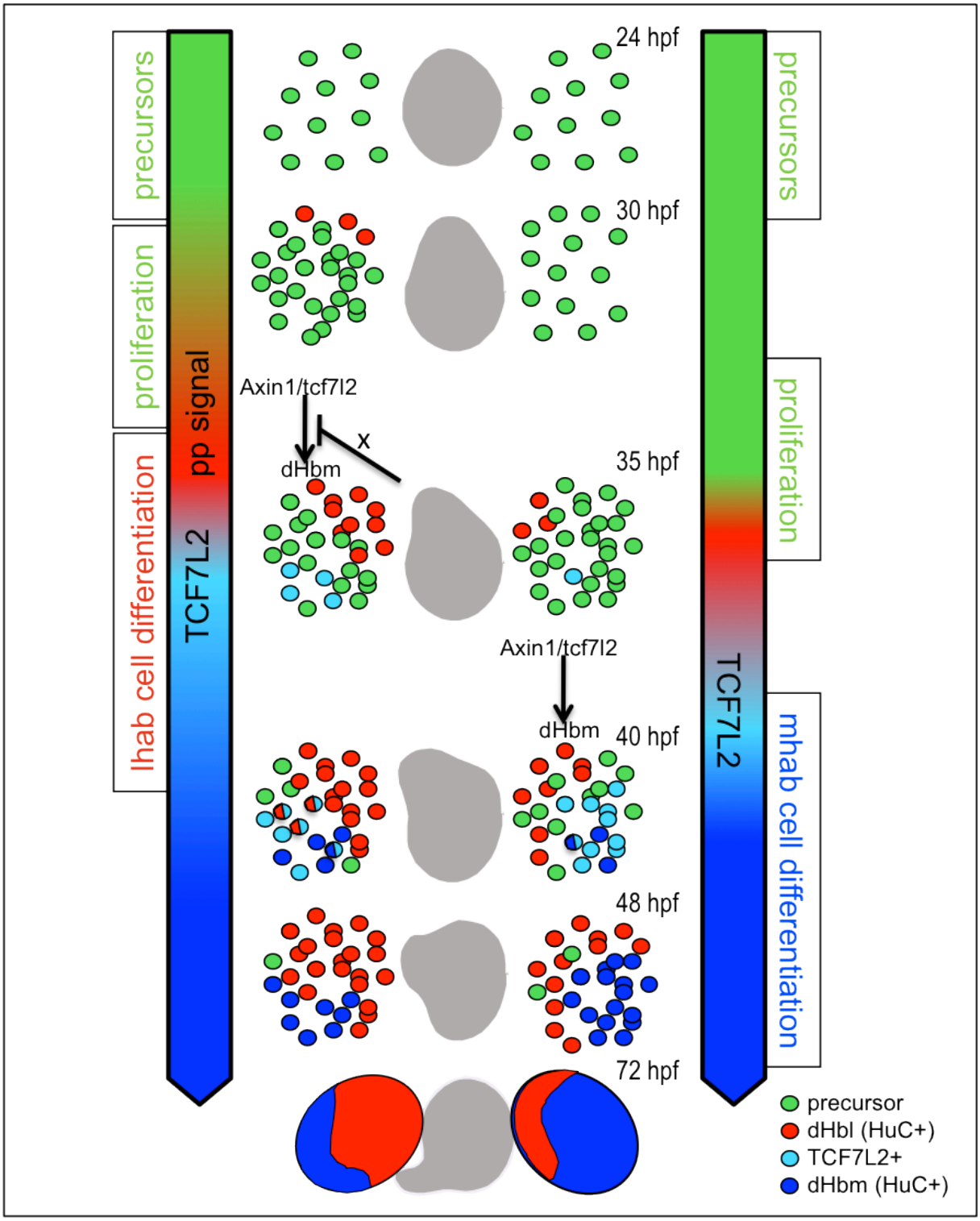

Figure 4.1: Model of habenular asymmetry establishment caused by Tcf7l2 and parapineal signals.

Initially, precursor cells (green) start to proliferate earlier on the left side than on the right. Subsequently cells differentiate into lateral dorsal habenula neurons (dHbl, red) on the left and slightly delayed right side. Left-biased Tcf7l2 expression (light blue) starts at 35 hpf and force the progenitors to differentiate into neurons with medial habenula character on the right side of the brain (dHbm. dark blue). On the left side parapineal signals prevent that the progenitor respond to the Tcf7l2-mediated Wnt signal. Thereby the cells bypass the original lateral fate program.

5 EXPERIMENTAL PROCEDURES

5.1 Fish Maintenance

AB and tupl wildtype lines and *tcf7l2*^{exl} (Muncan et al., 2007), masterblind/Axin1 (mbl^{tm213}) (Heisenberg et al., 2001), *tcf7l2*^{exl} x mbl^{tm213} and the u754 *tcf7l2* mutant (Wilson lab; UCL, UK) allele were used. In addition, the following transgenic lines were used: tg(mp558b:GFP) derived from an enhancer trap screen (Wen et al., 2008), *tcf7l2*^{exl} x tg(mp558b:GFP), tg(hsp70-brn3a:GFP) (Aizawa et al., 2005), *tcf7l2*^{exl} x tg(hsp70- brn3a:GFP), tg(foxD3:GFP); tg(flh:eGFP) (Concha et al., 2003; Gilmour et al., 2002), mbl^{tm213} x tg(foxD3:GFP); tg(flh:eGFP), tg(mp558b:GFP); tg(foxD3:GFP); tg(flh:eGFP), *tcf7l2*^{exl} x tg(mp558b:GFP); tg(foxD3:GFP); tg(flh:eGFP), tg(HuC/HuD:GFP) (Park et al., 2000), *tcf7l2*^{exi} x tg(HuC/HuD:GFP), tg(hsp70-deltatcf:GFP) (Weidinger et al., 2005) and tg(7xtcf:mCherry); tg(foxD3:GFP); tg(flh:eGFP) (Moro et al., 2012).

Zebrafish were maintained, bred and staged according to standard procedures (Westerfield et al., 1995). Embryos were raised in E3 embryo medium including 0.2 mM 1- phenyl-2 thiourea (Sigma; Munich) to avoid pigmentation. The medium was changed daily.

When the collected embryos obtained the right stage of development, they were anaesthetized in a Tricaine stock solution and fixated in 4 % paraformaldehyd (PFA; Sigma) in PBS (Invirtogen) for 4 hours at room temperature (RT) or over night at 4 °C. Embryos were transferred into a petridish containing 1x PBST (PBS + 1% Tween (Sigma)) after fixation. The chorion was removed with tweezers (No. 5 Dumont & Fils) under a light binocular. After washing the embryos two times for 10 minutes in PBST, the fish were rinsed 15 minutes in 50 % methanol/PBST (Sigma) and stored in 100 % methanol at -20 °C.

E3 embryo medium	5mM NaCl (Sigma) 0.17 mM KCl (Sigma) 0.33 mM CaCl2 (Sigma) 0.33 mM MgSO4 (Sigma) 1 % methylene blue (Sigma).
Tricaine stock solution (pH 7)	400 mg tricaine powder (Ethyl 3-aminobenzoale methanesulfonate salt, Sigma) 97.9 ml DD water ~2.1 ml 1 M Tris (pH 9; Sigma)

5.2 Identification of *tcf7l2* mutant fish

All shown experiments were performed on homozygote *tcf7l2* mutant embryos. Therefore heterozygote parental fish and the homozygote descendants had to be identified.

5.2.1 DNA extraction

Potential *tcf7l2* mutant carriers were anaesthetized in a tricaine solution (4,2 ml stock solution in 100 ml tank water). A small piece of the fin was cut and incubated in 40 µl lysis buffer containing 220 µg/ml proteinase K (Sigma) at 55 °C overnight.
Similar, the tail of fixed embryos was cut with tweezers and inserted in a well of a 96-well plate. The Methanol evaporated by letting the open plate incubate on a PCR machine (Mastercycler, Eppendorf) at 37 °C with the lid open. 20 µl lysis buffer containing 220 µg/ml proteinase K (Sigma) were added before incubating for 4 hours.
After incubation, each tube/plate was vortexed, shortly spun down and incubated for another 2 hours at 55 °C. Finally, the solution was incubated for 10 minutes at 95 °C to inactivate the proteinase K activity. The extracted DNA was stored at -20 °C.

Lysis buffer	10 mM Tris/HCl (pH 8, Sigma)
	1mM EDTA (Sigma)
	0,3% Tween (Sigma)
	0,3% Glycerol (Sigma)

5.2.2 PCR

A nested Polymerase chain reaction (PCR) was used to amplify the DNA area including the potential point-mutation of the *tcf7l2* gene. The subsequent digestion of the amplified segment with a restriction enzyme, which specifically cut at the mutation side, allowed the identification of the mutant carriers.

Following primer pairs were used:

first primers tcf7l2$^{exl-/-}$	F-5'- AACCGATGCACCGTGTTG-3'
	R-5'-AAATGCCGCAGCTGAACG-3'

nested primers tcf7l2$^{exl-/-}$	F-5'-GACGAAGGCGAGCAGGAGG-3′
	R-5-GAAATGCAACGAAACACAGGGAATGC-3′
first primers tcf7l2^{u754}	F-5'- CCTAGCGGATGGGGAATC-3'
	R-5'-CAACATCGTGGCTGCCTC -3'
nested primers tcf7l2^{u754}	F-5'-TGTTCAATTGTGTATCTCACAAAGG-3′
	R-5'-GTGGAGGCCTTGGGGTTC -3′
first primers tcf7l2^{u763}	F-5'- AACCGATGCACCGTGTTG-3'
	R-5'-AAATGCCGCAGCTGAACG-3'
nested primers tcf7l2^{u763}	F-5'-TTCAATGCATTCCCTGTGTT-3′
	R-5'-GTCCTGTGCAAAAACAAAAAG-3′

The PCR reaction mix contained 10 µl of 5x GoTaq polymerase buffer, 10 µl Q-Solution, 5 mM magnesium chloride, 0,5 µl of each primer, 1 µl of 10 mM desoxynucleotide triphosphate, 1 U GoTaq polymerase (all Qiagen) and 3 µl DNA in total volume of 50 µl. The amplified product was diluted 1:20 with DD water. For the nested PCR 2 µl were used. The polymerase chain reaction was performed according to the following programs:

first amplification tcf7l2$^{exl-/-}$

95 °C	2 min
95 °C	30 sec
63°C	30 sec
72 °C	30 sec
go to step 2, repeat the cycle 30 times	
72 °C	5 min
10 °C	for ever

second amplification tcf7l2$^{exl-/-}$

95 °C	2 min
95 °C	30 sec
56°C	30 sec
72 °C	30 sec
go to step 2 and repeat the cycle 35 times	
72 °C	5 min
10 °C	for ever

first amplification tcf7l2^{u754}

95 °C	2 min
95 °C	30 sec
58,4°C	30 sec
72 °C	40 sec
go to step 2 and repeat the cycle 30 times	
72 °C	5 min
10 °C	for ever

second amplification tcf7l2^{u754}

94 °C	2 min
94 °C	30 sec
55°C	30 sec
72 °C	30 sec
go to step 2 and repeat the cycle 44 times	
72 °C	5 min
10 °C	for ever

first amplification tcf7l2^{u763}		second amplification tcf7l2^{u763}	
95 °C	2 min	94 °C	2 min
95 °C	30 sec	94 °C	30 sec
63°C	30 sec	55°C	30 sec
72 °C	30 sec	72 °C	30 sec
go to step 2 and repeat the cycle 30 times		go to step 2 and repeat the cycle 44 times	
72 °C	5 min	72 °C	5 min
10 °C	for ever	10 °C	for ever

To control the amplification of the right DNA fragment, 5 µl of the PCR product were loaded with 6 x loading dye (Fermentas) on a 1 % agarose gel.

5.2.3 Restriction Analysis

The final PCR product was digested with the restriction enzyme BsaJI (tcf7l2$^{exl-/-}$), NlaIV (tcf7l2^{u754}) or HphI (tcf7l2^{u763}, all New England Biolab) to identify the mutant zebrafish. An exchange of the bases adenine to guanine in the tcf7l2$^{exl-/-}$ mutant gene, guanine to adenine in tcf7l2^{u754} mutant and in tcf7l2^{u763} mutant disrupts the restriction sides. Therefore, 8 µl PCR product were digested with 2,5 U enzyme and 2 µl of 10x NEB buffer in a total volume of 20 µl. The reaction mix was incubated at 60°C (tcf7l2$^{exl-/-}$) or 37°C (tcf7l2^{u754}; tcf7l2^{u763}) for 4 hours. The product was loaded with 6 x loading dye on a 1,2 % (tcf7l2$^{exl-/-}$; tcf7l2^{u763}) or 3 % (tcf7l2^{u754}) agarose gel.

5.3 *In Situ* Hybridization Procedures

5.3.1 Bacteria transformation - Isolation of plasmid DNA

For the amplification of a vector including the sequence of a *in situ* hybridization target gene, *E. coli* were transformed with the plasmid using the One Shot® TOP10 Chemically Competent *E. coli* kit (Invitrogen). Thus, competent cells were defrosted on ice. 2 µl plasmid were pipetted into the vial. The solution was incubated on ice for 30 minutes. Subsequently, the solution was incubated exactly 30 seconds on 42°C thermomixer (Eppendorf). The vial was placed again on ice after heating. 250 µl SOC medium (Invitrogen) was added to the bacteria solution. Finally, the vial was shaked at 37°C for one hour at 225 rpm. 20 µl of the

transfection solution was spread to 200 µl with LB medium and distributed on LB plates. Plates were incubated at 37°C overnight.

Single colonies were picked and solved in 2 ml LB medium. The culture was incubated at 37°C overnight at 1000 rpm. The bacterial culture was centrifuged at 14,000 x g for 1 minute to pellet cells. After the supernatant was removed, the cells were resuspended in 0,3 ml of Solution I by gently vortexing. Afterwards, 0,3 ml of Solution II was added. The entire solution was incubated at room temperature for 5 minutes. 0,3 ml of 3 M potassium acetate (pH 5,5; Roth) was slowly added. The sample was placed on ice for 10 minutes. After incubation the solution was centrifuged for 10 minutes at 14,000 x g. The supernatant was transferred to a tube containing 0,8 ml isopropanol (Applichem). The tube was inverted a few times and placed on ice for 10 minutes. The sample was centrifuged again for 15 minutes at 14,000 x g at room temperature. Subsequently, the supernatant was carefully removed. The pellet was washed with 70% ethanol (Roth). After final centrifugation (5 minutes at 14,000 x g) and removing of the supernatant the pellet was solved in 40 µl DD water. After concentration and purity determination (Nanodrop system, Fischer) plasmid was stored at -20°C.

LB medium (pH 7)	1% Tryptone (Roth) 0,5% yeast Extract (Roth) 1,0% NaCl (Sigma) 0,3% Tween (Sigma) 0,3% Glycerol (Sigma) autoclave on liquid cycle 20 min and add antibiotic
LB plates	LB medium + 15 g/l LB agar (Roth)
Solution I	15 mM Tris/HCl (pH 8; Sigma) 10 mM EDTA (Sigma) 100 µg/ml RNase A (Qiagen) filter-sterilize
Solution II	0,2 N NaOH (Roth) 1% SDS (Applichem) filter-sterilize

5.3.2 Preparation of *in situ* probes

For synthetizing *in situ* probes, the plasmid DNA was linearized by enzymatic digestion. 4 µl DNA (1 µg/µl) were digested with 5 U of the appropriate restriction enzyme (NEB) and 2 µl of 10 x buffer in a total volume of 20 µl for 3 hours at 37 °C. The digestion product was cleaned from the endonucleases with the Qiagen purification Kit. Therefore 5 volumes of buffer PB were added to 1 volume of the linearized DNA and insert into the provided filtration column. After centrifugation for 60 seconds at 13,000 rpm the flow-through was discarded. Subsequently, 750 µl buffer PE were added to the column. Again a centrifugation step was performed at 13 000 rpm for 60 seconds and the flow-through was discarded. Centrifugation for additional one minute removed wash residues. The column was placed into a new 1,5 ml tube and the DNA was eluted in two steps with each 25 ml RNAse-free water, which was placed into the center of the membrane and centrifugation for 1 minute at 13 000 rpm. After the determination of the size of the fragment by gel-electrophoresis, the sample was stored at -20°C.

For the preparation of the RNA probe 3 µl of linearized plasmid were incubated with 10 U of the appropriate RNA polymerase, 16 U RNAse inhibitor, 2 µl of 10 x buffer (all NEB; including 100 mM DTT) and 2 µl of DIG (dioxigenin)- or FITC (fluorescein)-labeling mix (Roche) in a total volume of 20 µl for 3 hours at 37°C.

In situ probe	Enzyme for linearization	RNA polymerase	Reference
left-over/kcdt12.1	EcoRI	T7	Gamse et al., 2005
dexter/kcdt8	XhoI	Sp6	Gamse et al., 2005
right-on/kcdt12.2	EcoRI	T7	Gamse et al., 2005
tag1	NotI	T7	Gamse et al., 2003
cpd2	SalI	T7	Gamse et al., 2003
cxcr4b	BamHI	T7	Roussigné et al., 2009
gfi	NotI	T3	Dufourq et al., 2004
pitx2	SpeI	T7	Essner et al., 2000
spw	SpeI	T7	Long et al., 2003
tcf7l2	XbaI	T7	Young et al., 2002

After *in vitro* transcription the DIG-labeled RNA probe was purified using the Qiagen RNeasy Kit. The volume of the RNA solution was adjusted to 100 µl with RNase free water. 350 µl buffer RLT were added and mixed well. 250 µl of 100 % ethanol were added to the diluted RNA and mixed by pipetting. The solution was transferred into a Qiagen spin column and washed two times with 500 µl buffer RPE by centrifuging 15 seconds at 10,000 rpm.

After discarding the flow-through, the sample was again centrifuged for 2 minutes at 10,000 rpm. The column was placed into a new 1,5 ml Eppendorf tube and eluted in two steps with each 25 µl RNase free water by centrifuging 1 minute at 10 000 rpm. The *in situ* probe was checked for their purity and size by gel-electrophoresis and stored at -20°C

5.3.3 Whole mount *in situ* hybridization

All steps were performed in 1.5 ml tubes on a shaking plate or thermomixer (Eppedorf) except the incubation step with proteinase K. The embryos were rehydrated in 50 % methanol/PBST for 15 minutes and then washed two times in PBST for 10 minutes. Subsequently embryos were digested with 10 µg/ml proteinase K in PBST. The duration of incubation depends on the stage of embryos: Up to a stage of 26 somites the embryos were digested for 5 minutes, up to 24 hpf for 10 minutes, up to 48 hpf for 30 minutes and older embryos for 1 hour. No digestion is needed before somitogenesis stages. After washing the fish two times for 5 minutes in PBST, the embryos were fixated for 20 minutes in 4 % PFA at room temperature. The fixative was washed out 5 times for 5 minutes each with PBST. Subsequently, embryos were rinsed in hybridization mix and then pre-hybridized for at least 2 hours at 65 °C in hybridization mix. Before the probe was added to the embryos, the solution was diluted 1:100 and incubated for 10 minutes at 65°C. The fish were incubated in 300 µl of the solution at 65 °C overnight without shaking.

The next washing steps were all occurred at 65 °C. First, embryos were washed the next day 5 minutes in hybridization mix followed by a 30 minutes incubation in a mixture of 50 % hybridization mix and 2 x SSC. Then fish were incubated for 20 minutes in 2 x SSC. After washing two times in 0,2 x SSC for 35 minutes, the embryos were incubated for 15 minutes at room temperature in a 1:1 mixture of 0,2 x SSC and MAB. Subsequently, the embryos were washed two times for 5 minutes in MAB. To block the unspecific binding sites the embryos were incubated in 2 % blocking reagent (Roche) in MAB for 3 hours. The solution was replaced with an antibody mixture of anti-digoxigenin-alkaline phosphatase (1:2000) or anti-fluorescein-isothiocyanate phosphatase (1:1000) in 2 % blocking reagent/MAB and were incubated overnight at 4 °C on a turning plate.

At the next day the embryos were washed 4 times for 30 minutes in MAB at RT. After the washing embryos were equilibrated 3 times for 5 minutes in staining buffer (DIG or FITC). For detection the embryos were transferred into a 24-well plate, all liquid removed and incubated with the developing substrate at RT in the dark until the reaction was complete. For the DIG reaction 4,5 µl NBT (4-Nitro blue tetrazolium chloride) and 3,5 µl BCIP (4-toluidine salt; both Roche) were diluted in 1ml staining buffer and used as developing substrate. For FITC staining, one Naphtol tablet and one Tris buffer tablet (Sigma Fast Fast

Red Tr-Naphtol-604-44-4) were dissolved in 1 ml DD water. The solution was sterile filtered before application. To stop the reaction the embryos were washed several times in PBST and then fixated in 4 % PFA for 2 hours at RT or at 4 °C overnight. The fixative was washed out twice with PBST. Before the embryos could be stored in 75 % Glycerol/PBS at 4 °C, they were rinsed for 15 minutes in 50% Glycerol/PBS.

Hybridization mix (pH 6)	50 ml Formamide (Roth) 25 ml 20xSSC 1 ml Torula RNA (50 µg/ml; Sigma) 920 µl Cidric acid (1M; Sigma) 500 µl Tween 20 (Sigma) 50 µl Heparin (100 mg/ml; Applichem) fill up to 100 ml with DD water
20x SSC	88,23 g Sodium citrate (0,3 M; Sigma) 179 g NaCl (Sigma) fill up to 1 l with DD water
MAB	100 mM Maleicacid (pH 7,5; Sigma) 150 mM NaCl (Sigma) 0,1% Tween20 (Sigma)
Staining buffer (DIG)	5 ml 1 M Tris/HCl (pH 9; Sigma) 1 ml 5 M NaCl (Sigma) 2,5 ml 1 M MgCl2 (Sigma) 250 µl Tween20 (Sigma) fill up to 50 ml with DD water
Staining buffer (FITC)	0,1 M Tris/HCl (pH 8,3; Sigma) 0,1 % Tween20 (Sigma)

5.4 Whole mount antibody staining

For antibody staining, stored fish were rehydrated, digested and refixed as described in 5.3.3.. After the fixation, the fixative was washed out 5 times, for 5 minutes each, with PBSTr (PBS + 1% Triton-X-100; Roth). To block unspecific binding, embryos were subsequently incubated in Incubation buffer (IB) for at least one hour on a shaker. The primary antibody was diluted in 1 ml IB. The solution was added to the embryo sample and incubated at 4 °C over night on a shaking plate.

At the next day the primary antibody was removed by rinsing the embryos 3 times in PBSTr. The sample was washed 4 - 6 times for 30 minutes with PBSTr. Then, the secondary antibody was diluted in IB and added to the embryos. Fish were incubated at 4 °C on shaker in the dark over night on a shaking plate.

Fish were rinsed 3 times in PBSTr the next morning and washed 4 times for 30 minutes. Subsequently a nuclei counterstaining was performed. Therefore embryos were incubated in PBS, 0.8% Triton X-100, 1% bovine serum albumin (BSA) containing ToPro3 (1:1000, Molecular Probes-T3605) or Sytox orange (1:10000, Invitrogen-S11368) for 30 minutes on shaker. The nuclei labeling substrate was washed out three tines with PBS. The fish were immediately mounted and imaged.

Incubation buffer (IB)	10% NGS (normal goat serum; Invitrogen) 1% DMSO (Dimethyl Sulfoxide; Sigma) 0,8 % Triton-X-100 (Roth) in PBS (Sigma)

Antibody	**Dilution**	**Brand**	**Order No.**
Mouse anti-TCF3,4	1:400	USBiological	T2025.200
Rabbit anti-GFP	1:1000	Torrey Pines Biolabs	TP401
Rabbit anti-HuC/HuD	1:500	Molecular Probes	A21271
Alexa Fluor 488 Goat Anti-Mouse IgG	1:200	Invitrogen	A11001
Alexa Fluor 488 Goat Anti-Rabbit IgG	1:200	Invitrogen	A11034
Alexa Fluor 647 Goat Anti-Mouse IgG	1:200	Invitrogen	A21235
Alexa Fluor 647 Goat Anti-Rabbit IgG	1:200	Invitrogen	A21244

5.5 Labeling of habenular efferent projections

4 dpf tg(mp558b:GFP) wild type, tcf7l2$^{exl-/-}$ mutant and drug treated larvae were fixed by overnight incubation at 4°C in 4% paraformaldehyde + 4% sucrose (Sigma) in PBS (no Triton). At the next day the fixative was replaced by PBS.

Before every dye application, tungston needles (Tungston) had to be sharpened to a fine point by electrolytically eroding. Therefore tungsten filaments were covered with tin foil and clamped to the kathode of a transformer (Mascot). The anode was a metal rod. The filament was gently dipped into a saturated NaOH solution (Sigma) under a voltage of 8 - 19 mV till the solution formed bubbles. The procedure was repeated until the wire was sharp enough.

For dissection of the embryo brain, the fish were pined lateral with sharpened tungston needles in the trunk on a sylgard dish (Dowcorning). Dissection was performed with extrafine forceps (No. 5 Bio extrafine Dumont). Eyes were removed by cutting around the edges of the eyecup. The embryo had to be unpined to the other side for the removal of the second eye. The needles were then used to cut through the tissue from just above the notochord ventrally through the jaw and cardiac tissue at the anterior/posterior level of the otic vesicle. Subsequently, the needles and forceps were used to cut the skin between the main body and the yolk sac to remove the yolk as an intact structure. Forceps and needles were used to peel away the intestines and the jaw from the underside of the brain. Finally, the skin and hardtissue covering the brain were removed with the forceps by trying to grip flaps of skin and pull them rostrally. After dissection the brain should be free of any surrounding tissue and still attached to the body.

Dissected embryos were pinned dorsal up. Fluorescent carbocyanine dyes (1,1-dioctadecyl-3,3,3,3-tetramethylindocarbocyanine perchlorate (DiI; Sigma-D282) and 3,3'-dioctadecyloxacarbocyanine perchlorate (DiO; Sigma-D275) were applied to the tungsten needle. The dyes were resolved in ethanol and pipetted in small quantities (5 µl) onto a glass slide. The glass slide was moved around with the liquid dye as it dries. The procedure was repeated 5 times until a sticky goo formed. The tungston wire was gently turned in the dye. The needle was attached to micromanipulator (Narishige) and sticked into the habenulae and hold there for 3 minutes. The needle should not enter the ventral tissue to avoid unspecific staining and background signal. The procedure, including needle sharpening and dye application, was repeated 3 times on each habenula. After application the fish were unpinned and incubated overnight on 4 °C in PBS. At the next day, proper labeled brains were detached from the body and mounted in agarose (ventral side down/objective side) (see 5.9).

5.6 Laser cell ablation

Focal ablation of single parapineal cells in 27 - 30 hpf old tg(foxD3:GFP); tg(flh:eGFP) double transgenic and tg(mp558b:GFP); tg(foxD3:GFP); tg(flh:eGFP) triple transgenic embryos was performed using two-photon excitation at 800nm with a Chameleon tunable laser (Coherent) on an inverted microscope of A1R MP setup (Nikon).
For ablation and subsequent imaging a 40x water-immersion LWD 40xWI λS NA 1.15 Nano Crystal Coated objective (Nikon) was used. Anaesthetized embryos were immobilized in 1,2% low melt agarose containing 0,04 mg/ml tricaine. 29-31% laser power was used for acquisition as well as for laser ablation. 800nm laser beam was used to scan through 40x zoomed in region. 4 - 7 beams (4 msec each) were needed to destroy the parapineal region at the point of delamination from the pineal. Ablation was just performed when the parapineal cell cluster did not exhibit the left-orientation yet.
Embryos were imaged immediately and 3 days after ablation with a 3x zoom. In between fish were demounted from the agarose and let grown according to standard maintenance. At 4 dpf embryos were fixed for antibody staining and in situ hybridization.

5.7 Heatshock and IWR treatments

Heatshock treatments were performed with 33 hpf old tg(hsp70delta-tcf:GFP) embryos. Therefore embryos were dechorionated and transferred in a 50 ml tube filled with embryo medium. The tube was placed in a 40°C warm water bath for 30 minutes. Fish recovered for 30 minutes at room temperature before they were placed again for 30 minutes at 40°C. After 2 hours fish were sorted for their heatshock activated transgenic GFP fluorescence.
For drug treatment, dechorionated tg(mp558b:GFP) and tg(*fox*D3:GFP); tg(*flh*:eGFP) embryos were incubated in IWR-1 endo or IWR1-exo (4-(1,3,3a,4,7,7a-Hexahydro-1,3-dioxo-4,7-methano-2H-isoindol-2-yl)-N-8-quinolinyl-Benzamid, both 0.1 mM, Sigma-I0161) at 32 hpf for 12 hours or as indicated. Drugs were dissolved in 100% DMSO to a concentration of 10 mM. For drug treatment the solution was dissolved in embryo medium. After incubation, embryos were rinsed 4 times in embryo medium before they were bred till fixation under standard conditions.

5.8 Temperature shift and Morpholino injection

Laterality randomization was caused by raising 5 hpf old tg(*fox*D3:GFP); tg(*flh*:eGFP) double transgenic embryos for 16 hours at 22°C (Roussigné et al., 2009).
For manipulating Nodal signaling *no tail* (Nasevicius and Ekker, 2000; 8 ng/embryo) and *spw* (Long et al., 2003; 10 ng/embryo) morpholino oligonucleotides (MO; Gene Tools - Philomat) were injected at one cell stage into tg(*fox*D3:GFP); tg(*flh*:eGFP) transgenic fish.

MO *no tail*	5'- GACTTGAGGCAGGCATATTTCCGAT-3'
MO *spw*	5'- GCACGCTATGACTGGCTGCATTGCG-3'

5.9 Microscopy, Image manipulation and Statistical analysis

For differential interference contrast pictures a CTR6000 compound microscope (20x and 40x objectives; Leica) was used. Embryos were mounted in 75% glycerol between microscopic slides and cover glass for acquisition.
For confocal microscopy, a SP5 confocal laser-scanning microscope (Leica) was used. Therefore, stained and dissected embryo heads were mounted in 1.2% low melt agarose on the bottom of glass bottom dishes (LabTek Chamber slides-734-2057). Another possibility to mount the embryos was used by position the fish in glass rings. Therefore a microscopy slide was placed on the dissecting microscope. A 22x22 coverslip was placed on the slide and a glass ring (18x18; self-production) with silicon grease on top and bottom was pressed onto the slip. The warm agarose including the embryos were poured in the ring till it was 70% filled. After the embryos were positioned on the bottom and the agarose had been tried, PBS was filled in to form a convex meniscus over the top of the ring. Another slide was pressed down onto the top of the glass ring till it formed a watertight seal. The preparation was inverted and used for microscopy.
Z-stacks were acquired in 0.75-2 µm intervals using a 40x oil-immersion objective lense (40x1.3 Oil DIC III). Three-dimensional projections and maximum intensity projections were reconstructed from the stack of images using Volocity (Improvision). Pseudocoloring was performed using Photoshop CS4 (Adobe) software.
Three-dimensional projections were used to identify anti-Tcf7l2 and anti-HuC/D stained habenular cells. The outer cell layer was counted. Average, SD and percentage of Tcf7l2+ and/or HuC/D positve habenula cells were calculated using Prism 4 software (GraphPad Software).

6 REFERENCES

Abu-Khalil, A., Fu, L., Grove, E. A., Zecevic, N., & Geschwind, D. H. (2004). Wnt genes define distinct boundaries in the developing human brain: implications for human forebrain patterning. J Comp Neurol, 474(2), 276-288. doi: 10.1002/cne.20112

Agathocleous, M., Iordanova, I., Willardsen, M. I., Xue, X. Y., Vetter, M. L., Harris, W. A., & Moore, K. B. (2009). A directional Wnt/beta-catenin-Sox2-proneural pathway regulates the transition from proliferation to differentiation in the Xenopus retina. Development, 136(19), 3289-3299. doi: 10.1242/dev.040451

Agetsuma, M., Aizawa, H., Aoki, T., Nakayama, R., Takahoko, M., Goto, M., . . . Okamoto, H. (2010). The habenula is crucial for experience-dependent modification of fear responses in zebrafish. Nat Neurosci, 13(11), 1354-1356. doi: 10.1038/nn.2654

Aizawa, H., Bianco, I. H., Hamaoka, T., Miyashita, T., Uemura, O., Concha, M. L., . . . Okamoto, H. (2005). Laterotopic representation of left-right information onto the dorso-ventral axis of a zebrafish midbrain target nucleus. Curr Biol, 15(3), 238-243. doi: 10.1016/j.cub.2005.01.014

Aizawa, H., Goto, M., Sato, T., & Okamoto, H. (2007). Temporally regulated asymmetric neurogenesis causes left-right difference in the zebrafish habenular structures. Dev Cell, 12(1), 87-98. doi: 10.1016/j.devcel.2006.10.004

Amo, R., Aizawa, H., Takahoko, M., Kobayashi, M., Takahashi, R., Aoki, T., & Okamoto, H. (2010). Identification of the zebrafish ventral habenula as a homolog of the mammalian lateral habenula. J Neurosci, 30(4), 1566-1574. doi: 10.1523/JNEUROSCI.3690-09.2010

Arce, L., Yokoyama, N. N., & Waterman, M. L. (2006). Diversity of LEF/TCF action in development and disease. Oncogene, 25(57), 7492-7504. doi: 10.1038/sj.onc.1210056

Augustin, H. G., & Reiss, Y. (2003). EphB receptors and ephrinB ligands: regulators of vascular assembly and homeostasis. Cell Tissue Res, 314(1), 25-31. doi: 10.1007/s00441-003-0770-9

Bajoghli, B., Aghaallaei, N., Soroldoni, D., & Czerny, T. (2007). The roles of Groucho/Tle in left-right asymmetry and Kupffer's vesicle organogenesis. Dev Biol, 303(1), 347-361. doi: 10.1016/j.ydbio.2006.11.020

Baker, J. M., Stidworthy, M., Gull, T., Novak, J., Miller, J. M., & Antczak, D. F. (2001). Conservation of recognition of antibody and T-cell-defined alloantigens between species of equids. Reprod Fertil Dev, 13(7-8), 635-645.

Barami, K., Iversen, K., Furneaux, H., & Goldman, S. A. (1995). Hu protein as an early marker of neuronal phenotypic differentiation by subependymal zone cells of the adult songbird forebrain. J Neurobiol, 28(1), 82-101. doi: 10.1002/neu.480280108

Barker, N., Huls, G., Korinek, V., & Clevers, H. (1999). Restricted high level expression of Tcf-4 protein in intestinal and mammary gland epithelium. Am J Pathol, 154(1), 29-35. doi: 10.1016/S0002-9440(10)65247-9

Barth, K. A., Miklosi, A., Watkins, J., Bianco, I. H., Wilson, S. W., & Andrew, R. J. (2005). fsi zebrafish show concordant reversal of laterality of viscera, neuroanatomy, and a subset of behavioral responses. Curr Biol, 15(9), 844-850. doi: 10.1016/j.cub.2005.03.047

Beretta, C. A., Dross, N., Guiterrez-Triana, J. A., Ryu, S., & Carl, M. (2012). Habenula circuit development: past, present, and future. Front Neurosci, 6, 51. doi: 10.3389/fnins.2012.00051

Bianco, I. H., Carl, M., Russell, C., Clarke, J. D., & Wilson, S. W. (2008). Brain asymmetry is encoded at the level of axon terminal morphology. Neural Dev, 3, 9. doi: 10.1186/1749-8104-3-9

Bianco, I. H., & Wilson, S. W. (2009). The habenular nuclei: a conserved asymmetric relay station in the vertebrate brain. Philos Trans R Soc Lond B Biol Sci, 364(1519), 1005-1020. doi: 10.1098/rstb.2008.0213

Binder, J. (2000). The new neuroanatomy of speech perception. Brain, 123 Pt 12, 2371-2372.

Bluske, K. K., Vue, T. Y., Kawakami, Y., Taketo, M. M., Yoshikawa, K., Johnson, J. E., & Nakagawa, Y. (2012). beta-Catenin signaling specifies progenitor cell identity in parallel with Shh signaling in the developing mammalian thalamus. Development, 139(15), 2692-2702. doi: 10.1242/dev.072314

Caldecott-Hazard, S. (1988). Interictal changes in behavior and cerebral metabolism in the rat: opioid involvement. Exp Neurol, 99(1), 73-83.

Caneparo, L., Huang, Y. L., Staudt, N., Tada, M., Ahrendt, R., Kazanskaya, O., . . . Houart, C. (2007). Dickkopf-1 regulates gastrulation movements by coordinated modulation of Wnt/beta catenin and Wnt/PCP activities, through interaction with the Dally-like homolog Knypek. Genes Dev, 21(4), 465-480. doi: 10.1101/gad.406007

Carl, M., Bianco, I. H., Bajoghli, B., Aghaallaei, N., Czerny, T., & Wilson, S. W. (2007). Wnt/Axin1/beta-catenin signaling regulates asymmetric nodal activation, elaboration, and concordance of CNS asymmetries. Neuron, 55(3), 393-405. doi: 10.1016/j.neuron.2007.07.007

Caron, A., Xu, X., & Lin, X. (2012). Wnt/beta-catenin signaling directly regulates Foxj1 expression and ciliogenesis in zebrafish Kupffer's vesicle. Development, 139(3), 514-524. doi: 10.1242/dev.071746

Chapple, S. J., Siow, R. C., & Mann, G. E. (2012). Crosstalk between Nrf2 and the proteasome: therapeutic potential of Nrf2 inducers in vascular disease and aging. Int J Biochem Cell Biol, 44(8), 1315-1320. doi: 10.1016/j.biocel.2012.04.021

Clevers, H., & Nusse, R. (2012). Wnt/beta-catenin signaling and disease. Cell, 149(6), 1192-1205. doi: 10.1016/j.cell.2012.05.012

Concha, M. I., Molina, S., Oyarzun, C., Villanueva, J., & Amthauer, R. (2003). Local expression of apolipoprotein A-I gene and a possible role for HDL in primary defence in the carp skin. Fish Shellfish Immunol, 14(3), 259-273.

Concha, M. L., Burdine, R. D., Russell, C., Schier, A. F., & Wilson, S. W. (2000). A nodal signaling pathway regulates the laterality of neuroanatomical asymmetries in the zebrafish forebrain. Neuron, 28(2), 399-409.

Concha, M. L., Russell, C., Regan, J. C., Tawk, M., Sidi, S., Gilmour, D. T., . . . Wilson, S. W. (2003). Local tissue interactions across the dorsal midline of the forebrain establish CNS laterality. Neuron, 39(3), 423-438.

Concha, M. L., & Wilson, S. W. (2001). Asymmetry in the epithalamus of vertebrates. J Anat, 199(Pt 1-2), 63-84.

Crease, D. J., Dyson, S., & Gurdon, J. B. (1998). Cooperation between the activin and Wnt pathways in the spatial control of organizer gene expression. Proc Natl Acad Sci U S A, 95(8), 4398-4403.

Danos, M. C., & Yost, H. J. (1995). Linkage of cardiac left-right asymmetry and dorsal-anterior development in Xenopus. Development, 121(5), 1467-1474.

Dapretto, M., & Bookheimer, S. Y. (1999). Form and content: dissociating syntax and semantics in sentence comprehension. Neuron, 24(2), 427-432.

De Strooper, B., & Annaert, W. (2001). Where Notch and Wnt signaling meet. The presenilin hub. J Cell Biol, 152(4), F17-20.

Doll, C. A., Burkart, J. T., Hope, K. D., Halpern, M. E., & Gamse, J. T. (2011). Subnuclear development of the zebrafish habenular nuclei requires ER translocon function. Dev Biol, 360(1), 44-57. doi: 10.1016/j.ydbio.2011.09.003

Dufourcq, P., Rastegar, S., Strahle, U., & Blader, P. (2004). Parapineal specific expression of gfi1 in the zebrafish epithalamus. Gene Expr Patterns, 4(1), 53-57.

Ekstrom, P., & Ebbesson, S. O. (1988). The left habenular nucleus contains a discrete serotonin-immunoreactive subnucleus in the coho salmon (Oncorhynchus kisutch). Neurosci Lett, 91(2), 121-125.

Ekstrom, P., & Meissl, H. (2003). Evolution of photosensory pineal organs in new light: the fate of neuroendocrine photoreceptors. Philos Trans R Soc Lond B Biol Sci, 358(1438), 1679-1700. doi: 10.1098/rstb.2003.1303

Ellison, G. (2002). Neural degeneration following chronic stimulant abuse reveals a weak link in brain, fasciculus retroflexus, implying the loss of forebrain control circuitry. Eur Neuropsychopharmacol, 12(4), 287-297.

Essner, J. J., Amack, J. D., Nyholm, M. K., Harris, E. B., & Yost, H. J. (2005). Kupffer's vesicle is a ciliated organ of asymmetry in the zebrafish embryo that initiates left-right development of the brain, heart and gut. Development, 132(6), 1247-1260. doi: 10.1242/dev.01663

Falcon, J. (1999). Cellular circadian clocks in the pineal. Prog Neurobiol, 58(2), 121-162.

Falcon, J., Barraud, S., Thibault, C., & Begay, V. (1998). Inhibitors of messenger RNA and protein synthesis affect differently serotonin arylalkylamine N-acetyltransferase activity in clock-controlled and non clock-controlled fish pineal. Brain Res, 797(1), 109-117.

Faro, A., Boj, S. F., Ambrosio, R., van den Broek, O., Korving, J., & Clevers, H. (2009). T-cell factor 4 (tcf7l2) is the main effector of Wnt signaling during zebrafish intestine organogenesis. Zebrafish, 6(1), 59-68. doi: 10.1089/zeb.2009.0580

Fu, L., Zhang, C., Zhang, L. Y., Dong, S. S., Lu, L. H., Chen, J., . . . Guan, X. Y. (2011). Wnt2 secreted by tumour fibroblasts promotes tumour progression in oesophageal cancer by activation of the Wnt/beta-catenin signalling pathway. Gut, 60(12), 1635-1643. doi: 10.1136/gut.2011.241638

Galaburda, A. M. (1991). Asymmetries of cerebral neuroanatomy. Ciba Found Symp, 162, 219-226; discussion 226-233.

Gamse, J. T., Kuan, Y. S., Macurak, M., Brosamle, C., Thisse, B., Thisse, C., & Halpern, M. E. (2005). Directional asymmetry of the zebrafish epithalamus guides dorsoventral innervation of the midbrain target. Development, 132(21), 4869-4881. doi: 10.1242/dev.02046

Gamse, J. T., Shen, Y. C., Thisse, C., Thisse, B., Raymond, P. A., Halpern, M. E., & Liang, J. O. (2002). Otx5 regulates genes that show circadian expression in the zebrafish pineal complex. Nat Genet, 30(1), 117-121. doi: 10.1038/ng793

Gamse, J. T., Thisse, C., Thisse, B., & Halpern, M. E. (2003). The parapineal mediates left-right asymmetry in the zebrafish diencephalon. Development, 130(6), 1059-1068.

Geschwind, D. H. (2001). Sharing gene expression data: an array of options. Nat Rev Neurosci, 2(6), 435-438. doi: 10.1038/35077576

Geschwind, D. H., & Miller, B. L. (2001). Molecular approaches to cerebral laterality: development and neurodegeneration. Am J Med Genet, 101(4), 370-381.

Geschwind, N., & Levitsky, W. (1968). Human brain: left-right asymmetries in temporal speech region. Science, 161(3837), 186-187.

Gilmour, K. M., Shah, B., & Szebedinszky, C. (2002). An investigation of carbonic anhydrase activity in the gills and blood plasma of brown bullhead (Ameiurus nebulosus), longnose skate (Raja rhina), and spotted raffish (Hydrolagus colliei). J Comp Physiol B, 172(1), 77-86.

Glick, S. D., Ross, D. A., & Hough, L. B. (1982). Lateral asymmetry of neurotransmitters in human brain. Brain Res, 234(1), 53-63.

Grant, S. F., Thorleifsson, G., Reynisdottir, I., Benediktsson, R., Manolescu, A., Sainz, J., . . . Stefansson, K. (2006). Variant of transcription factor 7-like 2 (TCF7L2) gene confers risk of type 2 diabetes. Nat Genet, 38(3), 320-323. doi: 10.1038/ng1732

Gregorieff, A., Grosschedl, R., & Clevers, H. (2004). Hindgut defects and transformation of the gastro-intestinal tract in Tcf4(-/-)/Tcf1(-/-) embryos. EMBO J, 23(8), 1825-1833. doi: 10.1038/sj.emboj.7600191

Haddon, C., Smithers, L., Schneider-Maunoury, S., Coche, T., Henrique, D., & Lewis, J. (1998). Multiple delta genes and lateral inhibition in zebrafish primary neurogenesis. Development, 125(3), 359-370.

Halpern, M. E., Liang, J. O., & Gamse, J. T. (2003). Leaning to the left: laterality in the zebrafish forebrain. Trends Neurosci, 26(6), 308-313. doi: 10.1016/S0166-2236(03)00129-2

Hamada, H., Meno, C., Watanabe, D., & Saijoh, Y. (2002). Establishment of vertebrate left-right asymmetry. Nat Rev Genet, 3(2), 103-113. doi: 10.1038/nrg732

Harris, D. N., Bailey, S. M., Cowans, F., & Wertheim, D. (1996). Effect of optode separation on brain penetration in adults. Adv Exp Med Biol, 388, 133-135.

Harvey, S. A., Tumpel, S., Dubrulle, J., Schier, A. F., & Smith, J. C. (2010). no tail integrates two modes of mesoderm induction. Development, 137(7), 1127-1135. doi: 10.1242/dev.046318

Hayward, P., Kalmar, T., & Arias, A. M. (2008). Wnt/Notch signalling and information processing during development. Development, 135(3), 411-424. doi: 10.1242/dev.000505

Heisenberg, C. P., Houart, C., Take-Uchi, M., Rauch, G. J., Young, N., Coutinho, P., . . . Stemple, D. L. (2001). A mutation in the Gsk3-binding domain of zebrafish Masterblind/Axin1 leads to a fate transformation of telencephalon and eyes to diencephalon. Genes Dev, 15(11), 1427-1434. doi: 10.1101/gad.194301

Hirabayashi, Y., Itoh, Y., Tabata, H., Nakajima, K., Akiyama, T., Masuyama, N., & Gotoh, Y. (2004). The Wnt/beta-catenin pathway directs neuronal differentiation of cortical neural precursor cells. Development, 131(12), 2791-2801. doi: 10.1242/dev.01165

Holland, P. W., & Graham, A. (1995). Evolution of regional identity in the vertebrate nervous system. Perspect Dev Neurobiol, 3(1), 17-27.

Hoppler, S., & Kavanagh, C. L. (2007). Wnt signalling: variety at the core. J Cell Sci, 120(Pt 3), 385-393. doi: 10.1242/jcs.03363

Houart, C., Caneparo, L., Heisenberg, C., Barth, K., Take-Uchi, M., & Wilson, S. (2002). Establishment of the telencephalon during gastrulation by local antagonism of Wnt signaling. Neuron, 35(2), 255-265.

Huang, S., Shetty, P., Robertson, S. M., & Lin, R. (2007). Binary cell fate specification during C. elegans embryogenesis driven by reiterated reciprocal asymmetry of TCF POP-1 and its coactivator beta-catenin SYS-1. Development, 134(14), 2685-2695. doi: 10.1242/dev.008268

Hurlstone, A. F., Haramis, A. P., Wienholds, E., Begthel, H., Korving, J., Van Eeden, F., . . . Clevers, H. (2003). The Wnt/beta-catenin pathway regulates cardiac valve formation. Nature, 425(6958), 633-637. doi: 10.1038/nature02028

Husken, U., & Carl, M. (2012). The Wnt/beta-catenin signaling pathway establishes neuroanatomical asymmetries and their laterality. Mech Dev. doi: 10.1016/j.mod.2012.09.002

Inbal, A., Kim, S. H., Shin, J., & Solnica-Krezel, L. (2007). Six3 represses nodal activity to establish early brain asymmetry in zebrafish. Neuron, 55(3), 407-415. doi: 10.1016/j.neuron.2007.06.037

Itoh, M., Kim, C. H., Palardy, G., Oda, T., Jiang, Y. J., Maust, D., . . . Chitnis, A. B. (2003). Mind bomb is a ubiquitin ligase that is essential for efficient activation of Notch signaling by Delta. Dev Cell, 4(1), 67-82.

Jiang, Y. J., Brand, M., Heisenberg, C. P., Beuchle, D., Furutani-Seiki, M., Kelsh, R. N., . . . Nusslein-Volhard, C. (1996). Mutations affecting neurogenesis and brain morphology in the zebrafish, Danio rerio. Development, 123, 205-216.

Kanwar, S. S., Poolla, A., & Majumdar, A. P. (2012). Regulation of colon cancer recurrence and development of therapeutic strategies. World J Gastrointest Pathophysiol, 3(1), 1-9. doi: 10.4291/wjgp.v3.i1.1

Kemali, M., Sada, E., & Fiorino, L. (1990). Superficial and deep blood vessel distribution in the frog telencephalon. Reference to morphological brain asymmetries. Z Mikrosk Anat Forsch, 104(2), 305-315.

Klein, D. C., & Moore, R. Y. (1979). Pineal N-acetyltransferase and hydroxyindole-O-methyltransferase: control by the retinohypothalamic tract and the suprachiasmatic nucleus. Brain Res, 174(2), 245-262.

Korinek, V., Barker, N., Willert, K., Molenaar, M., Roose, J., Wagenaar, G., . . . Clevers, H. (1998). Two members of the Tcf family implicated in Wnt/beta-catenin signaling during embryogenesis in the mouse. Mol Cell Biol, 18(3), 1248-1256.

Kuan, Y. S., Gamse, J. T., Schreiber, A. M., & Halpern, M. E. (2007). Selective asymmetry in a conserved forebrain to midbrain projection. J Exp Zool B Mol Dev Evol, 308(5), 669-678. doi: 10.1002/jez.b.21184

Kuan, Y. S., Yu, H. H., Moens, C. B., & Halpern, M. E. (2007). Neuropilin asymmetry mediates a left-right difference in habenular connectivity. Development, 134(5), 857-865. doi: 10.1242/dev.02791

Lagutin, O. V., Zhu, C. C., Kobayashi, D., Topczewski, J., Shimamura, K., Puelles, L., . . . Oliver, G. (2003). Six3 repression of Wnt signaling in the anterior neuroectoderm is essential for vertebrate forebrain development. Genes Dev, 17(3), 368-379. doi: 10.1101/gad.1059403

Larsen, J. P., Hoien, T., Lundberg, I., & Odegaard, H. (1990). MRI evaluation of the size and symmetry of the planum temporale in adolescents with developmental dyslexia. Brain Lang, 39(2), 289-301.

Lecourtier, L., & Kelly, P. H. (2005). Bilateral lesions of the habenula induce attentional disturbances in rats. Neuropsychopharmacology, 30(3), 484-496. doi: 10.1038/sj.npp.1300595

Lecourtier, L., Neijt, H. C., & Kelly, P. H. (2004). Habenula lesions cause impaired cognitive performance in rats: implications for schizophrenia. Eur J Neurosci, 19(9), 2551-2560. doi: 10.1111/j.0953-816X.2004.03356.x

Lee, E. H., & Huang, S. L. (1988). Role of lateral habenula in the regulation of exploratory behavior and its relationship to stress in rats. Behav Brain Res, 30(3), 265-271.

Liang, J. O., Etheridge, A., Hantsoo, L., Rubinstein, A. L., Nowak, S. J., Izpisua Belmonte, J. C., & Halpern, M. E. (2000). Asymmetric nodal signaling in the zebrafish diencephalon positions the pineal organ. Development, 127(23), 5101-5112.

Linask, K. K., Han, M., Cai, D. H., Brauer, P. R., & Maisastry, S. M. (2005). Cardiac morphogenesis: matrix metalloproteinase coordination of cellular mechanisms underlying heart tube formation and directionality of looping. Dev Dyn, 233(3), 739-753. doi: 10.1002/dvdy.20377

Lisoprawski, A., Herve, D., Blanc, G., Glowinski, J., & Tassin, J. P. (1980). Selective activation of the mesocortico-frontal dopaminergic neurons induced by lesion of the habenula in the rat. Brain Res, 183(1), 229-234.

Loewenstein, D. A., Amigo, E., Duara, R., Guterman, A., Hurwitz, D., Berkowitz, N., . . . et al. (1989). A new scale for the assessment of functional status in Alzheimer's disease and related disorders. J Gerontol, 44(4), P114-121.

Long, S., Ahmad, N., & Rebagliati, M. (2003). The zebrafish nodal-related gene southpaw is required for visceral and diencephalic left-right asymmetry. Development, 130(11), 2303-2316.

Lu, J., Ma, Z., Hsieh, J. C., Fan, C. W., Chen, B., Longgood, J. C., . . . Chen, C. (2009). Structure-activity relationship studies of small-molecule inhibitors of Wnt response. Bioorg Med Chem Lett, 19(14), 3825-3827. doi: 10.1016/j.bmcl.2009.04.040

MacDonald, B. T., Tamai, K., & He, X. (2009). Wnt/beta-catenin signaling: components, mechanisms, and diseases. Dev Cell, 17(1), 9-26. doi: 10.1016/j.devcel.2009.06.016

Mao, C. D., & Byers, S. W. (2011). Cell-context dependent TCF/LEF expression and function: alternative tales of repression, de-repression and activation potentials. Crit Rev Eukaryot Gene Expr, 21(3), 207-236.

Marlow, F., Gonzalez, E. M., Yin, C., Rojo, C., & Solnica-Krezel, L. (2004). No tail co-operates with non-canonical Wnt signaling to regulate posterior body morphogenesis in zebrafish. Development, 131(1), 203-216. doi: 10.1242/dev.00915

McGrew, L. L., Lai, C. J., & Moon, R. T. (1995). Specification of the anteroposterior neural axis through synergistic interaction of the Wnt signaling cascade with noggin and follistatin. Dev Biol, 172(1), 337-342. doi: 10.1006/dbio.1995.0027

McMahon, A. P., & Bradley, A. (1990). The Wnt-1 (int-1) proto-oncogene is required for development of a large region of the mouse brain. Cell, 62(6), 1073-1085.

Meyers, J. R., Hu, L., Moses, A., Kaboli, K., Papandrea, A., & Raymond, P. A. (2012). ss-catenin/Wnt signaling controls progenitor fate in the developing and regenerating zebrafish retina. Neural Dev, 7(1), 30. doi: 10.1186/1749-8104-7-30

Minguillon, C., Ferrier, D. E., Cebrian, C., & Garcia-Fernandez, J. (2002). Gene duplications in the prototypical cephalochordate amphioxus. Gene, 287(1-2), 121-128.

Moro, E., Ozhan-Kizil, G., Mongera, A., Beis, D., Wierzbicki, C., Young, R. M., . . . Argenton, F. (2012). In vivo Wnt signaling tracing through a transgenic biosensor fish reveals novel activity domains. Dev Biol, 366(2), 327-340. doi: 10.1016/j.ydbio.2012.03.023

Muller, M., Akinturk, H., Schindler, E., Brau, M., Scholz, S., Valeske, K., . . . Hempelmann, G. (2003). A combined stage 1 and 2 repair for hypoplastic left heart syndrome: anaesthetic considerations. Paediatr Anaesth, 13(4), 360-365.

Muller, Y. L., Yueh, Y. G., Yaworsky, P. J., Salbaum, J. M., & Kappen, C. (2003). Caudal dysgenesis in Islet-1 transgenic mice. FASEB J, 17(10), 1349-1351. doi: 10.1096/fj.02-0856fje

Muncan, V., Faro, A., Haramis, A. P., Hurlstone, A. F., Wienholds, E., van Es, J., . . . Clevers, H. (2007). T-cell factor 4 (Tcf7l2) maintains proliferative compartments in zebrafish intestine. EMBO Rep, 8(10), 966-973. doi: 10.1038/sj.embor.7401071

Munoz-Descalzo, S., Tkocz, K., Balayo, T., & Arias, A. M. (2011). Modulation of the ligand-independent traffic of Notch by Axin and Apc contributes to the activation of Armadillo in Drosophila. Development, 138(8), 1501-1506. doi: 10.1242/dev.061309

Nakaya, M. A., Biris, K., Tsukiyama, T., Jaime, S., Rawls, J. A., & Yamaguchi, T. P. (2005). Wnt3a links left-right determination with segmentation and anteroposterior axis elongation. Development, 132(24), 5425-5436. doi: 10.1242/dev.02149

Nascone, N., & Mercola, M. (1997). Organizer induction determines left-right asymmetry in Xenopus. Dev Biol, 189(1), 68-78. doi: 10.1006/dbio.1997.8635

Nasevicius, A., & Ekker, S. C. (2000). Effective targeted gene 'knockdown' in zebrafish. Nat Genet, 26(2), 216-220. doi: 10.1038/79951

Niikura, Y., Tabata, Y., Tajima, A., Inoue, I., Arai, K., & Watanabe, S. (2006). Zebrafish Numb homologue: phylogenetic evolution and involvement in regulation of left-right asymmetry. Mech Dev, 123(5), 407-414. doi: 10.1016/j.mod.2006.03.008

Oertel, V., Knochel, C., Rotarska-Jagiela, A., Schonmeyer, R., Lindner, M., van de Ven, V., . . . Linden, D. E. (2010). Reduced laterality as a trait marker of schizophrenia--evidence from structural and functional neuroimaging. J Neurosci, 30(6), 2289-2299. doi: 10.1523/JNEUROSCI.4575-09.2010

Oh, H., Chun, C. H., & Chun, J. S. (2012). Dkk-1 expression in chondrocytes inhibits experimental osteoarthritic cartilage destruction in mice. Arthritis Rheum, 64(8), 2568-2578. doi: 10.1002/art.34481

Ohi, Y., & Wright, C. V. (2007). Anteriorward shifting of asymmetric Xnr1 expression and contralateral communication in left-right specification in Xenopus. Dev Biol, 301(2), 447-463. doi: 10.1016/j.ydbio.2006.08.021

Ortiz, C. O., Faumont, S., Takayama, J., Ahmed, H. K., Goldsmith, A. D., Pocock, R., . . . Hobert, O. (2009). Lateralized gustatory behavior of C. elegans is controlled by specific receptor-type guanylyl cyclases. Curr Biol, 19(12), 996-1004. doi: 10.1016/j.cub.2009.05.043

Park, H. C., Kim, C. H., Bae, Y. K., Yeo, S. Y., Kim, S. H., Hong, S. K., . . . Huh, T. L. (2000). Analysis of upstream elements in the HuC promoter leads to the establishment of transgenic zebrafish with fluorescent neurons. Dev Biol, 227(2), 279-293. doi: 10.1006/dbio.2000.9898

Qu, J., Volpicelli, F. M., Garcia, L. I., Sandeep, N., Zhang, J., Marquez-Rosado, L., . . . Fishman, G. I. (2009). Gap junction remodeling and spironolactone-dependent reverse remodeling in the hypertrophied heart. Circ Res, 104(3), 365-371. doi: 10.1161/CIRCRESAHA.108.184044

Raya, A., Kawakami, Y., Rodriguez-Esteban, C., Buscher, D., Koth, C. M., Itoh, T., . . . Izpisua Belmonte, J. C. (2003). Notch activity induces Nodal expression and mediates the establishment of left-right asymmetry in vertebrate embryos. Genes Dev, 17(10), 1213-1218. doi: 10.1101/gad.1084403

Regan, J. C., Concha, M. L., Roussigne, M., Russell, C., & Wilson, S. W. (2009). An Fgf8-dependent bistable cell migratory event establishes CNS asymmetry. Neuron, 61(1), 27-34. doi: 10.1016/j.neuron.2008.11.030

Renteria, M. E. (2012). Cerebral asymmetry: a quantitative, multifactorial, and plastic brain phenotype. Twin Res Hum Genet, 15(3), 401-413. doi: 10.1017/thg.2012.13

Rodriguez-Esteban, C., Capdevila, J., Kawakami, Y., & Izpisua Belmonte, J. C. (2001). Wnt signaling and PKA control Nodal expression and left-right determination in the chick embryo. Development, 128(16), 3189-3195.

Roose, J., & Clevers, H. (1999). TCF transcription factors: molecular switches in carcinogenesis. Biochim Biophys Acta, 1424(2-3), M23-37.

Roussigne, M., Bianco, I. H., Wilson, S. W., & Blader, P. (2009). Nodal signalling imposes left-right asymmetry upon neurogenesis in the habenular nuclei. Development, 136(9), 1549-1557. doi: 10.1242/dev.034793

Saegusa, M., Hashimura, M., Kuwata, T., Hamano, M., & Okayasu, I. (2005). Upregulation of TCF4 expression as a transcriptional target of beta-catenin/p300 complexes during trans-differentiation of endometrial carcinoma cells. Lab Invest, 85(6), 768-779. doi: 10.1038/labinvest.3700273

Schier, A. F. (2001). Axis formation and patterning in zebrafish. Curr Opin Genet Dev, 11(4), 393-404.

Schlueter, J., & Brand, T. (2007). Left-right axis development: examples of similar and divergent strategies to generate asymmetric morphogenesis in chick and mouse embryos. Cytogenet Genome Res, 117(1-4), 256-267. doi: 10.1159/000103187

Schneider, I., Schneider, P. N., Derry, S. W., Lin, S., Barton, L. J., Westfall, T., & Slusarski, D. C. (2010). Zebrafish Nkd1 promotes Dvl degradation and is required for left-right patterning. Dev Biol, 348(1), 22-33. doi: 10.1016/j.ydbio.2010.08.040

Shitashige, M., Hirohashi, S., & Yamada, T. (2008). Wnt signaling inside the nucleus. Cancer Sci, 99(4), 631-637. doi: 10.1111/j.1349-7006.2007.00716.x

Signore, I. A., Guerrero, N., Loosli, F., Colombo, A., Villalon, A., Wittbrodt, J., & Concha, M. L. (2009). Zebrafish and medaka: model organisms for a comparative developmental approach of brain asymmetry. Philos Trans R Soc Lond B Biol Sci, 364(1519), 991-1003. doi: 10.1098/rstb.2008.0260

Struewing, I., Boyechko, T., Barnett, C., Beildeck, M., Byers, S. W., & Mao, C. D. (2010). The balance of TCF7L2 variants with differential activities in Wnt-signaling is regulated by lithium in a GSK3beta-independent manner. Biochem Biophys Res Commun, 399(2), 245-250. doi: 10.1016/j.bbrc.2010.07.062

Tabin, C. J. (2006). The key to left-right asymmetry. Cell, 127(1), 27-32. doi: 10.1016/j.cell.2006.09.018

Tanaka, S., Terada, K., & Nohno, T. (2011). Canonical Wnt signaling is involved in switching from cell proliferation to myogenic differentiation of mouse myoblast cells. J Mol Signal, 6, 12. doi: 10.1186/1750-2187-6-12

Tanaka, S. S., Kojima, Y., Yamaguchi, Y. L., Nishinakamura, R., & Tam, P. P. (2011). Impact of WNT signaling on tissue lineage differentiation in the early mouse embryo. Dev Growth Differ, 53(7), 843-856. doi: 10.1111/j.1440-169X.2011.01292.x

Teufel, C., Ghazanfar, A. A., & Fischer, J. (2010). On the relationship between lateralized brain function and orienting asymmetries. Behav Neurosci, 124(4), 437-445. doi: 10.1037/a0019925

Thisse, B., Heyer, V., Lux, A., Alunni, V., Degrave, A., Seiliez, I., . . . Thisse, C. (2004). Spatial and temporal expression of the zebrafish genome by large-scale in situ hybridization screening. Methods Cell Biol, 77, 505-519.

Toga, A. W., & Thompson, P. M. (2003). Mapping brain asymmetry. Nat Rev Neurosci, 4(1), 37-48. doi: 10.1038/nrn1009

Tran, H. T., Sekkali, B., Van Imschoot, G., Janssens, S., & Vleminckx, K. (2010). Wnt/beta-catenin signaling is involved in the induction and maintenance of primitive hematopoiesis in the vertebrate embryo. Proc Natl Acad Sci U S A, 107(37), 16160-16165. doi: 10.1073/pnas.1007725107

Vacik, T., & Lemke, G. (2011). Dominant-negative isoforms of Tcf/Lef proteins in development and disease. Cell Cycle, 10(24), 4199-4200. doi: 10.4161/cc.10.24.18465

Valjakka, A., Vartiainen, J., Tuomisto, L., Tuomisto, J. T., Olkkonen, H., & Airaksinen, M. M. (1998). The fasciculus retroflexus controls the integrity of REM sleep by supporting the generation of hippocampal theta rhythm and rapid eye movements in rats. Brain Res Bull, 47(2), 171-184.

Veeman, M. T., Axelrod, J. D., & Moon, R. T. (2003). A second canon. Functions and mechanisms of beta-catenin-independent Wnt signaling. Dev Cell, 5(3), 367-377.

Veeman, M. T., Slusarski, D. C., Kaykas, A., Louie, S. H., & Moon, R. T. (2003). Zebrafish prickle, a modulator of noncanonical Wnt/Fz signaling, regulates gastrulation movements. Curr Biol, 13(8), 680-685.

Veien, E. S., Grierson, M. J., Saund, R. S., & Dorsky, R. I. (2005). Expression pattern of zebrafish tcf7 suggests unexplored domains of Wnt/beta-catenin activity. Dev Dyn, 233(1), 233-239. doi: 10.1002/dvdy.20330

Wang, H., Lei, Q., Oosterveen, T., Ericson, J., & Matise, M. P. (2011). Tcf/Lef repressors differentially regulate Shh-Gli target gene activation thresholds to generate progenitor patterning in the developing CNS. Development, 138(17), 3711-3721. doi: 10.1242/dev.068270

Wang, R., Xie, H., Huang, Z., Ma, J., Fang, X., Ding, Y., & Sun, Z. (2011). T cell factor 1 regulates thymocyte survival via a RORgammat-dependent pathway. J Immunol, 187(11), 5964-5973. doi: 10.4049/jimmunol.1101205

Warner, J. F., Lyons, D. C., & McClay, D. R. (2012). Left-Right Asymmetry in the Sea Urchin Embryo: BMP and the Asymmetrical Origins of the Adult. PLoS Biol, 10(10), e1001404. doi: 10.1371/journal.pbio.1001404

Weidinger, G., Thorpe, C. J., Wuennenberg-Stapleton, K., Ngai, J., & Moon, R. T. (2005). The Sp1-related transcription factors sp5 and sp5-like act downstream of Wnt/beta-catenin signaling in mesoderm and neuroectoderm patterning. Curr Biol, 15(6), 489-500. doi: 10.1016/j.cub.2005.01.041

Wen, L., Wei, W., Gu, W., Huang, P., Ren, X., Zhang, Z., . . . Zhang, B. (2008). Visualization of monoaminergic neurons and neurotoxicity of MPTP in live transgenic zebrafish. Dev Biol, 314(1), 84-92. doi: 10.1016/j.ydbio.2007.11.012

Wes, P.D.; Bargmann, C.I. (2001). C. elegans odour discrimination requires asymmetric diversity in olfactory neurons. Nature, 410(6829), 698-701.

Wree, A., Zilles, K., & Schleicher, A. (1981). Growth of fresh volumes and spontaneous cell death in the nuclei habenulae of albino rats during ontogenesis. Anat Embryol (Berl), 161(4), 419-431.

Yanagawa, N., Sakabe, M., Sakata, H., Yamagishi, T., & Nakajima, Y. (2011). Nodal signal is required for morphogenetic movements of epiblast layer in the pre-streak chick blastoderm. Dev Growth Differ, 53(3), 366-377. doi: 10.1111/j.1440-169X.2010.01244.x

Yanez, J., & Anadon, R. (1994). Afferent and efferent connections of the habenula in the larval sea lamprey (Petromyzon marinus L.): an experimental study. J Comp Neurol, 345(1), 148-160. doi: 10.1002/cne.903450112

Yang, L. M., Hu, B., Xia, Y. H., Zhang, B. L., & Zhao, H. (2008). Lateral habenula lesions improve the behavioral response in depressed rats via increasing the serotonin level in dorsal raphe nucleus. Behav Brain Res, 188(1), 84-90. doi: 10.1016/j.bbr.2007.10.022

Yost, C., Farr, G. H., 3rd, Pierce, S. B., Ferkey, D. M., Chen, M. M., & Kimelman, D. (1998). GBP, an inhibitor of GSK-3, is implicated in Xenopus development and oncogenesis. Cell, 93(6), 1031-1041.

Young, R. M., Reyes, A. E., & Allende, M. L. (2002). Expression and splice variant analysis of the zebrafish tcf4 transcription factor. Mech Dev, 117(1-2), 269-273.

Yu, S., Avery, L., Baude, E., & Garbers, D. L. (1997). Guanylyl cyclase expression in specific sensory neurons: a new family of chemosensory receptors. Proc Natl Acad Sci U S A, 94(7), 3384-3387.

Zhang, M., Zhang, J., Lin, S. C., & Meng, A. (2012). beta-Catenin 1 and beta-catenin 2 play similar and distinct roles in left-right asymmetric development of zebrafish embryos. Development, 139(11), 2009-2019. doi: 10.1242/dev.074435

Zilles, K., Dabringhaus, A., Geyer, S., Amunts, K., Qu, M., Schleicher, A., . . . Steinmetz, H. (1996). Structural asymmetries in the human forebrain and the forebrain of non-human primates and rats. Neurosci Biobehav Rev, 20(4), 593-605.

Zilles, K., Schleicher, A., & Wingert, F. (1976). [Quantitative growth analysis of limbic nuclei areas fresh volume in diencephalon and mesencephalon of an albino mouse ontogenic series. I. Nucleus habenulare]. J Hirnforsch, 17(1), 1-10.

7 APPENDIX

7.1 Transient interference of Wnt/beta-catenin signaling

hpf	wt	rev	bi-left	bi-right	absent	n
IWRendo 32-48 *lov*	11 (100)	0 (0)	89 (0)	0 (0)	0 (0)	35 (21)
IWRendo 32-48 *dex*	100 (100)	0 (0)	0 (0)	0 (0)	0 (0)	32 (26)
IWRendo 32-48 *mp558:GFP*	15 (100)	0 (0)	85 (0)	0 (0)	0 (0)	27 (10)
IWRendo 32-48 *brn3a:GFP*	88 (100)	0 (0)	0 (0)	12 (0)	0 (0)	16 (14)
IWRendo 32-48 DiI/DiO	27 (100)	0 (0)	73* (0)	0 (0)	0 (0)	11 (5)
Hsp70-Dtcf:GFP hs: 33 *lov*	61 (100)	8 (0)	31 (0)	0 (0)	0 (0)	13 (12)
Hsp70-Dtcf:GFP hs: 33 *dex*	100 (100)	0 (0)	0 (0)	0 (0)	0 (0)	12 (12)
IWR 28-30	100	0	0	0	0	20
IWR 30-32	90	0	10	0	0	20
IWR 32-33	80	0	20	0	0	20
IWR 32-33	80	0	20	0	0	20
IWR 32-34	20	0	80	0	0	10
IWR 34-35	25	0	75	0	0	20
IWR 34-36	10	0	90	0	0	10
IWR 35-36	20	0	80	0	0	20
IWR 36-37	75	0	25	0	0	20
IWR 36-38	30	0	70	0	0	10
IWR 37-39	70	0	30	0	0	20
IWR 39-41	100	0	0	0	0	20
IWR 41-43	91	0	9	0	0	11
IWR 43-47	100	0	0	0	0	10
IWR 47-51	100	0	0	0	0	12
IWR 51-55	100	0	0	0	0	10

In brackets IWR: IWRexo treatments; in brackets heat shock: Not green embryos after heat shock; * bi-dorsal, 4 complete and 4 partial

7.2 Original pictures of anti-Tcf7l2 stainings

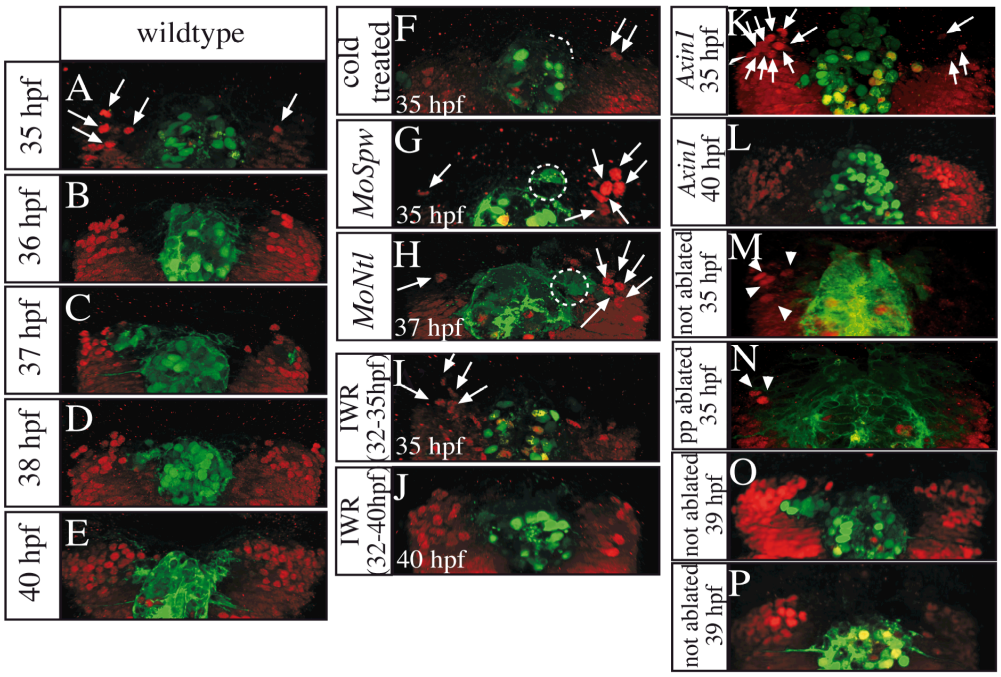

7.3 Numbers of Tcf7l2 and/or HuC/D expressing cells

HuC/D positive cells in wildtype

	wildtype		*tcf7l2*	
	L	**R**	**L**	**R**
39 hpf	22	17	19	14
	12	9	20	18
	17	16	13	8
	23	15	24	21
	16	13	13	11
	14	8	12	11
	11	6	14	9
	24	18	21	18
	20	17	23	15
	22	17	19	14
48 hpf	40	31	33	26
	38	27	49	37
	28	20	31	20
	34	26	38	45
	22	18	28	20
	27	24	31	32
	40	34	28	17
	32	26	24	19
	45	38	33	37
	29	21	46	37
	40	31	33	26
	38	27	49	37

Tcf7l2 positive cells in wildtype

	L	R
34 hpf	0	0
	0	0
	0	0
	0	0
	0	0
	0	0
	0	0
	0	0
	0	0
	0	0
35 hpf	6	2
	6	2
	5	1
	4	2
	5	3
	6	2
	4	0
	2	0
	4	2
	6	1
36 hpf	11	6
	13	7
	14	9
	15	8
	11	6
	13	10
	9	6
	9	11
	10	6
	14	6

	L	R
37 hpf	23	20
	24	20
	16	16
	14	17
	15	9
	16	9
	13	12
	16	9
	17	14
	12	11
38 hpf	17	22
	23	26
	34	26
	25	17
	21	18
	23	23
	27	25
	20	15
	14	16
	27	17
40 hpf	31	46
	41	29
	27	31
	33	35
	41	33
	32	37
	42	48
	37	31
	30	26
	26	22

Co-expression of HuC/D and Tcf7l2

	L			R		
	HuC/D+	TCF+	HuC/D and TCF	HuC/D+	TCF+	HuC/D and TCF
38 hpf	15	14	4	6	11	1
	15	17	8	13	15	7
	14	15	9	9	11	4
	12	10	8	7	5	5
	16	13	8	12	12	7
	11	10	6	8	9	3
	8	12	4	4	11	0
	11	11	3	8	7	4
	6	12	3	4	11	2
40 hpf	23	24	13	9	15	8
	32	34	36	31	34	31
	41	41	41	29	35	29
	35	37	35	28	30	27
	18	27	13	20	28	13
	30	29	27	24	26	22
	25	21	17	11	17	7
	31	33	31	23	27	23
	34	36	34	27	28	25
	28	34	26	23	28	23

***Axin1* mutants and IWRendo treated embryos**

	Axin1		IWRendo	
	L	R	L	R
35 hpf	18	11	3	0
	19	9	2	1
	18	6	2	0
	22	17	6	2
	12	8	7	3
	11	5	1	0
	13	6	2	1
	6	3	3	2
	6	3	1	0
	9	5	2	0
40 hpf	36	31	24	15
	45	31	18	10
	49	45	24	27
	32	27	9	4
	27	25	7	6
	30	21	8	5
	22	24	14	17
	22	19	20	14
	23	35	21	17
	37	31	17	13

Nodal manipulation

	coldtreated		Mo*Ntl*		Mo*Spw*	
	L	**R**	**L**	**R**	**L**	**R**
35 hpf	1	0	1	1	1	1
/	2	0	2	2	2	7
37 hpf	3	0	3	5	3	7
(MoNtl)	4	4	4	4	4	3
	5	3	5	1	5	4
	6	2	6	5	6	5
	7	4	7	6	7	5
	8	3	8	0	8	2
	9	3	9	4	9	2
	10	5	10	4	10	5
39 hpf	26	24	30	28	30	28
	28	24	28	20	28	20
	27	30	19	20	19	20
	21	23	28	24	28	24
	26	22	27	23	27	23
	23	24	25	26	25	26
	24	27	19	21	19	21
	24	19	26	23	26	23
	27	22	29	34	29	34
	27	25	26	29	26	29

Parapineal (PP) ablation

	pp not ablated		pp ablated	
	L	**R**	**L**	**R**
35 hpf	6	2	0	0
	6	2	2	1
	5	1	2	0
	4	2	3	2
	5	3	3	1
	6	2	4	2
	4	0	6	4
	2	0	2	1
	4	2	-	-
	6	1	-	-
39 hpf	26	24	30	28
	28	24	28	20
	27	30	19	20
	21	23	28	24
	26	22	27	23
	23	24	25	26
	24	27	19	21
	24	19	26	23
	27	22	29	34
	27	25	26	29
	-	-	20	19
	-	-	23	21

7.4 Lists of figures and abbreviations

List of figures

Figure 1.1:	Asymmetric regions of the zebrafish brain.	4
Figure 1.2:	Habenula-IPN asymmetry in the zebrafish brain.	6
Figure 1.3:	Model of asymmetric habenular development.	8
Figure 1.4:	Functions of Wnt/beta-catenin signaling during the establishment of brain asymmetry.	15
Figure 1.5:	Three different *tcf7l2* mutations cause symmetric dHbl marker expression.	17
Figure 3.1:	*tcf7l2* mutant exhibit double left sided lateral marker expression.	21
Figure 3.2:	*tcf7l2* mutant exhibit symmetric medial and absent right-sided marker expression.	22
Figure 3.3:	*tcf7l2* mutant develop symmetric habenulae with left-sided character symmetrically innervating the dorsal IPN.	23
Figure 3.4:	The expression of precursor cell marker *cxcr4b* is not altered in *tcf7l2* mutant.	24
Figure 3.5:	The early steps of habenula formation are not affected in *tcf7l2* mutants.	25
Figure 3.6:	*Axin1* acts upstream *tcf7l2* during formation of habenular asymmetry.	27
Figure 3.7:	Transient inhibition of Wnt/beta-catenin signaling causes an increase of dHbl cells on the right side.	29
Figure 3.8:	Artificial downregulation of Wnt/beta-catenin signaling with IWRendo mimic *tcf7l2* mutant phenotype.	30
Figure 3.9:	Wnt signaling is asymmetric active in the dorsal diencephalon as from 34 hpf.	33
Figure 3.10:	Artificial downregulation of Wnt signaling around 35 hpf results in an increased right dHbl subnucleus.	34
Figure 3.11:	*tcf7l2* expression in the diencephalon during habenula development.	35
Figure 3.12:	Anti-Human TCF3,4 detects zebrafish Tcf7l2 protein.	36
Figure 3.13:	Tcf7l2 protein is asymmetrically expressed across the left-right axis.	37
Figure 3.14:	Tcf7l2 is expressed in habenula precursor cells.	39

Figure 3.15: Tcf7l2 is expressed in differentiating habenula neurons. 39
Figure 3.16: Tcf7l2 is expressed in the entire dorsal habenula at 4dpf. 40
Figure 3.17: Tcf7l2 expression in habenular cells is regulated by Wnt signaling. 41
Figure 3.18: Nodal gene laterality is not altered in *tcf7l2* mutants. 44
Figure 3.19: Altered Nodal signaling does not influence asymmetrically Tcf7l2 distribution. 45
Figure 3.20: Left-directed parapineal migration is not altered in *tcf7l2* mutant. 46
Figure 3.21: Absence of parapineal cells does not influence *tcf7l2* mutant phenotype. 47
Figure 3.22: Absence of parapineal cells does not influence Tcf7l2 expression. 48
Figure 4.1: Model of habenular asymmetry establishment caused by Tcf7l2 and parapineal signals. 63

List of abbreviations

A	adenosine
ace	acerebellar
ALP	alster paullone
ANP	anterior neural plate
APC	adenomatous polyposis coli
BCIP	4-toluidine salt
bp	basepairs
brn3a	brain 3a
BSA	bovine serum albumin
C	cytosine
c. elegans	Caenorhabditis elegans
cpd2	cerebellum postnatal development associated protein 2
CTNNB1	catenin (cadherin-associated protein), beta 1
cxcr4b	C-X-C chemokine receptorr 4b
cyc	cyclops
d	dorsal
DNA	deoxyribonucleic acid
DD	double destilated
DDC	dorsal diencephalic conduction system
dex	dexter
dHb	dorsal habenula

dHbl	lateral dorsal habenula
dHbm	medial dorsal habenula
DIG	digoxigenin-alkaline
DiI	1,1-dioctadecyl-3,3,3,3-tetramethylindocarbocyanine perchlorate
DiO	3,3'-dioctadecyloxacarbocyanine perchlorate
DMSO	dimethylsulfoxide
dNTP	deoxyribonucleosidtriphosphate
dpf	days post fertilization
E. coli	Escherichia coli
e. g.	exempli gratia
EDTA	ethylendiamintetraacetate
eGFP	enhanced green fluorescent protein
ENU	N-ethyl-N-nitrosourea
FGF	fibroblast growth factor
FITC	fluorescein-isothiocyanate
flh	floating-head
fow	foward
FR	fasciculus retroflexus
G	guanine
GFP	green fluorescent protein
GSK3	Glykogen Synthase Kinase 3
HMG	high mobility group
hpf	hours post fertilization
hsp	heatshock promoter
i. e.	id est
IPN	interpeduncular nucleus
IWR	4-(1,3,3a,4,7,7a-Hexahydro-1,3-dioxo-4,7-methano-2H-isoindol-2-yl)-N-8-quinolinyl-Benzamid
kb	kilobase
KCTD	potassium channel tetramization domain
KV	Kuppfer's vesicle
L	left
lhab	lateral habenula
lov	left-over
LPM	lateral plate mesoderm
LRP	leucine-responsive regulatory protein
M	molarity

mbl	masterblind
mhab	medial habenula
mib	mindbomb
min	minute
Mo	morpholino
NBT	4-Nitro blue tetrazolium chloride
ntl	no-tail
oep	one-eyed pinhead
ON	over night
P	propability
PBS	phosphate buffered saline
PC	pineal complex
PCP	planar cell polarity
PCR	polymerase chain reaction
PFA	paraformaldehyde
pitx2	paired-loke homeodomain transcription factor2
pp	parapineal
PTU	1- phenyl-2-thiourea
R	right
rev	reverse
RNA	ribonucleic acid
ron	right-on
RT	room temperature
SD	standard deviation
SDS	sodiumdodecylsulfat
sec	seconds
spw	southpaw
sur	schmalspur
T	thyamine
tag1	transiently expressed glycoprotein1
Taq	Thermophilus aquaticus
Tcf	T-cell specific transcripton factor
tg	transgene
Tris	Tris(hydroxymethyl)aminomethan
v	ventral
wt	wildtype
µ	micro